Karianne Talset

Effect of vertical load on lateral response and p-y curves for piles in cohesive soil

Numerical analyses of large diameter monopiles

June 2020

NTNU
Norwegian University of
Science and Technology
Faculty of Engineering
Department of Civil and Environmental Engineering

Master's thesis

2020

Karianne Talset

Master's thesis

NTNU
Norwegian University of
Science and Technology

NTNU
Norwegian University of
Science and Technology

NTNU
Norwegian University of
Science and Technology

Effect of vertical load on lateral response and p-y curves for piles in cohesive soil

Numerical analyses of large diameter monopiles

Karianne Talset

Civil and Environmental Engineering
Submission date: June 2020
Supervisor: Professor Gudmund R. Eiksund
Co-supervisor: Professor Amir M. Kaynia
Dr. Nallathamby Sivasithamparam, NGI

Norwegian University of Science and Technology
Department of Civil and Environmental Engineering

Preface

This master thesis was conducted at the Geotechnical division at the Norwegian University of Science and Technology (NTNU) during the spring semester of 2020. It is the final part of a MSc in Civil and Environmental Engineering.

The thesis is written for NTNU, as a part of the course TBA4900 and counts 30 credits for geotechnical students at the Department of Civil and Environmental Engineering. The topic of this master thesis was suggested by Professor Amir M. Kaynia and Dr. Nallathamby Sivasithamparam from the Norwegian Geotechnical Institute (NGI).

Trondheim, 2020-06-10

Karianne Talset

Acknowledgement

The summer of 2019, I worked as a summer intern at NGI. I got to work with Professor Amir M. Kaynia on my project thesis on dynamic analyses of an offshore wind turbine with a monopile foundation in SIMA. For the master thesis, Professor Amir M. Kaynia suggested looking into the effect of vertical loading on p-y curves as a topic for my master thesis. I was set in contact with Dr. Nallathamby Sivasithamparam, who guided me along the way.

I would like to thank Professor Gudmund R. Eiksund and Professor Amir M. Kaynia for their valuable guidance and suggestions along the way. I would especially like to thank Dr. Nallathamby Sivasithamparam for invaluable help during the difficult working conditions due to coronavirus outbreak during the spring of 2020. I am very grateful for the many skype calls and encouragement during this study. I would also like to thank NTNU and the professors for inspiration during my five years as a student. Lastly, I would like to thank my parents and all the new friends I have gained along the way.

K.T

Abstract

Pile foundations are usually exposed to simultaneous vertical and lateral loads. In integrated analyses of offshore wind turbines with a monopile foundation, the lateral foundation behaviour is usually represented by a set of non-linear springs (p-y curves) along the length of the pile. The p-y curves are then often derived from design regulations provided by API and DNV. The recommendations are based on slender piles and not large diameter monopiles used for offshore wind turbines. In the p-y curve methodology, the effect of vertical loading is neglected, and the lateral and vertical response is considered as uncoupled. This may give an inaccurate representation of the lateral pile behaviour. In this study, the effect of vertical loading on the lateral response of a large diameter pile installed in clay is studied in a series of three-dimensional finite element analyses in Plaxis 3D. The ultimate lateral response is limited by a wedge failure at shallow depth and by flow-around failure at larger depth. This study is limited to the p-y curves derived from the flow-around soil failure mechanism.

A large diameter pile installed in an idealised homogeneous clayey soil profile is analysed in Plaxis 3D. The pile is modelled with a linearly elastic material, and the soil material is modelled with the Hardening Soil (HS) model. The full length of the pile is modelled to evaluate the effect of vertical loads on the lateral response. A significant reduction in the lateral capacities is observed for applied vertical loads above 60% of the vertical capacities. Furthermore, the effect of the pile slenderness ratio, L/D-ratio, is evaluated. For piles with $L/D > 10$, the effect of vertical loading on the lateral pile response appears to be limited. However, for non-slender piles, $L/D < 10$, vertical loading significantly reduces the lateral capacity.

In addition, the effect of vertical loading on lateral p-y curves derived from a pile slice governing the flow-around soil failure mechanism is evaluated. The results indicate a limited effect of vertical loading on the lateral p-y curves. Although a significant effect of vertical loading was observed in the soil material close to the pile, further away from the pile, the effect is marginal. For lateral loading, on the other hand, shear stresses are mobilised at a considerable distance from the pile. Consequently, the ultimate lateral capacity is mainly governed by soil material which is not affected by vertical loading.

The overall conclusion in this study is that it is necessary with a full three-dimensional finite element analysis of the entire length of the pile to evaluate the effect of simultaneous vertical and lateral loading on the lateral pile behaviour. For non-slender piles installed in a clayey soil, it is unconservative to neglect the effect of vertical loads above 60% of the vertical capacity on the lateral pile response. Furthermore, the flow-around soil failure mechanism often used for derivation of p-y curves, as represented by a pile slice in Plaxis 3D, is not able to represent the effect of vertical loading on the lateral p-y curves.

Sammendrag

Pel fundamenter utsettes som oftest for både vertikale og horisontale laster samtidig. I integrerte analyser av offshore vindturbiner med monopelfundament modelleres horisontale jordreaksjoner vanligvis ved et sett av ikke-lineære fjærkurver (p-y kurver) langs pelens lengde. Fjærkurvene konstrueres da ofte fra standarder som er gitt av API og DNV. Anbefalinger gitt i disse standardene er basert på lange slanke peler, og ikke store monopeler brukt for offshore vindturbiner. Ved beregning av p-y kurvene neglisjeres da effekten av vertikal last og det antas det at de vertikale og horisontale jordreaksjonene er uavhengige av hverandre. Dette kan føre til feilaktig beregning av de horisontale jordreaksjonene rundt pelen. I dette studiet er det sett på effekten av vertikal last på den horisontale responsen til en pel installert i leire og på de horisontale p-y kurvene som representerer bruddformen for horisontal jordstrømning rundt pelen.

En stor diameter pel installert i idealisert homogen leire er analysert i elementmetodeprogrammet Plaxis 3D. Pelen er modellert med lineært elastisk materiale, og leiren er modellert med Hardening Soil (HS) modellen. Full lengde av pelen er modellert for å evaluere effekten av vertikale last på den horisontale responsen. Resultatene viser en betydelig reduksjon av den horisontale kapasiteten for vertikale laster over 60% av den vertikale kapasiteten. Videre ble effekten av pelens slankhetsforhold, L/D-forhold, vurdert. For peler med $L/D > 10$ ble det observert en marginal effekt av vertikal last på den horisontale kapasiteten. For peler med $L/D < 10$, ble det derimot observert en betydelig reduksjon som følge av vertikal last på den horisontale kapasiteten.

Effekten av vertikal last på de horisontale p-y fjærkurvene ble evaluert ved å se på en pel skive som representerer bruddformen for horisontal jordstrømning rundt pelen. En begrenset effekt av vertikal last ble observert på de horisontale p-y kurvene. Til tross for at det ble funnet en betydelig effekt av vertikal last på jordmateriale nær pelen, er effekten marginal lenger borte fra pelen. For horisontale laster derimot, mobiliseres skjærspenninger i en betydelig avstand fra pelen. Dermed er den ultimate horisontale kapasiteten dominert av jordmateriale som ikke er påvirket av vertikal last.

Hovedkonklusjonen i dette studiet er at det er nødvendig med en full tre-dimensjonal elementmetode-analyse av hele pelens lengde for å kunne evaluere effekten av vertikal last på den horisontale kapasiteten. Resultater fra dette studiet viser at for store monopeler med lave L/D-forhold, er det ikke-konservativt å neglisjere effekten av vertikale laster over 60% av den vertikale kapasiteten på horisontal kapasiteten av pelen. Videre er bruddformen for horisontal jordstrømning, modellert som en pel skive i Plaxis 3D, ikke i stand til å representere effekten av vertikal last på de horisontale p-y kurvene.

Contents

List of Figures

List of Tables

List of symbols

A_p = cross-sectional area of the pile

D = pile diameter

E_{py} = modulus of p-y curve

E^*_{py} = initial modulus of p-y curve

$E_p I_p$ = flexural rigidity of the pile

E_s = soil modulus

H = horizontal force applied

J = coefficient used in the equation for calculating the ultimate soil resistance for p-y curves in clay

L = pile length

M = bending moment applied

N = axial force

N_c = bearing capacity factor for vertical loading

N_p = bearing capacity factor for lateral loading

o = periphery of the cross-section of the pile

p = the reaction from the soil due to the deflection of the pile

p_{ult} = the ultimate lateral capacity

Q_t = vertical load used for deriving the vertical bearing capacity of the pile

Q_p = mobilised tip resistance

Q_s = mobilised side friction

Q_{pn} = mobilised net tip resistance

s_u = undrained shear strength of the soil

Vc = vertical capacity

W_p = weight of pile

y = deflection

y_{50} = a specific deflection for p-y curves in clay

z = depth below the seabed

R_{inter} = interface roughness factor

r_s = factor used in the equation for calculating the shear stress acting along the pile shaft for vertical capacity

γ = unit weight of soil

γ' = submerged unit weight of soil

ϵ_{50} = strain corresponding to one-half of the maximum principal stress difference

σ = normal stress

σ' = effective stress

σ_1 = major principle stress

σ_3 = minor principle stress

τ = shear stress

τ_s = shear stress along the pile shaft

α = proposed correction factor for the effect of vertical loading on the ultimate lateral capacity

Acronyms

ALS Accidental Limit State

API American Petroleum Institute

DNV Det Norske Veritas

FEA Finite Element Analysis

FEM Finite Element Method

FLS Fatigue Limit State

REDWIN REDucing cost of offshore WINd by integrated structural and geotechnical design

SLS Serviceability Limit State

ULS Ultimate Limit State

Chapter 1

Introduction

1.1 Background

Monopiles represent 81% of all installed substructures in Europe (Ramirez, Fraile, & Brindley, 2020), and is currently installed in water depths of up to 40 m. As the wind turbines are continuing to increase in size, larger diameter monopiles are required. The foundation response of an offshore wind turbine in an integrated analysis is often represented by rather simple methods, and the lateral and vertical behaviours of piles are most often analysed separately. In the offshore industry, the common calibration method for representing the soil-structure interaction is the use of discrete lateral and vertical uncoupled non-linear springs distributed along the length of the pile. The lateral foundation response is then represented by a set of p-y curves, where the pile is modelled as a beam and the soil is represented by a series of discrete uncoupled non-linear springs. The lateral and vertical behaviour is considered as uncoupled, and interaction effects are neglected. This assumption may lead to an unconservative estimate of the lateral capacity in clayey soils.

In this thesis, a series of three-dimensional finite element analyses are carried out in Plaxis 3D. The purpose is to evaluate the influence of vertical loading on the lateral response for large diameter piles installed in clayey soil. Furthermore, calculating the p-y curves requires a comprehensive study to derive dimensional loads. The use of three-dimensional finite element analyses for calculating p-y curves is, therefore, a complex and time-consuming process. A method of deriving p-y curves from Plaxis 3D will be investigated to see if it is possible to include a static vertical load in the model. The purpose is to evaluate the effect of vertical loading on the lateral p-y curves, and investigate if it is possible to propose a correction factor to account for this effect.

1.2 Problem Formulation

The main objective of this master thesis is:

- What is the effect of vertical load on the lateral loading response for a pile installed in normally consolidated

clay, and how can the p-y curves be modified to account for this effect?

The tasks to be answered along the way:

- What is the effect of vertical loading on the lateral response of a large diameter pile in clay?
- How can a vertical load be included in the flow-around soil failure mechanisms represented by a pile slice in Plaxis 3D?
- What is the effect of vertical loading on the lateral p-y curves represented by a pile slice in Plaxis 3D?
- What is the impact of the undrained shear strength of the soil on the effect of vertical loading on the lateral pile behaviour?
- What is the impact of the pile slenderness ratio on the effect of vertical loading on the lateral pile behaviour?
- Is it possible to propose a correction factor to account for the effect of vertical loading on the lateral p-y curves representing the flow-around soil failure mechanism?

The study is to be presented as a technical report with an introduction, objectivities, literature study, presentation of results, illustrations of figures, summary, and conclusion.

1.3 Method

This master thesis consists of theory in addition to relevant studies and literature on the subject, and calculations in Plaxis 3D, Python, Matlab and Excel. The theory and literature study are based on well-known publications and books. Most of the references are available through the university library database. In addition, lecture books and compendiums from courses lectured at NTNU is used. The calculations are done through Plaxis 3D, Python, Matlab and Excel. Python is used to generate scripts for creating models in Plaxis 3D and for extracting results. Matlab and Excel are used for calculations and presentation of the results.

As a part of answering the main objectivity, several tasks were conducted. This method chapter includes these tasks.

The main objectivity is solved by studying a model of the full length of the pile and a model representing the plane strain flow-around soil failure mechanism in Plaxis 3D. The models are exposed to both static vertical and lateral load simultaneously, and the effect of vertical loading is evaluated. In addition, the effect of vertical loading on the lateral p-y curves is compared to the effect of vertical loading on the lateral-load deflections obtained from a model of the full length of the pile.

The first task illustrates the effect of vertical loading on the lateral pile deflection. The full length of the pile is modelled in Plaxis 3D. Vertical capacity analyses are used to apply vertical loads equal to 20%, 40%, 60% and 80% of the vertical capacity. The purpose is to evaluate the lateral response of the full length of the pile when the pile is

exposed to both vertical and lateral loading. Several analyses were performed with varying vertical loads to see the effect on the pile response.

The second task consists of attempts to model only a slice of the pile. Several attempts are performed in Plaxis 3D, and two methods will be presented. The pile slice is modelled with a plane strain condition to restrict the soil surrounding the pile to move in the lateral directions, representing the horizontal flow-around mechanism. Therefore, the full length of the pile is first modelled to load the pile vertically prior to creating the slice.

The first model consists of removing soil volume from the full length of the pile to create the slice. The second model consists of creating smooth surfaces to allow for horizontal movement of the slice, independent of the rest of the model. Several analyses are performed to confirm the results obtained from the FE models for pure lateral loading.

The third task is answered by evaluating the results from the two models representing a pile slice in Plaxis 3D. Vertical capacity analyses are used to apply vertical loads equal to 20%, 40%, 60% and 80% of the vertical capacity.

The fourth and fifth task is answered by changing the undrained shear strength of the soil and the pile slenderness ratio, L/D-ratio. The slenderness ratio is changed by changing the diameter of the pile while the length remains constant. From the results, the impact of the undrained shear strength and the pile slenderness ratio is evaluated.

The last task is answered by studying the results from a model of a pile slice in Plaxis 3D. The results are analysed and compared to the results obtained by the model of the full length of the pile.

1.4 Use of references

The references used in this thesis is referred to with the American Psychological Association (APA). The references are listed in alphabetical order after the last name of the authors.

1.5 The outline of the thesis

Chapter 2 gives an introduction to offshore wind turbines installed today.

Chapter 3 gives an introduction to the theory used in the project, in addition to the existing solutions.

Chapter 4 presents the 3D finite element model representing the full length of the pile used in this project.

Chapter 5 presents the effect of axial load on the lateral response from the 3D finite element model representing the full length of the pile.

Chapter 6 presents two possible methods of deriving p-y curves for combined vertical and lateral loads by modelling a slice of the pile in Plaxis 3D.

Chapter 7 presents the results from the two models of a pile slice and the effect of vertical load on the lateral p-y curves.

Chapter 8 gives the conclusion.

Chapter 9 gives recommendations for further work.

The appendix includes graphs, results, and scripts and will be referred to in the text.

1.6 Limitations

The scope of this project is limited to the following features:

- A constant undrained shear strength profile is assumed. In reality, the strength profile of a soil varies with depth.
- The nature of loading considered is only static loading.
- A full rough pile is considered.
- An isotropic stress condition is assumed.
- The finite element model used for deriving the p-y curves is based on a plane strain flow-around soil failure mechanism. Deriving p-y curves from the failure mechanism characterised by a conical wedge is beyond the scope of this project.
- The slice model is based on ideal soil behaviour. Plane strain condition analyses ignore out of plane deformations and soil shear forces between the soil elements at different depths.

Chapter 2

Offshore Wind Turbines

The first offshore wind farm was constructed at Vindeby, Denmark, in 1991 (WindEurope, 2020). Since then, the development of the offshore wind market has grown rapidly in Europe. With the focus on reducing greenhouse gas emissions and the increasing energy demand in the world, renewable sources of energy are alternatives to fossil fuels. The last decade sustainable development policies have been initiated across Europe. In 2009, the European Union leaders established a policy that 20% of all energy should originate from renewable energy sources by 2020. In 2018, a new target of 32% of energy should originate from renewable energy sources by 2030 was set (*Renewable energy directive*, 2020).

With increasing interest in renewable energy sources to help mitigate climate change and reduce CO_2 emissions, wind energy appears as a clean alternative with enormous potential. The wind quality for generating electricity is better at sea than on land, with a stronger and less turbulent wind. In addition, as large areas are required for wind farms, placing the turbines at sea leads to less disturbance for the public. There are now 110 installed offshore wind farms across 12 countries in Europe (Ramirez et al., 2020). The average installed turbine capacity in 2019 was 7,8 MW, an increase of 15% from 2018 (Ramirez et al., 2020). The Dogger Bank Wind Farm to be constructed at the North East coast of England will be the first project in Europe to install 12MW machines (*Dogger Bank Wind Farm*, 2020).

This chapter introduces the terminology used for OWTs and the different foundation models used. In this project, a monopile is of interest, and the monopile foundation will be presented in further detail.

2.1 General

The general terminology of a wind turbine is given in Figure 2.1. It is taken from the Arkona offshore wind farm consisting of 60 turbines with monopile foundations, installed 35 kilometers northeast of the island of Rügen, Germany. The turbine capacity installed was 6MW. As indicated on the figure, the blades are connected to the hub, which is the rotating component of the wind turbine. The nacelle consists of the rotor, shaft, gearbox, and generator, and is located on the figure behind the blades. The tower is connected to the foundation by a transition piece.

The transition piece is installed on top of the foundation, and the foundation is below the water level in the figure.

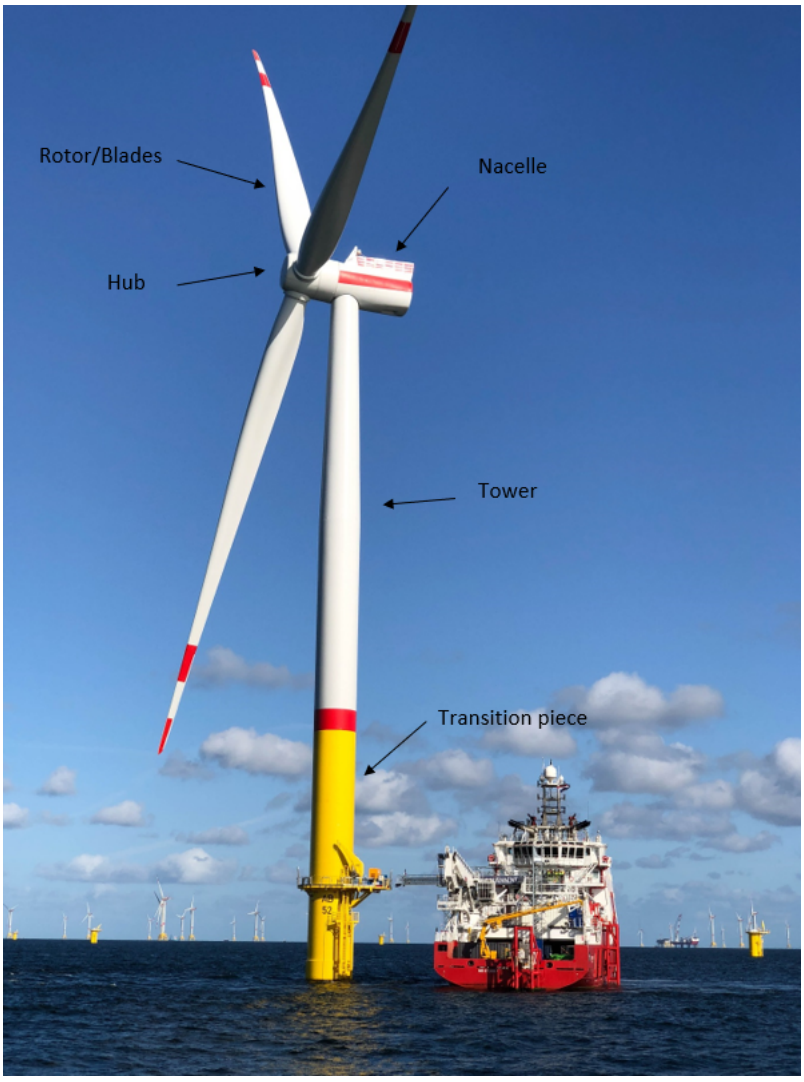

Figure 2.1: The Arkona offshore wind farm, 35 kilometres northeast of the island of Rügen, Germany. Edited from Equinor (2018)

Figure 2.2 illustrates the common support structures used in the design of offshore wind turbines. The gravity-based foundation is suitable for rocky seabed where pile driving complicated and expensive. The foundation achieves its stability by the self-weight of the structure at the seabed. It is the second most installed foundation type in Europe, consists of 5.7% of the installed foundations (Ramirez et al., 2020). The monopile is the most installed support structure in Europe, representing 81% of installed support structures in Europe. The support structure is rather simple to fabricate, and the tower is connected to a pile through a transition piece. The jacket and tripod foundations provide a stable support structure with multi-leg configurations connected to the transition piece with suction caissons or piles supporting each leg. Suction caisson foundations rest on the seabed with skirts penetrating the soil. The support structure achieves its stability by pressure difference generated between the inside of the bucket and the water surrounding it. The stable support structure of the jacket and tripods makes the structures

more suitable in deeper water depths, then the monopile and gravity-based structures.

The design of offshore wind turbines depends on the local site conditions. Environmental conditions such as water level data, wave data, current data, wind data and soil data are conditions determining the support structure (De Vries, 2011). As the offshore wind turbines are continuing to increase in size and installed at deeper depths, both the gravity-based foundation and the suction caisson foundations are considered competitive in comparison with other support structures. Also, environmental restrictions regarding noise emission from pile driving are avoided with these foundations.

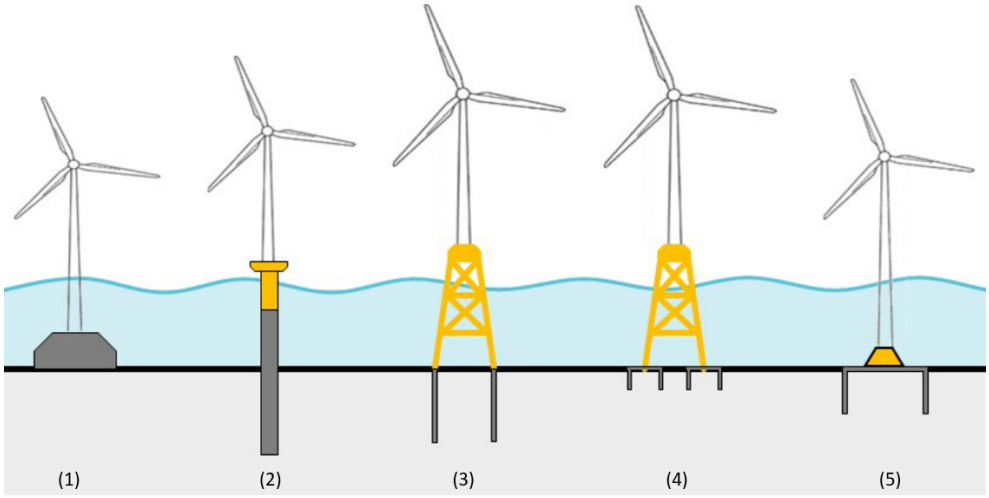

Figure 2.2: Typical foundations (1) gravity-based (2) monopile, (3) piled jacket structure, (4) suction caisson jacket structure (5) mono caisson (Skau et al., 2018)

2.2 Design of offshore wind turbines

Offshore wind turbines are dynamically sensitive structures (Skau et al., 2018). In the offshore environment, the wind turbines are exposed to irregular cyclic loads from wind, waves, and the operation of the turbine, which is highly coupled and non-linear. The design requires integrated dynamic non-linear analyses to capture the structural response. An integrated analysis is an analysis of the entire offshore wind turbine with the contributions from aerodynamic and hydrodynamic loads. Although advanced models often are used for modelling the wind and wave loads, and the operation of the turbine, rather simple models are used to represent the foundation and soil response.

The natural frequency of the support structure determines the dynamic behaviour of the offshore wind turbine (De Vries, 2011). As the offshore wind turbine is exposed to aero- and hydrodynamic forces, the response of the structure is determined by the frequency of the excitation. If the frequency response is close to the natural frequency, resonance occurs, and the response is amplified.

2.3 Monopile foundations

Monopiles are long steel tubes driven into the seabed by a hydraulic piling hammer. The monopiles are the most installed support structure today, as it is simple to fabricate, and easy to install and maintain. The vertical loads are transferred to the soil through wall stiffness and tip resistance, and the lateral loads are transferred to the foundation through bending (De Vries, 2011). The lateral loads, due to wind and wave loads, are much larger than the vertical loads. To provide the necessary stiffness, the diameter of the pile has to be large enough (De Vries, 2011). Therefore, as the size of the wind turbines continues to increase, larger diameter monopiles are required.

2.3.1 Current practice

A variety of numerical models have been developed to represent the foundation behaviour during dynamic and cyclic loading. However, integrated analysis often use rather simple models for representing the foundation behaviour. One such example is RIFLEX. RIFLEX is a computer tool for analyses of flexible risers and slender structures based on finite element theory (SINTEF-Ocean, 2019). The program is used for static, dynamic and Eigenvalue analysis, and can be used for modelling offshore wind turbines. The soil-structure interaction can be modelled either by non-linear soil springs or by the recent development to include a macro-element model. Nevertheless, the non-linear soil springs are the most common representation of the soil-structure interaction. SIMA is used to provide a 3D graphical representation of the objects modelled. SIMA is developed as a Joint Industry Project by SINTEF Ocean and former Statoil (Equinor) and is a tool for modelling within the field of marine technology. Figure 2.3 illustrates a model of an offshore wind turbine with a monopile foundation in SIMA for an integrated analysis. The pile is modelled down to the seabed. The red point at the end of the pile indicates the beginning of the foundation either modelled with a set of p-y springs or a macro element model.

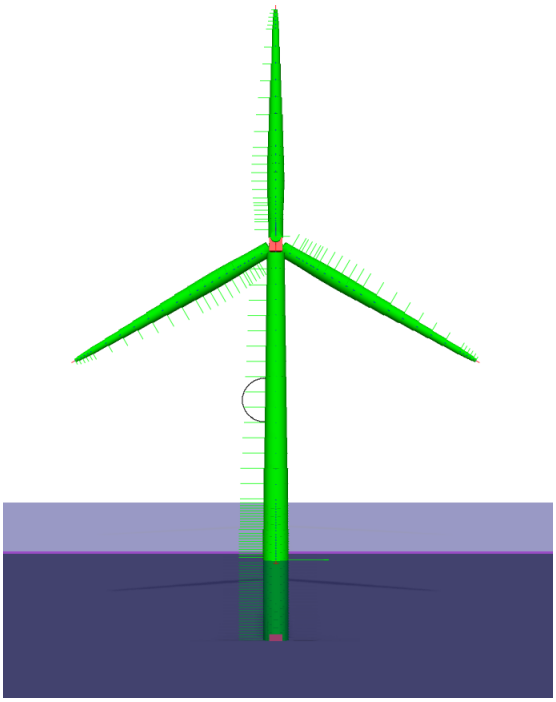

Figure 2.3: Offshore wind turbine modelled in SIMA

The current design regulations used for design of the offshore wind turbines, such as standards provided by the American Petroleum Institute (API) and Det Norske Veritas (DNV), base the lateral foundation behaviour design on p-y curves. As the p-y curve methodology is still used for analyses of offshore wind turbines, neglecting the effect of simultaneous vertical and lateral loading on the pile foundations will give an inaccurate representation of the pile behaviour.

In this thesis, a large diameter pile installed in a normally consolidated clay is analysed by three-dimensional finite element (FE) analyses in Plaxis 3D. The purpose is to evaluate the effect of vertical loading on the lateral pile behaviour and evaluate if it is possible to propose a correction factor to be included in the p-y curve formulations.

Chapter 3

Theory and existing solutions

3.1 Introduction

This chapter provides an introduction to the theory used in this project. The chapter includes an introduction to the origin of p-y curves, limitations, and assumptions. The chapter also includes existing studies on the effect of vertical load on the lateral response.

3.2 Pile design

To verify that piles have sufficient capacity to resist failure and no damaging deformation occurs, piles are designed in accordance with the limit states used in the design codes. A limit state is defined as a state in which the structure no longer satisfies the requirements (DNV, 2014). Both the installed capacity of the pile and the capacity of the soil-structure interaction is considered in the design. The pile capacity is depending on the pile material, design, and dimensions.

According to DNV (2014), the pile shall be designed according to the following limit states (a) the pile design and installed capacity shall be greater or equal to the design loads or load actions, Ultimate Limit State (ULS), (b) the pile shall be able to maintain its design purpose without excessive settlements, erosion or physical deterioration, Serviceability Limit State (SLS), (c) the pile shall be designed to not exceed ULS for accidental loads even with a low probability of occurrence, Accidental Limit State (ALS), (d) the pile shall be designed to not exceed ULS for cyclic or varying loads, Fatigue Limit State (FLS).

3.3 Soil-pile behaviour under lateral loading

In the offshore industry piles supporting offshore structures needs to be designed for large horizontal forces from wind and waves. The behaviour of a pile under lateral loading is depending on the resistance from the surrounding soil and the deflection of the pile. Figure 3.1a illustrated the pile bending due to lateral loading, H on a cylindrical

pile. The soil resistance, p, and pile deflection, y, is depending on the depth below the surface, z. Figure 3.1b illustrates a slice of the pile at a depth, z_1 and the resisting forces from the soil acting on the pile before and during lateral loading of the pile. The pile deflection, y_1, is a function of the lateral resistance from the soil, p_1.

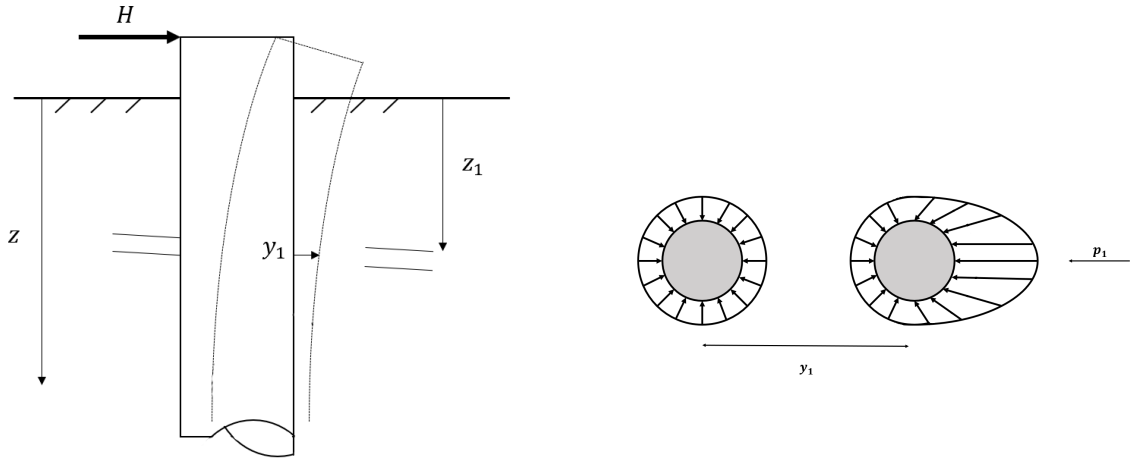

(a) Pile bending (b) Pile slice

Figure 3.1: Piles under lateral loading, edited after Reese and Van Impe (2011)

3.3.1 Loading

The nature of loading at the pile head is of great importance when determining the pile behaviour. Loading can be divided into active and passive loading. Passive loading can occur when soil is moving along the length of the pile. For active loading, the possible loading types are short term static, cyclic, sustained, or dynamic loading. Static loading seldom occurs in practice but is useful to find correlations between lateral force and displacement, and can also be used as a baseline for determining behaviour from other types of loading. In this project, only static loading will be evaluated.

3.3.2 Winkler approach

The simplest method to model the soil-structure interaction during lateral loading of a pile is to model the pile as an elastic beam and the soil as a series of uncoupled springs along the length of the pile. The lateral soil resistance deflection, p, is related to the lateral soil deflection, y, through a set of uniformly distributed p-y curves along the length of the pile. The pile is discretised into a chosen number of structural elements, connected through nodal points. The surrounding soil is modelled as springs attached to the nodal points, and the lateral forces are applied at the pile head. As the springs are uncoupled, they are independent of each other. This method is known as the Winkler idealisation (M. Randolph & Gourvenec, 2011). Figure 3.2 illustrates a beam exposed to axial force, N, horizontal force, H, and moment M, represented by a set of non-linear springs for each element along the length of the beam. The derivation of the differential equation for one beam-column element is given in the next section.

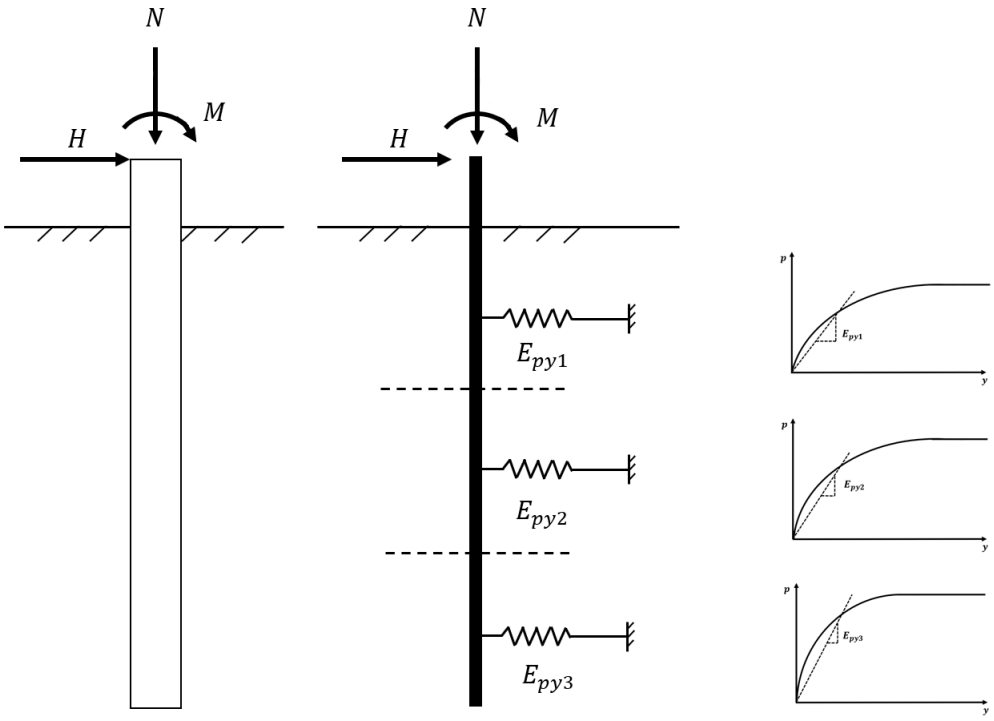

Figure 3.2: Winkler beam approach, edited after Sørensen et al. (2012)

3.3.3 Derivation of the differential equation for laterally loaded piles

The p-y curves are based on analysing the pile based on the derivation of the differential equation of a beam element. The derivation is based on classical beam theory, also known as Euler-Bernoulli beam theory. The following derivation of the differential equations is based on Reese and Van Impe (2011). A beam-column element exposed to shear forces, V, moment, M, and axial load, N, is illustrated in Figure 3.3.

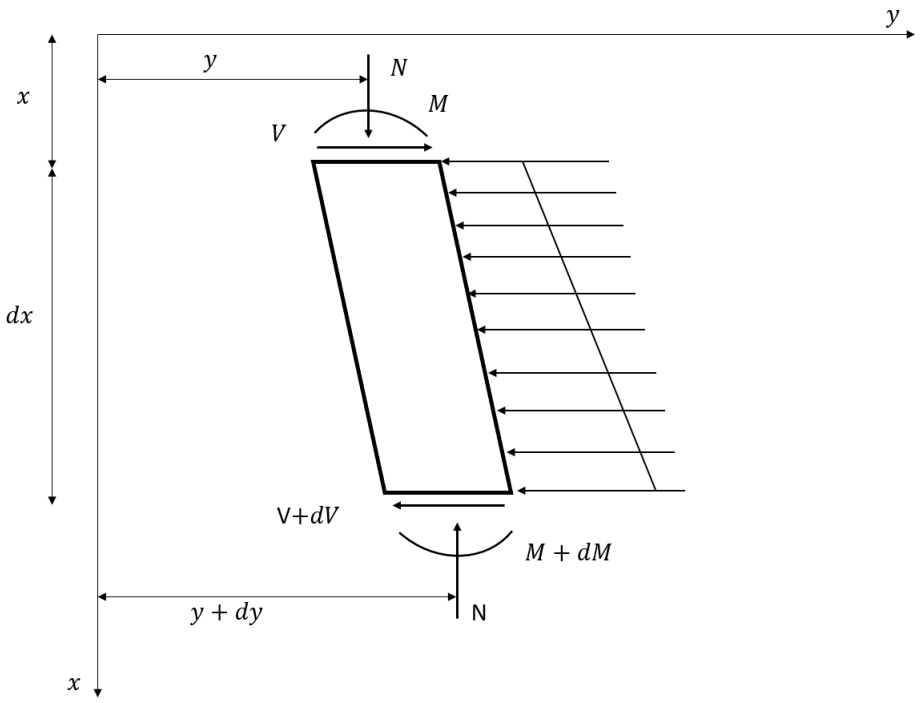

Figure 3.3: Beam-column element, edited after Reese and Van Impe (2011)

The equations are derived based on moment equilibrium of the element where second-order terms are neglected,

$$(M + dM) - M + N dy - V dx = 0 \tag{3.1}$$

Rewriting Equation 3.1,

$$\frac{dM}{dx} + N\frac{dy}{dx} - V = 0 \tag{3.2}$$

By differentiating Equation 3.2 with respect to x,

$$\frac{d^2M}{dx^2} + N\frac{d^2y}{dx^2} - \frac{dV}{dx} = 0 \tag{3.3}$$

Introducing the following relations,

$$\frac{d^2M}{dx^2} = E_p I_p \frac{d^4y}{dx^4}$$
$$\frac{dV}{dx} = p$$
$$p = E_{py} y$$

where $E_p I_p$ is the flexural rigidity of the pile, p is the lateral soil resistance, and E_{py} is the reaction modulus. The reaction modulus will be explained further in the next section.

By substituting the relations introduced above into 3.3, the fourth-order differential equation for laterally loaded

piles is given by,

$$E_p I_p \frac{d^4 y}{dx^4} + N \frac{d^2 y}{dx^2} + E_{py} y = 0 \tag{3.4}$$

This equation is derived based on the following assumptions for the pile, (a) a straight pile with a uniform cross-section, (b) the loads and reactions lie in the plane of symmetry, (c) homogeneous and isotropic pile material, (d) the pile material does not exceed the proportional limit (d) same modulus of elasticity in tension and compression, (d) static loading of the pile, (e) small deflections from shear stresses.

3.4 Soil behaviour defined by p-y curves

The lateral soil-pile interaction can be described by p-y springs, defined by the lateral soil resistance, p, and the lateral pile deflection, y, as a function of depth. An example of a p-y curve and resulting soil modulus are illustrated in Figure 3.4.

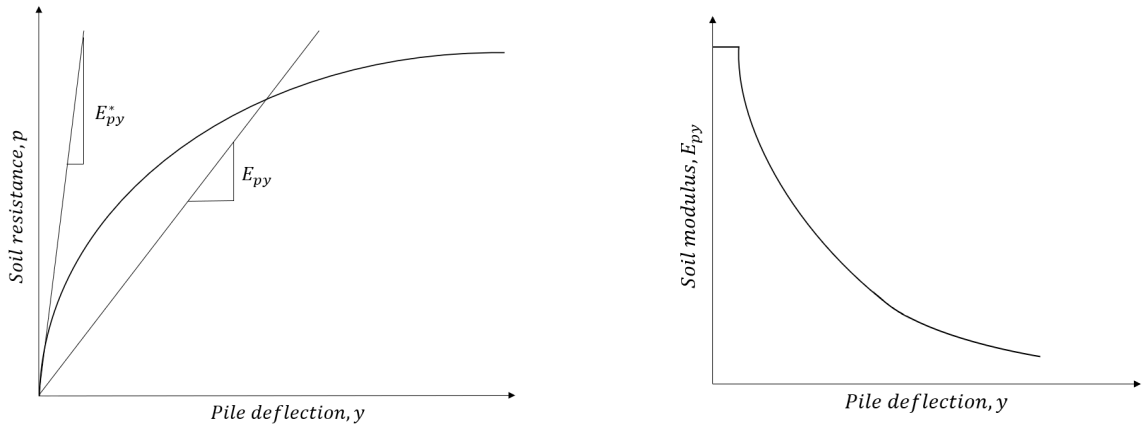

(a) p-y curve

(b) Soil modulus

Figure 3.4: A p-y curve with resulting soil modulus, edited after Reese and Van Impe (2011)

Even though the pile and soil stiffness are known, the soil-pile interaction governing the slope of the p-y curves is unknown. The interaction stiffness is defined as the reaction modulus for a pile under lateral loading, E_{py}, and is defining the slope of the p-y curves. Figure 3.4b, illustrated the reaction modulus to the p-y curve given in 3.4a. Hence, the lateral soil resistance can be written,

$$p = E_{py} y \tag{3.5}$$

As observed from the p-y curve presented in Figure 3.4a, the load-displacement response of the pile during lateral loading is non-linear. This was discovered by field investigations at Lake Austin and Sabine River reported in Matlock (1970). The strain increases in the soil during the lateral loading of the pile, and the stiffness decreases. The parameter E_{py} is constant for small displacements, referred to as the initial stiffness, E^*_{py}, and decreases as the displacement increases. The parameter is depending on the soil material, but it does not depending on a partic-

ular soil parameter alone (Reese & Van Impe, 2011). As the soil approaches failure, the ultimate lateral resistance, p_{ult}, is reached, defining the upper limit of the p-y curves. The ultimate soil resistance is depending on the pile cross-section and soil properties.

3.5 p-y curve formulations for piles in cohesive soils

In the late 1940's and 1950's energy companies showed interest in research related to construction of p-y curves for the design of large offshore structures exposed to large horizontal forces from wind and waves. Since then, numerous different p-y curve formulations have been proposed. Some of the most common p-y curve formulations for static behaviour of piles installed in cohesive soils are presented. Only the formulations made by Matlock (1970) and Reese, Cox, and Koop (1975) will be discussed. These formulations are referred to in design regulations given by API and DNV for installation of piles in soft and stiff clay.

3.5.1 Matlock (1970)

In the 1950s field pile tests were performed at Lake Austin and Sabine River. Two static loading tests were performed at both field locations. From the field tests and laboratory investigations, p-y curve formulations were developed based on correlations for design of laterally loaded piles in soft clay for offshore structures. The field tests consisted of free-head tests and restrained-head pile conditions with a pile diameter of $D = 324mm$ and pile length of $L = 12.80m$. This results in a slenderness ratio of $L/D = 40$. The p-y curves are obtained by empirical curve fitting of the full-scale field tests. The recommendations from Matlock (1970) are given for naturally consolidated or slightly overconsolidated clays and is considered to apply to open-ended, circular cross-sectional piles. From the field tests, it was discovered that the soil resistance and lateral displacement of the pile were found to be highly non-linear and inelastic. In addition, from the comparison between the free-head and restrained-head pile condition, the lateral resistance and deflection characteristics appear to be the same. The p-y curve formulations proposed by Matlock (1970) have been used as a framework for deriving p-y curves for piles installed in soft clays given in regulations provided by API and DNV. The p-y curve formulations provided by API will be presented in the next section.

3.5.2 Reese, Cox, and Koop (1975)

In the 1960s field studies were performed at a location northeast of Austin, Texas, called the Manor site. Two pile diameters of $D = 152mm$ and $D = 641mm$ were tested for lateral loading. The length of the piles was $L = 18.30m$, resulting in pile slenderness ratios of $L/D = 120$ and $L/D = 29$ for the two piles. The soil condition at the Manor site consisted of stiff, preconsolidated clays. Based on the experimental results, a method of predicting p-y curves for piles installed in stiff clay was reported in Reese et al. (1975). The resulting p-y curve formulation from the field test of larger diameter piles was used to analyse the behaviour of the smaller piles. The comparison from the analysis and field tests showed considerable disagreement for the lateral deflection at the surface. However, the reason for the disagreement was not discovered, and the p-y curve formulation recommended is based on the

larger diameter piles. The p-y curve formulation proposed in Reese et al. (1975) from experiments at the Manor site, is recommended by API for stiff clay.

3.6 Standards

The most commonly used design regulation for load-deformation curves for laterally loaded piles in the offshore industry today is provided by API. API recommendations are based on Matlock (1970) for the design of p-y curves for soft clays. The recommendations will be presented in this section.

The p-y curves are constructed based on the failure mechanism occurring in the soil surrounding the pile. For a homogeneous clay, the failure mechanism is different in the soil close to the ground surface and the soil at deeper depths, as shown in Figure 3.5. The failure mechanism close to the surface is characterised by a conical wedge. Resisting forces acting on the wedge preventing it from failure, is friction on the pile shaft from the surrounding soil, shear forces in the soil, and the weight of the wedge. The failure mechanism at deeper depths is governed by soil flowing around the pile shaft in the horizontal plane.

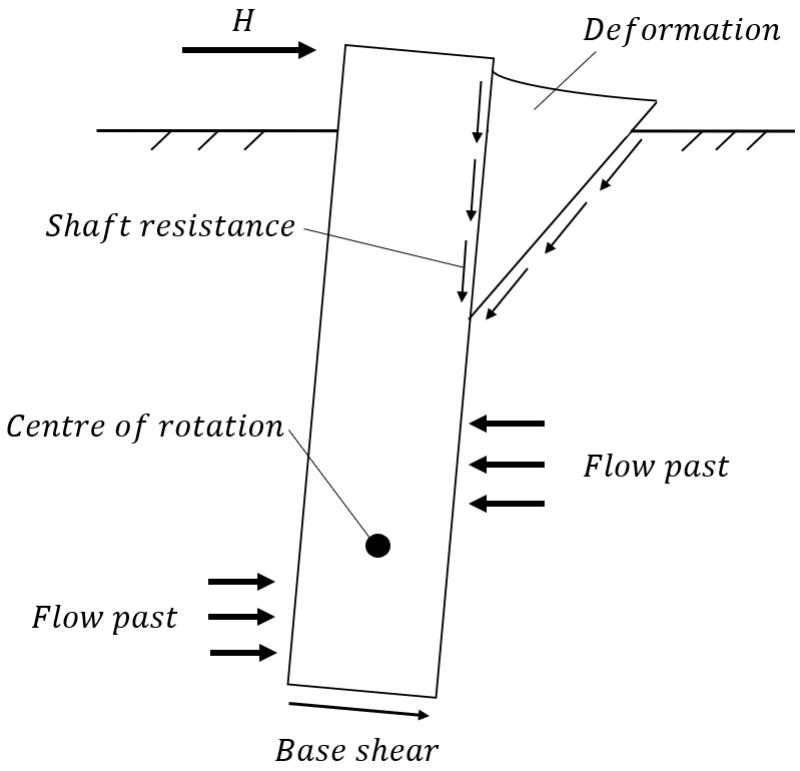

Figure 3.5: The failure mechanism in the clay surrounding the pile under lateral loading, edited after M. Randolph and Gourvenec (2011)

For static loading in soft clays in the presence of free water, the p-y curves are calculated based on the following

relationship,

$$\frac{p}{p_{ult}} = 0.5(\frac{y}{y_{50}})^{1/3} \leq 1 \tag{3.6}$$

The ultimate lateral resistance is calculated based on the failure mechanism. In the soil closer to the surface, where wedge failure is the governing failure mechanism, the ultimate lateral resistance is reduced to allow for the different modes of deformation. Equation 3.7 is used for the failure mechanism characterised by a conical wedge, and Equation 3.8 is used for the failure mechanism governed by soil flowing around the pile shaft.

$$p_{ult} = [3 + \frac{\gamma`}{s_u}z + \frac{J}{D}z]s_u D \tag{3.7}$$

$$p_{ult} = 9 s_u D \tag{3.8}$$

where γ' represents the submerged soil unit weight, J is a coefficient depending on the clay material. Experimental studies indicate that the coefficient J is about 0.5 for soft clay, and 0.25 for somewhat stiffer clays (Matlock, 1970). The deflection y_{50} is given by $y_{50} = 2.5\epsilon_{50}D$, and ϵ_{50} is the strain corresponding half of the maximum principal stress difference. s_u is the undrained shear strength of the soil material. The shear strength of soil material on a total stress basis is relevant for short term loading in cohesive soils, such as clay or fine silt, when the condition in the soil may be assessed as undrained. The lateral soil resistance p is given to be constant for deflections above $y = 8y_{50}$.

Figure 3.6 show characteristic p-y curves for static loading in soft clay in the presence of free water based on the API p-y curve formulations.

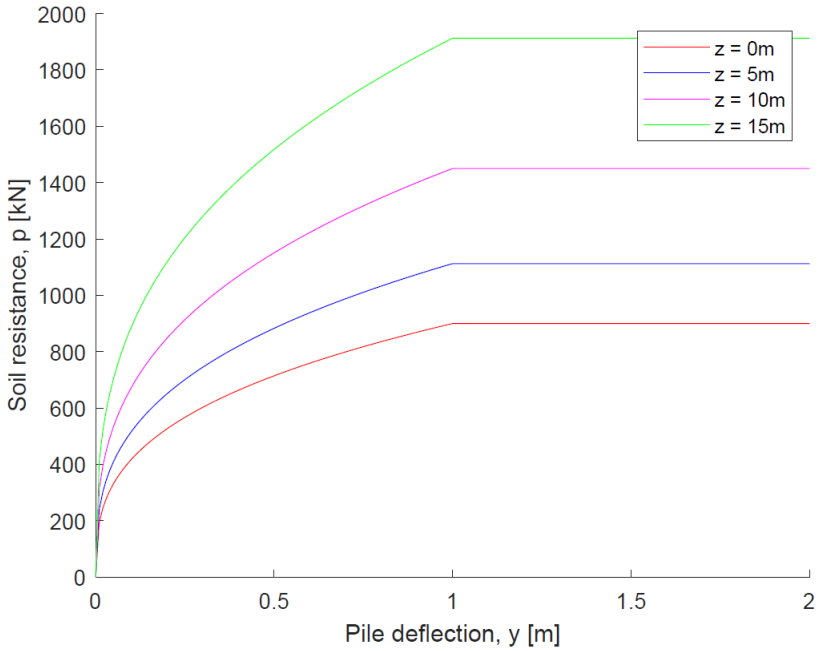

Figure 3.6: Characteristic p-y curves for static loading for soft clay in the presence of free water

The characteristic p-y curves presented in Figure 3.6 is calculated based on a large diameter pile used in Chapter 5, with a diameter of $D = 5m$ and a pile length of $L = 15m$. The soil properties used are given in Table 3.1.

Table 3.1: The soil properties used for deriving the API p-y curves

Undrained shear strength $[kPa]$	$s_{u,ref}$	60
Increasing undrained shear strength $[kPa/m]$	$s_{u,inc}$	2
Soil unit weight $[kN/m^3]$	γ	20

For normally consolidated clays, representative values for strain corresponding to one-half of the maximum principal stress difference given in Reese and Van Impe (2011) are presented in Table 3.2. The p-y curves presented in Figure 3.6 is derived based on a medium clay, and $\epsilon_{50} = 0.01$ is used.

Table 3.2: Representative values for ϵ_{50} (Reese & Van Impe, 2011)

Consistency of clay	Average undrained shear strength	ϵ_{50}
Soft	$s_u < 48kPa$	0.02
Medium	$s_u = 48 - 96kPa$	0.01
Stiff	$s_u = 96 - 192kPa$	0.005

3.7 Slice method

The ultimate lateral resistance is calculated based on the failure mechanism in the soil. In this study, the p-y curves will be derived based on the failure mechanism governed by the soil flowing around the pile shaft in the horizontal plane. M. F. Randolph and Houlsby (1984) studied the limiting pressure on a circular pile in cohesive soils for pure lateral loading. By representing the soil as perfectly plastic material, the failure mechanism can be modelled as a plane strain flow-around mechanism based on plasticity theory. The lateral load-deflection is then calculated on a long cylinder which moves through an infinite medium. Two approaches were considered for deriving an upper and lower bound for the limiting pressure of a circular pile in cohesive soil. For the lower bound, it is assumed a stress distribution in equilibrium with an applied load. Given that the stress field does not exceed the failure criteria, the applied load will be less or equal to the failure load. For the upper bound, a deformation mechanism was postulated with an associated velocity field. From the geometry of the failure mechanism, the limiting pressure is calculated based on the rate of dissipation of energy from the deformation of the soil mass and the work done by the applied load.

The ultimate lateral resistance per unit length of the pile is given by $p_{ult} = N_p s_u D$. M. F. Randolph and Houlsby (1984) suggested an upper and lower limit of the bearing capacity factor based on classical plasticity theory. M. F. Randolph and Houlsby (1984) stated that for most engineering purposes the limiting bearing capacity factor N_p could be calculated based on,

$$N_p = 9 + 3 * \alpha \tag{3.9}$$

where α is the roughness factor depending on the pile-soil interface. The factor varies from $\alpha = 0$ for a smooth

pile and $\alpha = 1$ for a rough pile. During lateral displacement, a rough pile will have a larger deformation area due to higher resistance, compared to a smooth pile, resulting in a higher bearing capacity factor. This is illustrated in Figure 3.7.

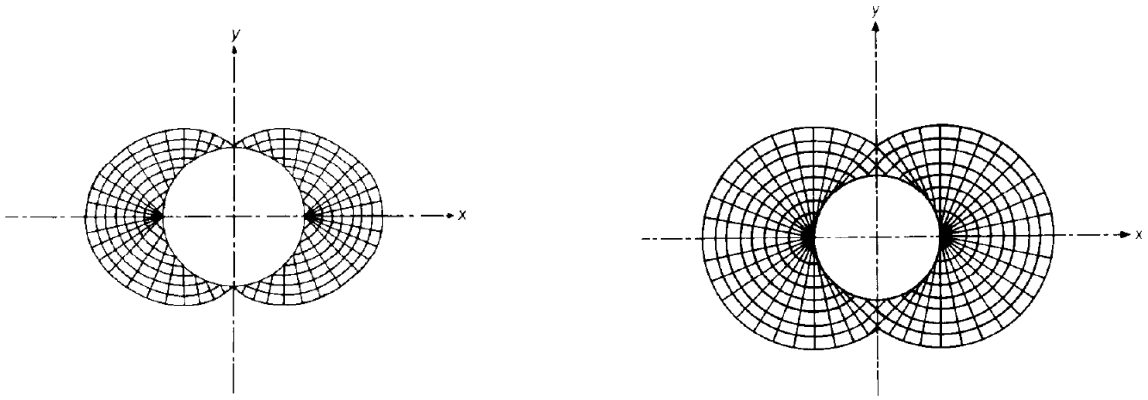

(a) Smooth pile $\alpha = 0$ (b) Rough pile $\alpha = 1$

Figure 3.7: Deformation area depending on the roughness factor (M. F. Randolph & Houlsby, 1984)

As stated by M. F. Randolph and Houlsby (1984), the solutions derived in the study are based on rigid, perfectly plastic responses in the soil, with an undrained shear strength, s_u, depending on the current stress level in the soil.

The plane strain flow-around mechanism is restricting the soil behind the pile to move only in the lateral direction preventing breakaway of the soil. In addition, the ultimate resistance is not influenced by elastic deformations. However, the elastic deformation of the soil could affect the ultimate resistance if the plastic region is fully confined by unyielding material.

Zhang and Andersen (2017) used a pile slice for scaling of lateral pile response in clay from laboratory stress-strain curves. In the study, only a slice of a slender pile was created. By using this method, p-y curves, as a function of depth, can be generated by changing the initial stresses in the slice.

In this study, p-y curves will be derived from a model of a pile slice in Plaxis 3D. The failure mechanism is modelled as a plane strain flow-around soil failure mechanism based on plasticity theory as described in M. F. Randolph and Houlsby (1984).

3.8 Limitations

The offshore wind turbines are continuing to increase in size, requiring larger monopile foundations. In the oil and gas industry, the p-y curves have successfully been applied for a long time (Page et al., 2016). As the p-y curve formulations are developed on slender piles, the validation of p-y curves for piles installed for offshore wind turbines has been questioned. The p-y curve formulations would ideally be derived from full-scale field tests, but for the large monopile foundations, this is difficult. There is currently no approved method for large diameter piles in the offshore industry, and therefore the design regulations provided by API and DNV still recommends the use of p-y curves. Some of the limitations of the p-y curves are discussed below.

The p-y curve methodology is based on applying the Winkler approach, and the assumptions listed in section 3.3.3 has to apply. Among the assumptions, the p-y curves are based on modelling the pile as a beam on elastic foundation. Consequently, a flexible pile is assumed. The recommendations given in Matlock (1970) is based on a limited number of field tests, for a constant slenderness ratio of $L/D = 40$. The typical slenderness ratio for piles installed for offshore wind turbines today is $L/D < 10$. The influence of the flexibility of the pile on the soil response has been investigated by several authors. Tomlinson (2001) described rigid piles as piles with a slenderness ratio below $L/D = 10 - 12$. Figure 3.8 illustrates the difference between flexible and rigid pile behaviour during lateral loading.

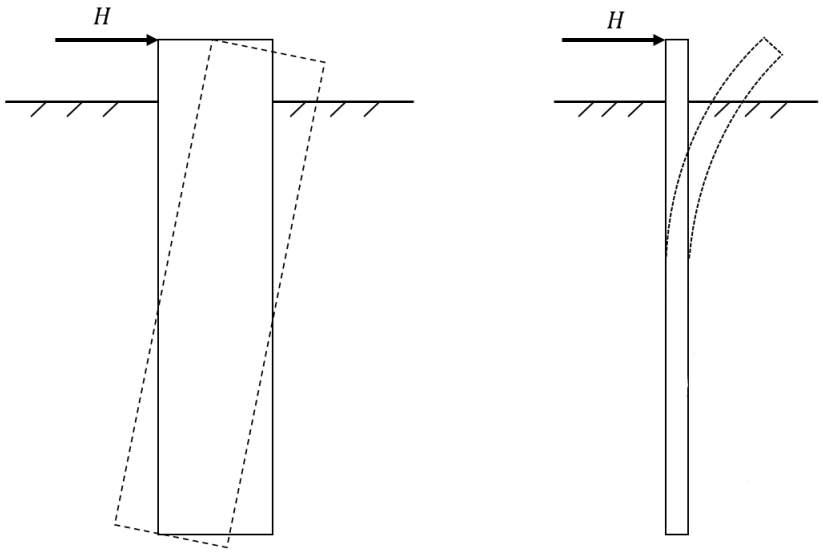

Figure 3.8: Rigid versus flexible pile behaviour, edited after Sørensen et al. (2012)

A rigid pile behaviour will first be discussed. As a lateral load, H, is applied at the pile head, passive soil resistance will form at the opposite side of the acting force. Also, passive soil resistance will also form at the pile tip on the same side as the applied force. This results in a rotation of the pile as illustrated to the left in Figure 3.8. The piles installed for other offshore structures are long slender piles, and the failure mechanism will differ from the rigid piles used for offshore wind turbines as illustrated to the right in Figure 3.8. For slender piles, the passive soil resistance acting on the same side as the applied force will be much higher. Hence no rotation of the pile will occur. The failure mechanism is more likely to occur at the point of a yielding moment.

Poulos and Hull (1989) proposed criteria for stiff and flexible piles. A rigid pile is defined as by the following criteria,

$$L < 1.48\left(\frac{E_p I_p}{E_s}\right)^{0.25} \tag{3.10}$$

where L is the length of the pile, E_p and E_s is the Young's modulus of elasticity of the pile and soil, respectively. I_p

is the moment of inertia of the pile. Furthermore, a flexible pile is defined by,

$$L < 4.44(\frac{E_p I_p}{E_s})^{0.25} \tag{3.11}$$

As the p-y curve formulations are based on an ultimate lateral resistance for flexible piles, the formulations need validations for rigid piles. In addition, the piles used in the oil and gas industry, are fixed at the pile head, while the piles used for the offshore wind turbines are free. However, as stated in Matlock (1970), the results from field investigations of both free-head tests and restrained-head tests resulted in the same lateral response.

Among design regulations for offshore wind turbine structures, the regulations provided by DNV is commonly used. According to DNV (2014), non-linear p-y curves are intended for evaluation of lateral pile capacity in the ULS. The design code states that the p-y curves are designed for *long slender jacket piles with a diameter of up to 1.0 m* (DNV, 2014), and that they are in general not applicable for large diameter piles used in the offshore wind industry. In addition, the design code recommends that the p-y curves used for foundation design of an offshore wind turbine should be validated against, for example, finite element analysis (FEA). However, as 3D finite element analyses are time-consuming, the p-y curves are still used for large diameter piles.

3.9 The influence of vertical load on the lateral response in clay

The vertical and horizontal behaviour for piles is today most often analysed separately. Similar to the p-y curves for pure lateral loading of piles, the vertical displacement is characterised by t-z curves for vertical loading. Both the p-y and t-z curves are uncoupled, and therefore the soil reactions in the one direction are considered uncoupled from the other direction, and interaction effects are neglected.

As the vertical load is most often small compared to the vertical capacity, the lateral capacity is most often governing in design. Some studies have been conducted to investigate the effect the static vertical and lateral loading on the lateral pile response. Anagnostopoulos and Georgiadis (1993), Hazzar, Hussien, and Karray (2017) and Karthigeyan, Ramakrishna, and Rajagopal (2007) have investigated this effect, and their results will be discussed.

3.9.1 Existing studies

Anagnostopoulos and Georgiadis (1993) investigated effects of lateral loading on axial pile displacement and stresses experimentally, and the effects of axial loading on lateral pile response. Six model tests were performed on close-ended piles with a diameter of 19mm, a wall thickness of 1.5mm, and a length of 500mm. This results in a slenderness ratio of $L/D = 26$. The soil tested was soft laboratory-prepared clay, with $s_u = 28 kN/m^2$. The findings from the study concluded with a rather limited effect of axial loading on the lateral pile response. Nevertheless, conventional methods assume no interaction between the axial and lateral load, and the methods are, therefore, not able to capture the interaction between the axial and lateral pile response. Based on the study, a non-linear three-dimensional finite element method is recommended for analysing the effect of the combined vertical and lateral loads.

Karthigeyan et al. (2007) investigated the effect of piles subjected to both vertical and lateral loads through a series of 3D finite element analyses. The pile was modelled as a linear elastic material with a varying square cross-section. The Von Mises constitutive model with associated flow rule was used for analysing homogeneous clayey soil profiles. For clayey soils, the effect of vertical loads on the lateral capacity was marginally reduced for piles with up to 60% of the vertical capacity utilised. For higher vertical loads the lateral capacities were reduced by as much as 20%. The effect of the pile slenderness ratio was also investigated by increasing the length of the pile. The results indicate that the effect of vertical load decreases for increasing slenderness ratio. For slenderness ratios larger than $L/D = 16$, the influence of vertical load was found to be constant, and the effect of vertical loads was found to be limited. For longer piles, the reduction in lateral capacity can be expected to decrease. The findings from the study highlight the importance of the effect of vertical load on the lateral response.

Hazzar et al. (2017) analysed the influence of vertical loads on the lateral pile response through a series of 3D finite differences analyses. The lateral capacities and bending moments were evaluated. The models were verified with full-scale load and laboratory model testing data. The soil was idealised with the Mohr-Coulomb constitutive model with a non-associated flow rule. Three clayey soil profiles were analysed, one with a varying shear modulus, $G = 300s_u$, one with a constant shear modulus, $G = 38.5MPa$, and one with two-layered strata. Several cases with different undrained shear strength, s_u, were considered for the clayey soil profile with a varying shear modulus. For an undrained shear strength below $s_u < 16kPa$, there was no effect of vertical load on the lateral response. Furthermore, the model with a constant undrained shear strength was compared to a model with increasing undrained shear strength. The results indicate a significant difference in lateral load-deflection between the two models, and the study indicates that the lateral load-deflection is depending on the variation of the undrained shear strength with depth. The study also indicates that for layered soil, the lateral load-deflection depends on both the characteristics of the soil surrounding the pile and the soil beneath the pile tip. The findings from the study indicate a reduced lateral capacity due vertical loading, compared to pure lateral loading in clayey soils. Based on the findings from the study, Hazzar et al. (2017) state that it is unconservative to assume no interaction between vertical and lateral loads for the design of piles installed in clay.

The studies mentioned above emphasise the importance of analysing the effect of vertical load on the lateral response. Piles installed for offshore wind turbines are exposed both vertical and lateral load simultaneously. The static vertical load originates from the self-weight of the turbine and foundation, and lateral loads from large wind and wave forces. As a possible reduction in the lateral capacity in clayey soil will affect the design capacity of the pile, the effect of vertical loading on the lateral response should be investigated further as there is limited research on the subject. The possibility of proposing a correction factor to account for the effect of vertical loads on the lateral p-y curves will be investigated in this study.

3.10 Vertical capacity

The vertical capacity is necessary to investigate the effect on the lateral response. The theory used for calculating the static bearing capacity of friction piles in total stress analysis is presented in this section. The theory is based on Nordal et al. (2016).

Figure 3.9 illustrates the forces acting on a pile for vertical static loading.

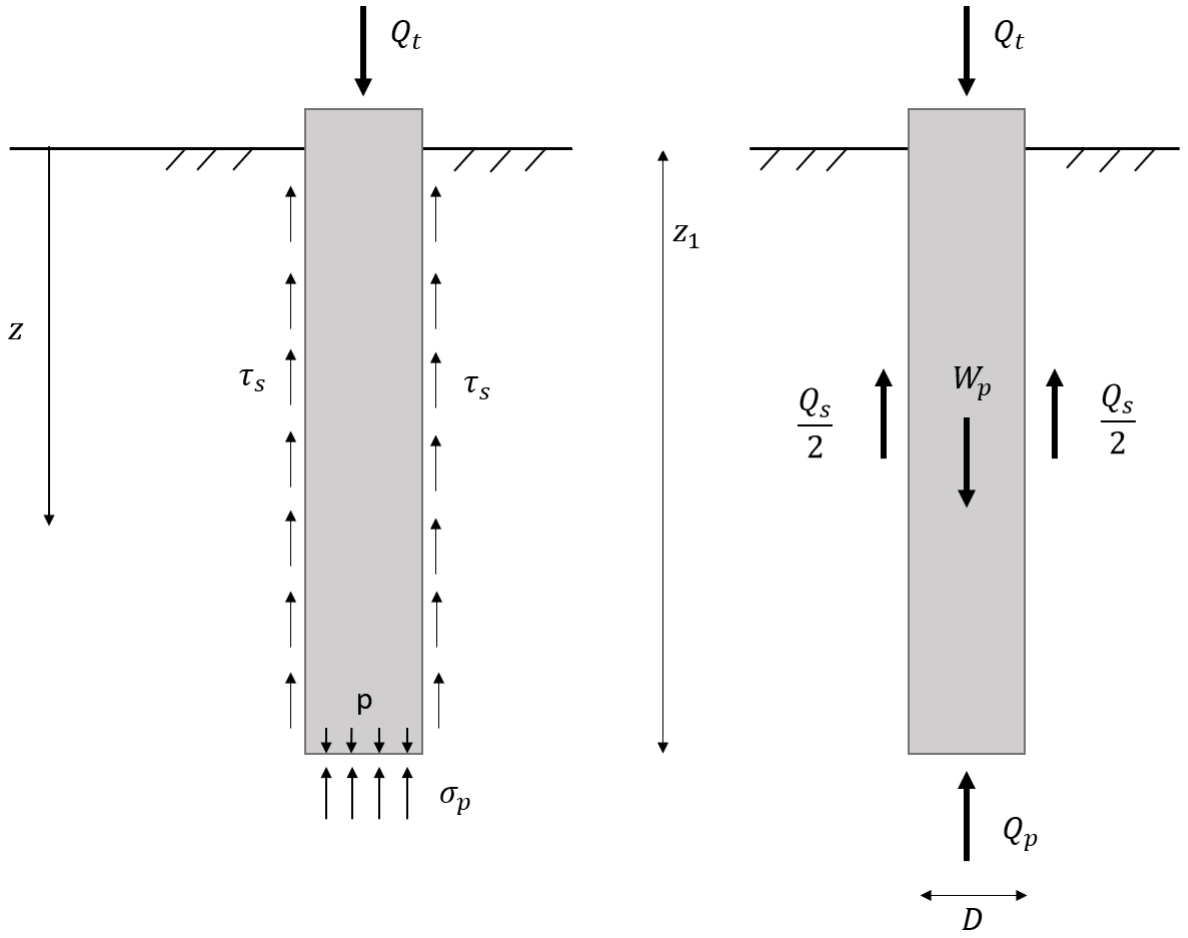

Figure 3.9: Bearing capacity of a pile, edited after Nordal et al. (2016)

The equation for the bearing capacity is derived based on vertical equilibrium,

$$Q_t = Q_p + Q_s - W_p \tag{3.12}$$

where W_p is the weight of the pile, Q_t, Q_p and Q_s is the vertical force at the pile head, the mobilised tip resistance, and the mobilised side friction respectively. As the unit weight of soils is about $\gamma \approx 20kN/m^3$, and the unit weight of concrete is about $\gamma \approx 24-25kN/m^3$, the net point resistance Q_{pn} is introduced. Assuming that the weight of the pile is approximately equal to an equivalent soil column, introducing $Q_{pn} = Q_p - W_p$ in equation 3.12, the bearing

capacity is given by,

$$Q_t = Q_{pn} + Q_s \tag{3.13}$$

Shaft friction

The shaft friction is estimated from classical earth pressure conditions. The mobilised shaft friction, Q_s, is given by,

$$Q_s = \int_{z=0}^{z=z_1} \tau_s o dz \tag{3.14}$$

where τ_s is the shear stress acting along the pile shaft at depth z from the surface, o is the periphery of the cross-section of the pile, and z_1 is the length of the pile below the surface. The shear stress acting along the pile shaft is given by,

$$\tau_s = r_s \tau_c \tag{3.15}$$

where τ_c is the critical shear stress in the soil at depth z, and r_s is a factor varying between $r_s = 0.3$ and $r_s = 1$, depending on the roughness ratio of the soil-pile interaction, and remoulding due to pile driving and following re-consolidation (Nordal et al., 2016). The shaft friction is illustrated in Figure 3.9, where the shaft friction is illustrated on both sides of the pile, $\frac{Q_s}{2}$, to illustrate that Q_s is the resulting force from shear stresses along the periphery of the cross-section of the pile.

Failure criterion on total stress basis

The shear strength on a total stress basis is relevant for a short-term loading condition. The short-term loading induces a sudden change in the total mean stress condition, causing an instant change in the pore pressure.

Assuming an idealised model of soil behaviour, the shear strength of the material is not considered to be influenced by the short-term changes in the mean stresses in the soil. As a result, the shear strength of the soil material is independent of the mean stress change.

The failure criterion is defined by the maximum shear stress in the soil material reaches a critical value. The yielding criterion can hence be written,

$$\tau_{max} = \frac{\sigma_1 - \sigma_3}{2} = \tau_c = s_u \tag{3.16}$$

This failure criterion was first proposed by Henri Tresca in 1864 and hence is referred to as the Tresca-criterion. The failure criterion is drawn in a Mohr-diagram and the corresponding critical failure element in Figure 3.10.

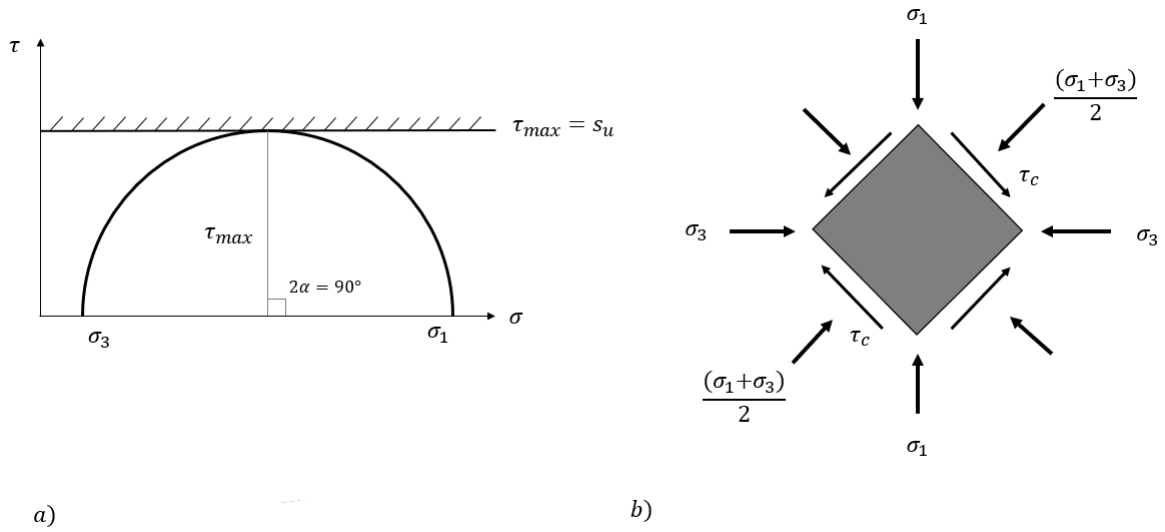

Figure 3.10: a) Yield criterion on total stress basis, b) critical failure element in the soil, edited after Nordal et al. (2016)

where τ_c is the critical shear stress in the soil material, and σ_1 and σ_3 are the major and minor principal stresses. The failure criterion is as shown depending on the maximum limiting shear stress, defined by the undrained shear strength of the soil material. For a soil element on the failure envelope, this is equal to the maximum radius in the Mohr circle. As illustrated on the figure, the maximum shear stresses and the principal stresses are acting along planes with an angle 45° in relation to each other.

Tip resistance of a deep foundation

The tip resistance is calculated based on the bearing capacity for a deep foundation. The equation governing the net tip resistance, Q_{pn}, is given by,

$$Q_{pn} = A_p \sigma_{pn} = A_p N_c \tau_c = A_p N_c s_u \tag{3.17}$$

where σ_{pn} is the net tip resistance represented by $\sigma_{pn} = \sigma_p - p$, and σ_p is the total vertical stresses at the tip of the pile, p is the weight of the soil, and A_p is the cross-sectional area of the pile tip. N_c is the bearing capacity factor.

Bearing capacity factor N_c

The bearing capacity factor is depending on the mechanical properties of the soil and the physical characteristics of the foundation. For a total stress analysis in a cohesive soil, a commonly used bearing capacity factor for deep quadratic foundations is $N_c = 9$ (M. Randolph & Gourvenec, 2011).

3.11 Numerical modelling

The three-dimensional finite element program Plaxis 3D has been used in this study. Plaxis 3D is a program developed for analysing deformation, stability and groundwater flow in geotechnical engineering (Brinkgreve, 2019). The program is a part of the PLAXIS product range, used for geotechnical engineering and design all around the world. It provides a fast generation of complex finite element models, and the computational results are presented by output facilities.

In Plaxis 3D, basis soil and structural elements are represented by 10-node tetrahedral elements and 6-node triangular elements, respectively. Figure 3.11a and 3.11b illustrate a 10-node and 6 node element. The nodes are represented by circles with local numbering, and the crosses represent the integration points. The soil behaviour is simulated by built-in soil models. The soil volume elements are numerically integrated using 4-point Gaussian integration. The nodes in each soil element have three translational degrees of freedom, u_x, u_y and u_z.

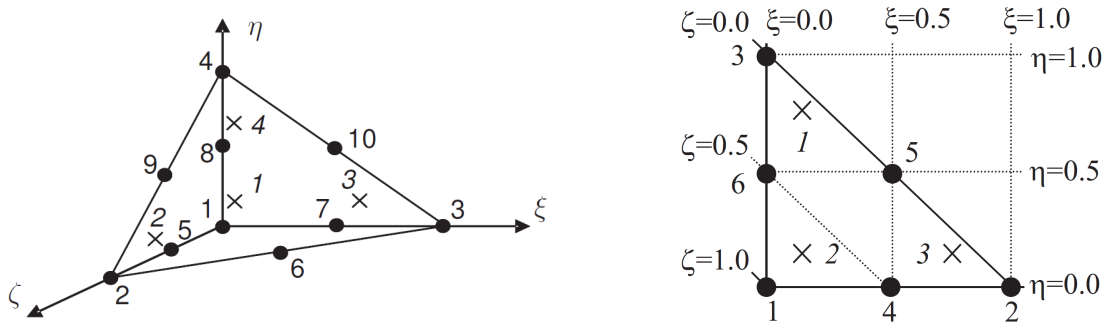

(a) A 10-node tetrahedral element

(b) A 6-node triangular element

Figure 3.11: Elements used for soil volume elements and for structural elements in Plaxis 3D, (Brinkgreve, 2019)

The finite element method (FEM) is a method of discretising a continuum domain into finite elements. The physical domain is represented by the number of elements used in the model, where the accuracy of the solution depends on the discretisation. Mesh refinement will improve the solution, and with enough iterations, the solution will converge towards a particular result.

Even though mesh refinement will improve the result and give a converge value, some situations might occur where the result does not converge. One of these situations is when stress singularities occur. A stress singularity is a point in the finite element model where the stress does not converge towards a particular value. The effect of stress singularities on the uniform stress field are local disturbances that remain local. This follows from St. Venant's Principle (Bell, 2014). Hence, stress singularities will not affect the solution away from the location of the singularity. Stress singularities may occur due to a point load, or corners of bodies or structures in contact.

In Plaxis 3D, the soil-structure interactions are modelled with interface elements to avoid stress singularities occurring in the contact area between the soil and structure. This is explained in the next section.

3.11.1 Soil-structure interaction

The soil-structure interaction is modelled by structural interface elements. The interface allows the soil and structure to move independently of each other by creating node pairs instead of single nodes. Figure 3.12 illustrates the soil-structure interaction with an interface and without an interface. The interaction between the nodes is represented by elastic-perfectly plastic springs. Each node has three translational degrees of freedom, (u_x, u_y, u_z), to model the gap and slip displacement between the soil and the structure(Brinkgreve, 2019).

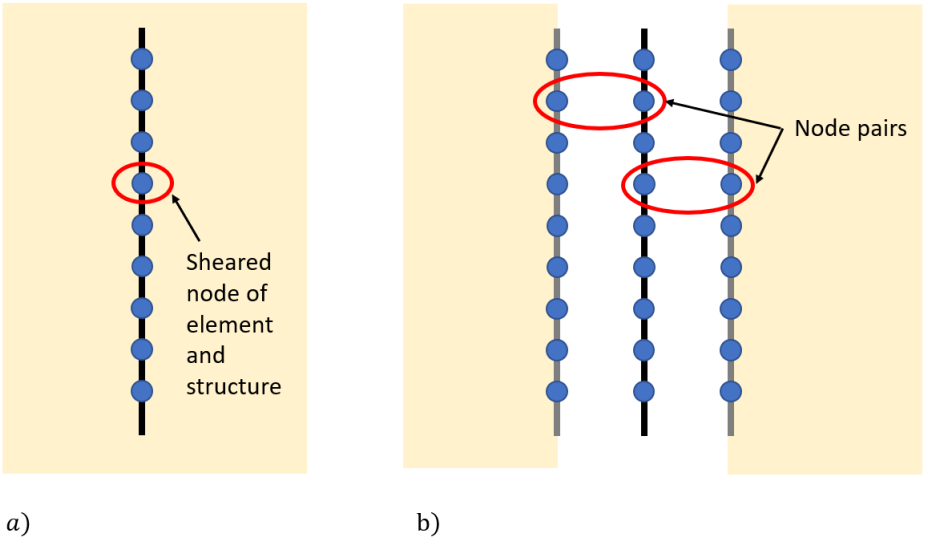

Figure 3.12: a) Plate element without an interface, b) Plate element with an interface, edited after *Plaxis | Modelling soil-structure interaction: interfaces* (2012)

Chapter 4

Methodology and finite element model

4.1 Introduction

The purpose of this study is to evaluate the effect of vertical loading on the lateral pile response. A series of three-dimensional the finite element analyses of the full length of the pile are performed in Plaxis 3D. The methodology and the finite element model are explained in this chapter. As installed monopiles for offshore wind turbines today are continuing to increase in size, low slenderness ratios were chosen to evaluate the effect of vertical loading on the lateral response.

4.2 Scripting

Plaxis 3D provides a fast generation of complex finite element models with a range of user-friendly drawing tools. A parametric study is performed on the lateral response with simultaneous vertical and lateral loads with the aid of Python scripting. A benefit of using Python scripting is the stepwise construction of the finite element model in a script with the possibility of fast generation of new models changing parameters of interest. The necessary Python components are automatically installed with the PLAXIS software. The text editor provided by default is SciTe but can be done with the text editor of choice. In this study, the scripting was done through the Scientific Python Development Environment (SPYDER). Spyder is a scientific environment with the possibility of advanced editing, analysis, and debugging (Spyder, 2020).

The results are extracted with Spyder and presented through the numerical computer program Matlab. Compared to using the drawing tools available in Plaxis 3D, with scripting, it is possible to show the process of creating the finite element model through the script. Appendix D presents example scripts from Spyder, for creating the models in this study in Plaxis 3D.

4.3 The Finite Element Model

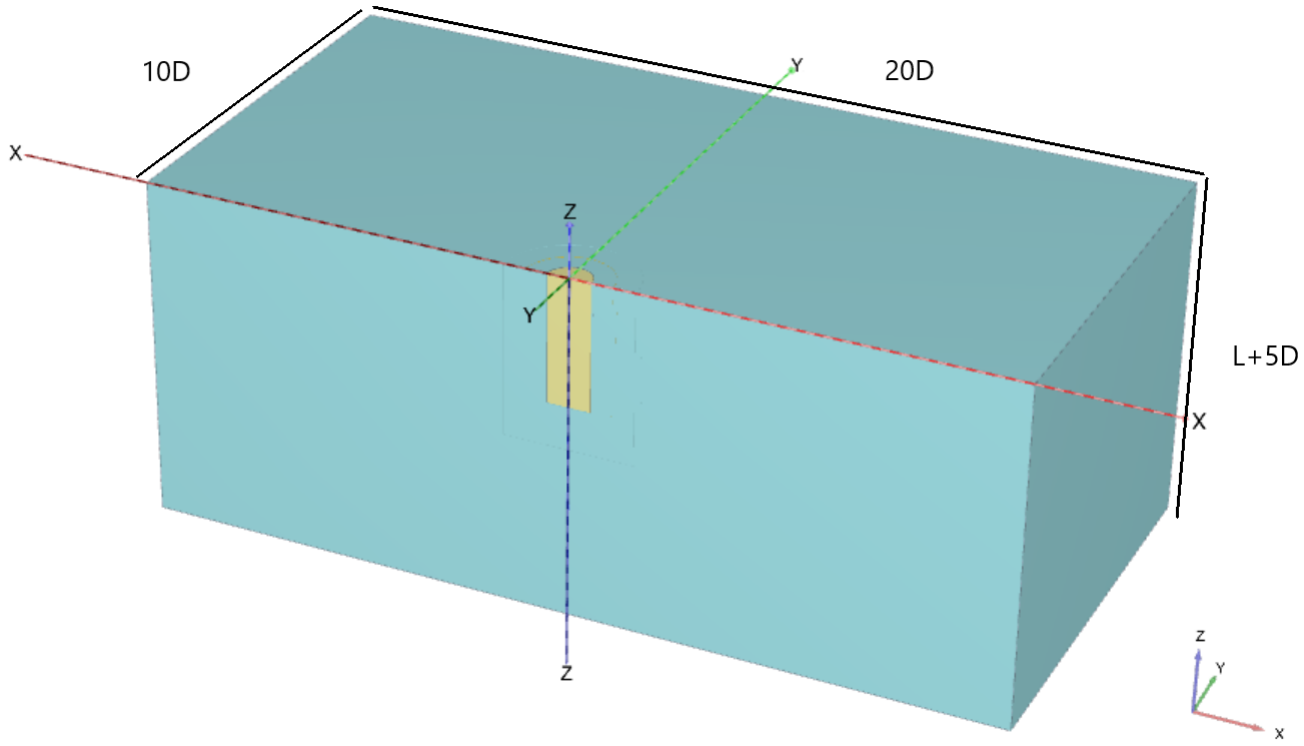

Figure 4.1: The 3D finite element model in Plaxis 3D

4.3.1 Pile

The 3D finite element model of the full length of the pile is presented in Figure 4.1. The surface of the model is representing the seabed. The pile is modelled from the surface of the model, with a circular cross-section with diameter D=5 m and a length L=15 m, resulting in a non-slender pile with a slenderness ratio of $L/D = 3$. Due to symmetry, only half of the pile is modelled in Plaxis 3D. In Table 4.1 the pile properties used in the analyses are presented. The pile is modelled as a non-porous linear elastic material with properties typical for steel material. For simplicity, the unit weight of the pile is equal to the unit weight of the soil. Further, as the FE model is to be used for creating a pile slice later in this study, representing a rigid body motion with plane strain flow-around soil failure mechanism, the pile is modelled as a full volume pile. The lateral response of the pile is analysed by the force-deflection response of the pile. If p-y curves were to be derived from the full length of the pile, an equivalent Young's modulus would be required to account for the effect of an open-ended pile. However, this is not done in this study.

The vertical capacity calculated based on this volumetric pile will over-estimate the actual vertical capacity of an open-ended pile, due to the base resistance. As the purpose of the full model is to evaluate the relative effect of vertical loading on the lateral response, a full volume pile is considered sufficient for this study.

Table 4.1: The pile properties

Linear elastic model		Pile
Unit weight of the pile [kN/m^3]	γ	20
Young's modulus [kPa]	E_{ref}	200e6
Poisson's ratio [-]	ν	0.3
Drainage type		Non-porous

4.3.2 Boundary conditions

From the centre of the pile, the lateral extent of the boundaries is selected to be 10 times in the lateral directions, as indicated in Figure 4.1. In the vertical direction, the boundary is the sum of the length of the pile and 5 times the diameter of the pile. The bottom vertical boundary is fully fixed, and all other boundaries in the model are modelled as normally fixed.

4.3.3 Soil

The soil material is represented with the Hardening Soil (HS) model. The HS model is a built-in soil model available in Plaxis 3D. It is an advanced model for simulating soil behaviour. The model is an elasto-plastic model with isotropic hardening connected to plastic yield surfaces. The soil stiffness is described by the triaxial stiffness E_{50}, the triaxial unloading stiffness E_{ur} and the oedometer loading stiffness E_{oed}. The model accounts for the stress-dependency of stiffness moduli, which means that the stiffness increase with pressure (Brinkgreve, 2019). As a total stress analysis is done, the yielding criteria is governed by the Tresca yield criterion, defined by the undrained shear strength of the soil.

An isotropic initial stress condition is modelled, with a homogeneous soil volume. Table 4.2 presents the soil parameters used in this study, representing typical values for a clayey soil profile. The drainage type used for the model is Undrained (B).

Table 4.2: The soil parameters for the HS model

Hardening Soil (HS) model		Clay
(Effective) cohesion [kPa]	c_u	60
Unit weight of the soil [kN/m^3]	γ	20
Secant stiffness in standard drained triaxial test [kPa]	E_{50}^{ref}	20 000
Tangent stiffness for primary oedometer loading [kPa]	E_{oed}^{ref}	20 000
unloading / reloading stiffness from drained triaxial test [kPa]	E_{ur}^{ref}	60 000
Power for stress-level dependency of stiffness [-]	m	1
(Effective) angle of internal friction [°]	ϕ'	0
Angle of dilatancy [°]	ψ	0
Drainage Type		Undrained (B)
Tension cut-off		x
Tensile strength	[kN/m^2]	0.00
Overconsolidation ratio	OCR	1

The soil-structure interaction is modelled with an interface surrounding the pile with 1 m extension at the bottom

of the pile, with an interface roughness factor $R_{inter} = 1$. The interface has the same strength properties as the adjacent soil, and no slipping is possible between the soil and pile. Hence the pile is considered as fully rough.

Tension cut-off

The allowable tensile stresses in the soil are controlled by tension cut-off. In reality, soil can not sustain any tensile stresses, if only very small tensile stresses (Brinkgreve, 2019). For vertical loading applied as compression, this would not be an issue. However, for lateral loading, tensile stresses will occur in the soil, and the tension cut-off, with a tensile strength of zero, controls that no tensile stresses occur in the soil. In reality, as the pile is loaded laterally, tensile stresses will occur both in front of the pile and at the back of the pile. This is illustrated in Figure 4.2.

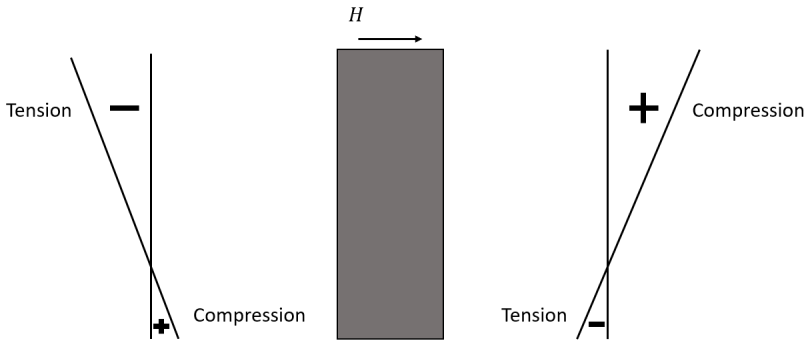

Figure 4.2: Illustration of the forces acting on the surrounding soil of a laterally loaded pile

During lateral loading, the soil in front of the pile, above the point of rotation, will experience compression as the load is transferred to the soil. Below the point of rotation, the rotation of the pile will induce tension forces in the soil as the pile is pushed in the opposite direction. At the back of the pile, the opposite response will occur in the soil. The tension occurring in front of the pile is not an issue, as there is no way the soil can make an opening. The tensile stresses at the back of the pile, on the other hand, will prevent the soil from making a gap opening. It should be noted that with the non-linear behaviour of the soil, the tension and compression forces as illustrated in Figure 4.2, is depending on the strength profile of the soil layers and that the illustration is only representing one possible case.

The correct way of modelling this behaviour would be to model a soil-structure interface at the front of the pile with no tension cut-off, to allow for the tensile stresses in front of the pile, and in the back of the pile, the tension cut-off is activated to allow for an opening in the soil. This is illustrated in Figure 4.3. The effect of creating two interfaces to allow for tensile stresses in front of the pile is tested. It is tested by creating a model with two interfaces, one with tension cut-off activated and one without tension cut-off.

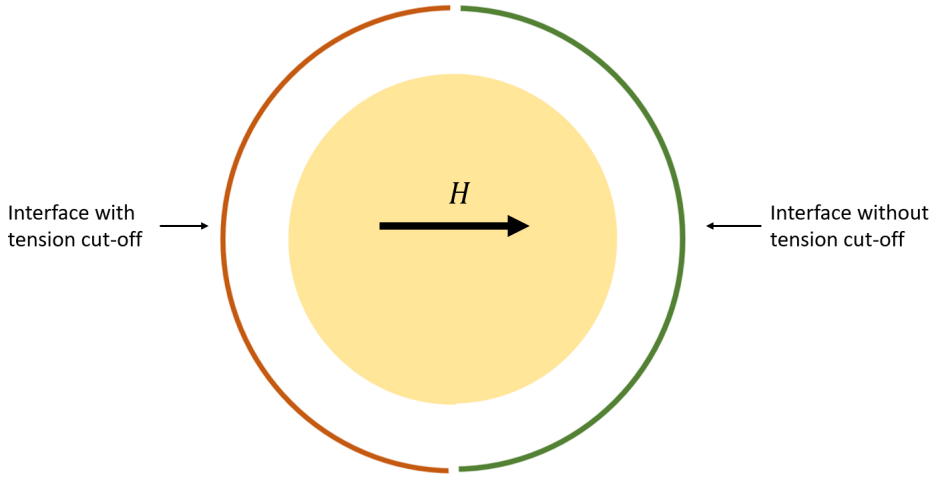

Figure 4.3: Illustration of modelling a pile with two different interfaces to control tension cut-off

4.3.4 Mesh Details

The finite element mesh used generates 70 309 soil elements. A refined mesh is used in one diameter in all directions outside the pile, and coarser mesh used in the soil outside. The coarseness factors used are 0.1 and 1. The purpose of using a coarser mesh is to save the computational time. The mesh refinement would be of importance if a safety factor were to be provided.

If a safety factor were to be provided, a scaling factor is necessary to give accurate vertical capacity. One possible consequence is numerical overshooting, resulting in a too high calculated vertical capacity, followed by applying a to high vertical load in relation to the vertical capacity. This would also result in a numerical overshoot of the lateral capacity. However, as the focus is on the relative effect on the lateral capacity, no scaling factor is considered necessary in this study.

4.4 Methodology in Plaxis 3D

The pile is modelled with a surface at the top of the pile, with the vertical static load is applied as constant surface pressure, σ_z, on top of the pile, whereas the lateral load is applied as a prescribed displacement at the surface of the pile head. The benefit of using a prescribed displacement instead of a load is that the force and displacement can be extracted directly from the output in Plaxis 3D. The calculation stages are divided into phases, calculated with the Plastic analysis, Stage construction. As the purpose is to analyse the effect of the combined vertical and lateral load on the lateral response, a node at the top of the pile is used to investigate the lateral deflection. The force and displacement of the pile are extracted from this node, at the centre of the pile head.

First vertical capacity analyses are performed. The vertical capacity is found by applying a vertical surface load at the pile head and loading until failure. The procedure for calculating the vertical capacity in Plaxis 3D is

further presented in Appendix A. After the vertical capacity analyses, the results are compared to theory. The pile is modelled as fully rough, and the factor r_s is set to a value of $r_s = 1$. In Plaxis 3D, a higher bearing capacity factor than the recommended value of $N_c = 9$, might occur due to the mesh refinement used. Therefore, the theoretical capacities are given as a range, with a lower limit with $N_c = 9$, and an upper limit with $N_c = 12$ is chosen. The results obtained through FEA are compared to the theoretical lower and upper limit for verification.

From the vertical capacity analyses, vertical loads equal to 20%, 40%, 60% and 80% of the vertical capacity is applied to the FE models prior to loading the pile laterally. Loads are chosen up to the value of 80% of the capacity as a vertical load equal to 100% will indicate failure of the pile, and no lateral loading can be applied. The models with combined vertical and lateral loads are then compared to a case of pure lateral loading.

In Plaxis 3D, the construction stages of a finite element model are defined by calculation phases. The calculation phases used for creating the finite element model presented in this chapter is listed below,

- **Phase 0**: Initial phase, the K0 calculation procedure is used to calculate the initial stress state of the soil material.
- **Phase 1**: Installation of the pile, the pile and interfaces are activated.
- **Phase 2**: Vertical loading, a vertical load is activated.
- **Phase 3**: Resetting displacements.
- **Phase 4**: Lateral loading, introduced in the model as prescribed lateral displacements.

The script used for creating the full model is presented in Appendix D.1.

4.4.1 Parametric study

A parametric study was performed to investigate which parameters affect the lateral response with combined vertical and lateral loading. A constant vertical load, corresponding to 20%, 40%, 60%, 80% of the vertical capacity, was applied at the top of the pile for each model and compare to a case with pure lateral loading. The parameters investigated are listed below.

- Effect of undrained shear strength,

$$s_u \text{ [kPa]: } 20, 40, 60, 80, 100$$

- Effect of increasing undrained shear strength.
- Effect of L/D -ratio,

$$L/D : 3, 5, 10, 15$$

Chapter 5

Effect of axial load on the lateral response

In this chapter, the results from the FE model described in Chapter 4 will be presented and discussed. The results will be compared to theoretical solutions and existing studies.

5.1 Results

5.1.1 Vertical capacity analysis

A vertical capacity analysis was performed. The results are presented in Table 5.1. As the model only represents half of the pile, the result is multiplied by two. The theoretical range is given for a bearing capacity factor of $N_c = 9$ and $N_c = 12$, for a lower and upper limit.

Table 5.1: Vertical capacity

		Theoretical vertical capacity $[kN]$	
Model	Vertical capacity $[kN]$	Low	High
Clay $s_u = 60kPa$	26 691	24 740	28 274

As observed from the table, the vertical capacity calculated from FEA is in the range of the theoretical capacity given. The vertical capacity is derived based on the multiplier M_{stage} in Plaxis 3D. A converged value of M_{stage} is difficult to obtain, and the analyses done in this chapter ended before a converged value was reached. When the calculation ends in Plaxis 3D, failure of the soil body has occurred during the calculation. This could be due to high stresses occurring in some soil elements surrounding the pile. The bearing capacity is reduced by the compressibility of the material leading to local shear failure. This will result in the calculation ends before the pile actually fails. The vertical capacity calculated by Plaxis 3D is resulting in the same side friction of the pile as theoretical solutions, as this is calculated based on the shear strength of the soil material. The vertical capacity coming from base resistance, however, is in general over-estimating the capacity. Therefore a converged value is often difficult to obtain. One method to avoid this is to use a displacement criterion. At what displacement, is

the pile considered to be failed. However, in this analysis, the vertical capacity is calculated based on the capacity indicated by the stage construction calculation ending.

Given that the side friction is fully mobilised for the vertical capacity calculated, the bearing capacity factor is $N_c = 10.7$. Resulting in a 19% higher bearing capacity factor compared to the commonly used value of $N_c = 9$.

It should be noted that vertical loads of 20%, 40%, 60% and 80% of the vertical capacity indicated further in this study are calculated as explained in this section, and no displacement criteria were used.

5.1.2 Lateral pile deflection

The full length of the pile is modelled to evaluate the effect of vertical loading on the lateral deflection. As a capacity calculation is time-consuming, the results are presented for lateral deflection of 4% of the diameter, 0.04D, resulting in 200mm displacement. The purpose of this is to have a comparative result for the different parameters tested later in this chapter. This gives an indication of the reduced capacity but is not representing the ultimate lateral capacity. For further presentation in this chapter, the results will be referred to as capacities for this displacement.

After a vertical capacity analysis, vertical loads equal to 20%, 40%, 60%, and 80% of the vertical capacity were applied at the pile head. The lateral force-displacement for models with vertical loads are compared to a case of pure lateral loading. The results are presented in Figure 5.1. The vertical load applied is given as a part of the vertical capacity (Vc).

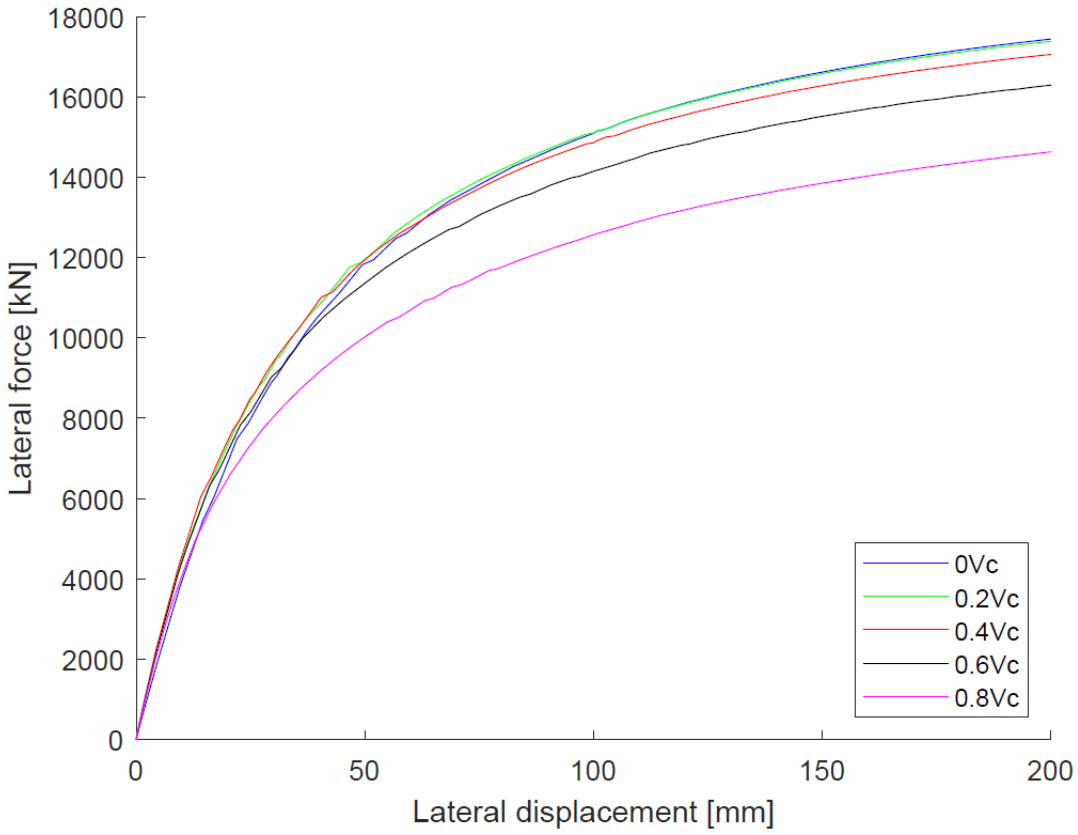

Figure 5.1: Lateral force - displacement

By studying the initial part of the pile deflection, it can be observed a higher initial stiffness for the models exposed to vertical loading. As this initial part of the lateral deflection curve is small, it is considered to have little consequence on the reached end capacity. Furthermore, it is observed a reduced lateral capacity with higher vertical loading compared to a case of pure lateral loading. The reduction in the lateral capacities for lateral deflection of 0.04D are calculated based on,

$$RLC = \frac{LC_{Vc} - LC}{LC} * 100\% \tag{5.1}$$

where RLC is the reduction in the lateral capacity, LC is the lateral capacity for pure lateral loading, and LC_{Vc} is the capacity with lateral loading. From this, the reduced capacities are presented,

$$Reduced\ lateral\ capacity = 100\% - RLC = \frac{LC_{Vc}}{LC} * 100\% \tag{5.2}$$

The reduced lateral capacities are presented in Table 5.2.

Table 5.2: The reduced lateral capacities for lateral deflection of 0.04D with combined vertical and lateral load

	Reduced lateral capacity [%]				
Model	0Vc	0.2Vc	0.4Vc	0.6Vc	0.8Vc
$s_u = 60kPa$	100	99.7	97.7	93.5	83.8

As can be observed from Table 5.2, for a vertical load of $0.2Vc$ and $0.4Vc$, the reduction in lateral capacity is marginal. The reduction from $0.4Vc$ to $0.6Vc$ is relatively small, and for a vertical load of $0.6Vc$, the lateral capacity is reduced by 6.5%. However, for a load of $0.8Vc$ the lateral capacity is reduced by 16.2%. This indicates a more significant effect for loads above $0.6Vc$.

The reduced lateral capacity for vertical loading is presented in Figure 5.2. It illustrates the larger effect of vertical loading above $0.6Vc$.

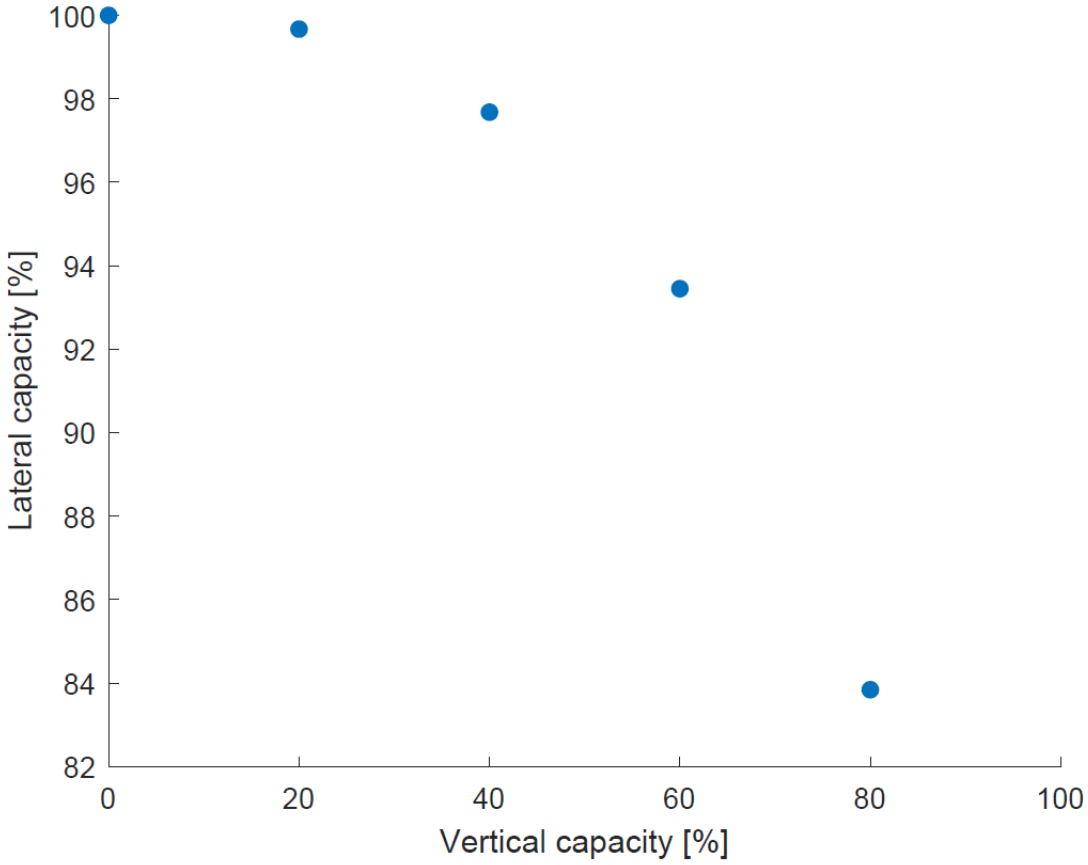

Figure 5.2: Reduced lateral capacity with vertical loading, for lateral deflection of 0.04D

Effect of tension cut-off

The effect of allowing tension to occur in the soil-structure interaction in front of the pile was tested. A model not allowing any tension, is compared to a model allowing tension to occur. As vertical loading is applied as compression, no tension will occur in the soil for vertical loading of the pile. Hence, this will only affect the lateral loading of the pile. Therefore, the models are compared for a case of pure lateral loading. The results are presented in Figure 5.3 and in Table 5.3.

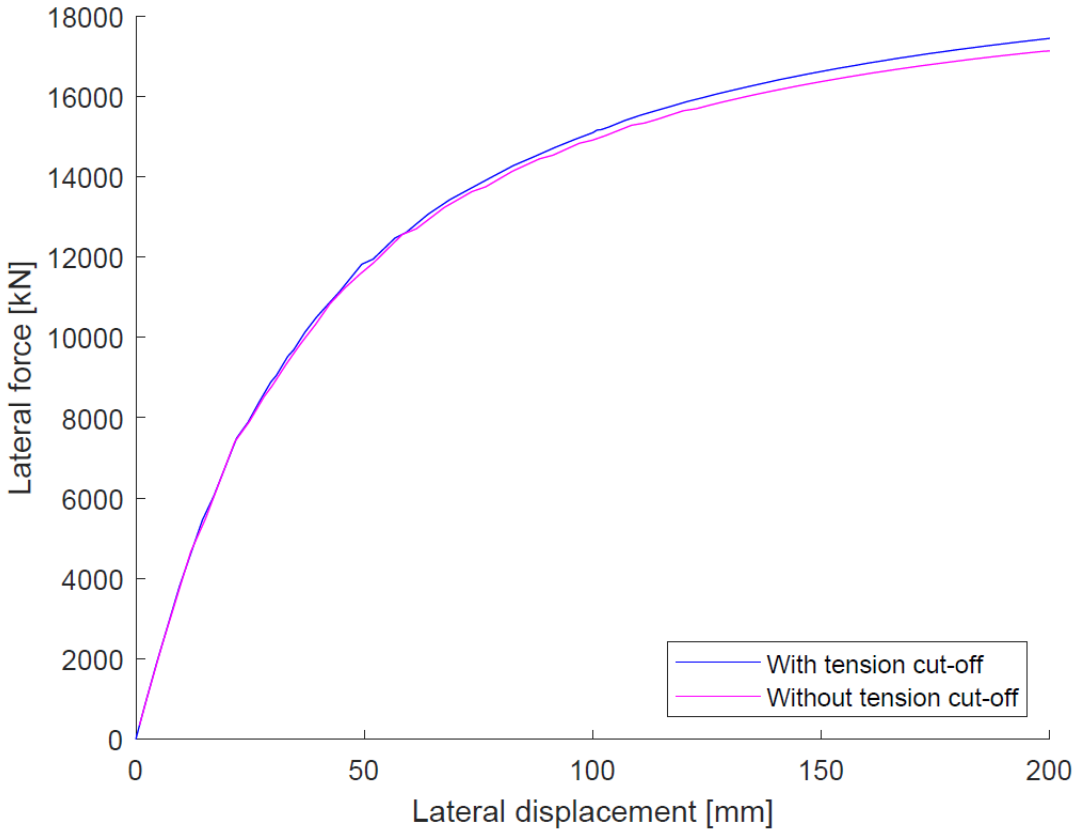

Figure 5.3: Comparison between lateral force-displacement for a pile with and without tension cut-off

Table 5.3: The lateral capacity for lateral deflection of 0.04D for pure lateral loading for evaluating the effect of tension cut-off

Model	Lateral capacity for lateral deflection of 0.04D
With tension cut-off	17 470 kN
Without tension cut-off	17 131 kN

As the results indicate, a marginal discrepancy of 2% is observed between the two models. Therefore, one interface, allowing no tension to occur in the soil, is used for further analyses as the purpose is to evaluate the relative effect of vertical loading on the lateral response.

5.2 Parametric study

5.2.1 Effect of undrained shear strength

Five models with different undrained shear strength s_u were analysed. The undrained shear strengths analysed were

$$s_u \text{ [kPa]} : 20, 40, 60, 80, 100$$

Vertical capacity calculations were performed, and the results are presented in Table 5.4 with the theoretical upper and lower limit. As can be observed from the results, the vertical capacities calculated from FEA is in the theoretical range given or close to it.

Table 5.4: The vertical capacities for the full model for different undrained shear strengths

		Theoretical vertical capacity [kN]	
Undrained shear strength	Vertical capacity [kN]	Low	High
$s_u = 20kPa$	9 631	8 247	9 425
$s_u = 40kPa$	18 146	16 493	18 850
$s_u = 60kPa$	26 691	24 740	28 274
$s_u = 80kPa$	35 103	32 987	37 699
$s_u = 100kPa$	43 345	41 233	47 124

The vertical capacity analyses were used to evaluate the effect of vertical load on the lateral capacities for 0.04D lateral deflection. The results are presented in Appendix B.1, and the reduced capacities are summarised in Table 5.5.

Table 5.5: The reduced lateral capacities for lateral deflection of 0.04D with combined vertical and lateral load for different undrained shear strengths

	Reduced lateral capacity [%]				
Undrained shear strength	0Vc	0.2Vc	0.4Vc	0.6Vc	0.8Vc
$s_u = 20kPa$	100	99.4	97.6	93.5	83.9
$s_u = 40kPa$	100	99.5	97.8	93.4	84.2
$s_u = 60kPa$	100	99.7	97.7	93.5	83.8
$s_u = 80kPa$	100	99.7	98.2	93.5	83.8
$s_u = 100kPa$	100	100	97.4	93.1	83.3

As can be observed from Table 5.5, the different undrained shear strengths indicate a similar reduction for vertical loading. The reduction in the lateral capacity is marginal for all models for vertical loads below 0.6Vc. A reduction of up to 1% and 2-3% is observed for vertical loading of 0.2Vc and 0.4Vc. For vertical loading of 0.6Vc and 0.8Vc, a reduction in the lateral capacity is observed of up to 6-7% and 16-17% respectively.

The lateral capacity calculation for the model with an undrained shear strength of $s_u = 20kPa$ for vertical loading of 0.8Vc ended before reaching a displacement of 0.04D. As a result, the lateral capacity for 0.8Vc is expected to be slightly higher. From the vertical capacity analysis, the vertical capacity calculated by FEA was above the theoretical range given, with a bearing capacity factor of $N_c = 12.5$. This results in slightly higher vertical loads applied to this model compared to the other models and could be the reason for the calculation in Plaxis ends before reaching the lateral deflection of 0.04D.

For the model with $s_u = 100kPa$ the lateral capacity given for vertical loading of 0.2Vc showed a higher capacity then for pure lateral loading. This is set in the table as 100%. This comes from the effect of the initial stiffness is slightly higher for vertical loading, and is affecting the result at the lateral deflection of 0.04D.

The results are presented in a scatter plot in Figure 5.4 to illustrate the reduced lateral capacities for vertical

loading. As can be observed from the scatter plot, the effect of vertical load on the lateral capacity shows a similar trend.

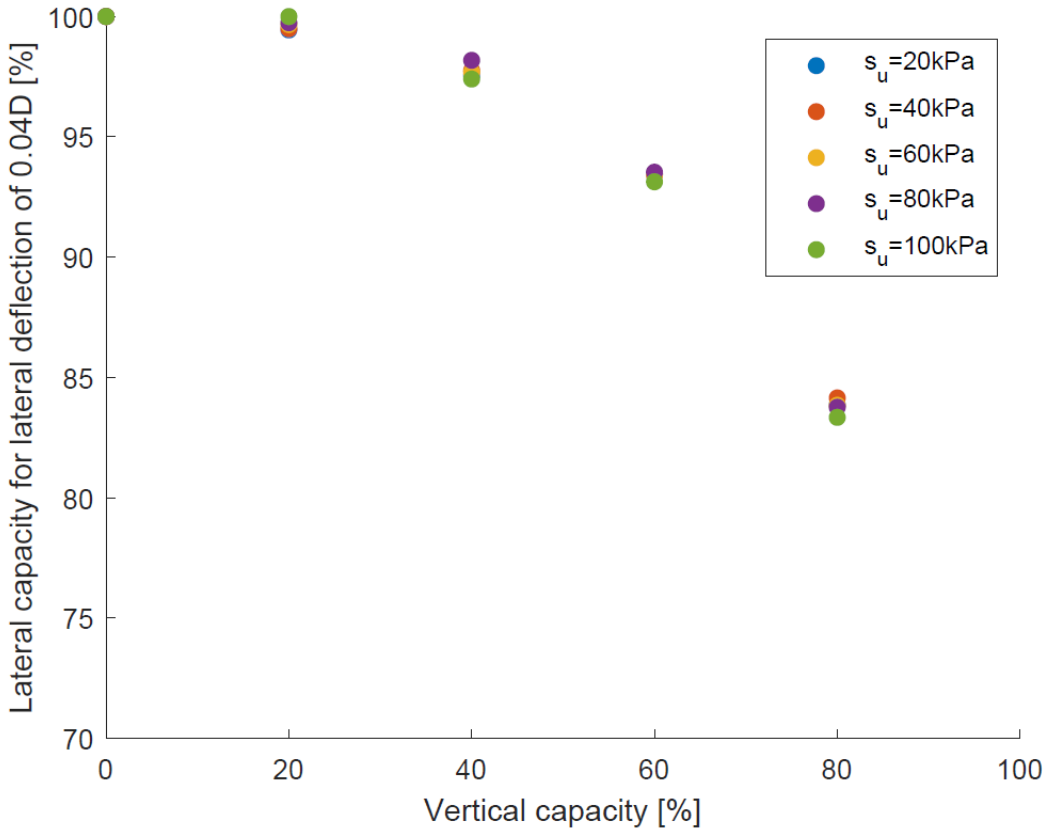

Figure 5.4: Reduced lateral capacity with vertical loading, for lateral deflection of 0.04D, for different undrained shear strengths

The results show a similar trend with only a marginal discrepancy for the different undrained shear strengths tested. Based on the FE analyses presented in this section, the effect of the vertical loading on the lateral response does not depend on the undrained shear strengths tested here.

5.2.2 Effect of increasing undrained shear strength

The undrained shear strength is, in reality, varying with depth. Assuming a constant undrained shear strength with depth was evaluated by considering a model with linearly increasing undrained shear strength with depth. A model with an increasing undrained shear strength of $s_u = 30kPa + 4kN/m^3 * z$, resulting in average shear strength of $s_{u,average} = 60kPa$, was compared to the model with a constant undrained shear strength of $s_u = 60kPa$. All other soil parameters used in the analysis were the same.

A vertical capacity analysis was done, and the results are presented in Table 5.6. The theoretical capacity is calculated based on an average undrained shear strength $s_{u,average} = 60kPa$ for the side friction and the base resistance is calculated based on the undrained shear strength at the pile tip, $s_{u,tip} = 90kPa$. As can be observed,

the capacity calculated is in the theoretical range.

Table 5.6: The vertical capacity for a model with an increasing undrained shear strength

		Theoretical vertical capacity [kN]	
Undrained shear strength	Vertical capacity [kN]	Low	High
$s_u = 30kPa + 4kN/m^3 * z$	32 936	30 041	35 343

Based on the vertical capacity analysis, vertical loads were applied at the pile head, to evaluate the lateral response for 0.04D lateral deflection. The results are presented in Table 5.7.

Table 5.7: The reduced lateral capacity for lateral deflection of 0.04D for a model with an increasing undrained shear strength

	Reduced lateral capacity [%]				
Undrained shear strength	0Vc	0.2Vc	0.4Vc	0.6Vc	0.8Vc
$s_u = 30kPa + 4kN/m^3 * z$	100	99.9	97.9	92.6	83.5

The results indicate a marginal response for the lateral loading below $0.6Vc$. For $0.6Vc$ and $0.8Vc$, the lateral capacity is reduced with 7.4% and 16.5% respectively. These results are similar to the model with a constant undrained shear strength of $s_u = 60kPa$. Based on these results, assuming a constant undrained shear strength with depth is not considered to affect the results.

5.2.3 Effect of L/D-ratio on the lateral capacity

The effect of the pile slenderness ratio was tested for four different L/D-ratios,

$$L/D: 3, 5, 10, 15$$

This was done by increasing the diameter of the pile, while the length of the pile remained constant. The lateral and vertical boundaries are changed in accordance with the model presented in Chapter 4, with 10D in the lateral directions and L+5D in the vertical direction.

As the cross-section change, the vertical capacity change. Vertical capacity analyses were performed, and the calculated vertical capacities are presented in Table 5.8, with the theoretical upper and lower limit.

Table 5.8: The vertical capacities for different slenderness ratio

		Theoretical vertical capacity	
Slenderness ratio	Vertical capacity [kN]	Low [kN]	High
$L/D = 3$	26 691	24 740	28 274
$L/D = 5$	12 886	12 299	13 572
$L/D = 10$	5 234	5 195	5 514
$L/D = 15$	3 221	3 252	3 393

As observed from the vertical capacity calculated based on FEA, for $L/D = 15$, it is below the theoretical range. Indicating that the calculation ended before the failure capacity was reached.

Based on the calculated vertical capacities, the effect of vertical loading on the lateral displacement is evaluated. The results are compared for a lateral displacement of 0.04D. The results are presented in Appendix B.3, and the reduced lateral capacities are summarised in Table 5.9.

Table 5.9: The reduced lateral capacities for lateral deflection of 0.04D with combined vertical and lateral loading for different L/D - ratios

	Reduced lateral capacity[%]				
Slenderness ratio	0Vc	0.2Vc	0.4Vc	0.6Vc	0.8Vc
$L/D = 3$	100	99.7	97.7	93.5	83.8
$L/D = 5$	100	99.9	98.6	95.1	85.5
$L/D = 10$	100	100	100	98.9	94.1
$L/D = 15$	100	100	100	100	99.2

As can be observed from Table 5.9, the effect of vertical loading on the lateral capacities decrease with higher L/D-ratio. For a slenderness ratio of $L/D = 5$, a reduction of 4.9% and 15% is observed for vertical loading of $0.6Vc$ and $0.8Vc$. This is a similar trend as observed for the pile with $L/D = 3$.

For slenderness ratios $L/D = 10$ and $L/D = 15$, a smaller effect is observed. For $L/D = 10$ the lateral capacity given for vertical loading of 0.2Vc and 0.4Vc showed a higher capacity then for pure lateral loading. The same is observed for $L/D = 15$ for vertical loads of 0.2Vc, 0.4Vc and 0.6Vc. This is set in the table as 100%. This comes from the effect of the initial stiffness is slightly higher for vertical loading, and for higher slenderness ratios the lateral force-displacement curves are observed to be further from a converged value for lateral deflection of 0.04D. In addition, from the vertical capacity calculations, for the model with $L/D = 15$, the vertical capacity calculated from FEA was not in the theoretical range, and it is expected a slightly higher vertical capacity for this model. This will affect the applied vertical loads and a slightly higher reduction in the lateral capacities for vertical loading then presented in the table above might be expected. Nevertheless, for vertical loading of 0.8Vc the reduced lateral capacity is 5.9% and 0.8% for $L/D = 10$ and $L/D = 15$, respectively. The results are presented in Figure 5.5 to illustrate the reduced lateral capacity with vertical loading.

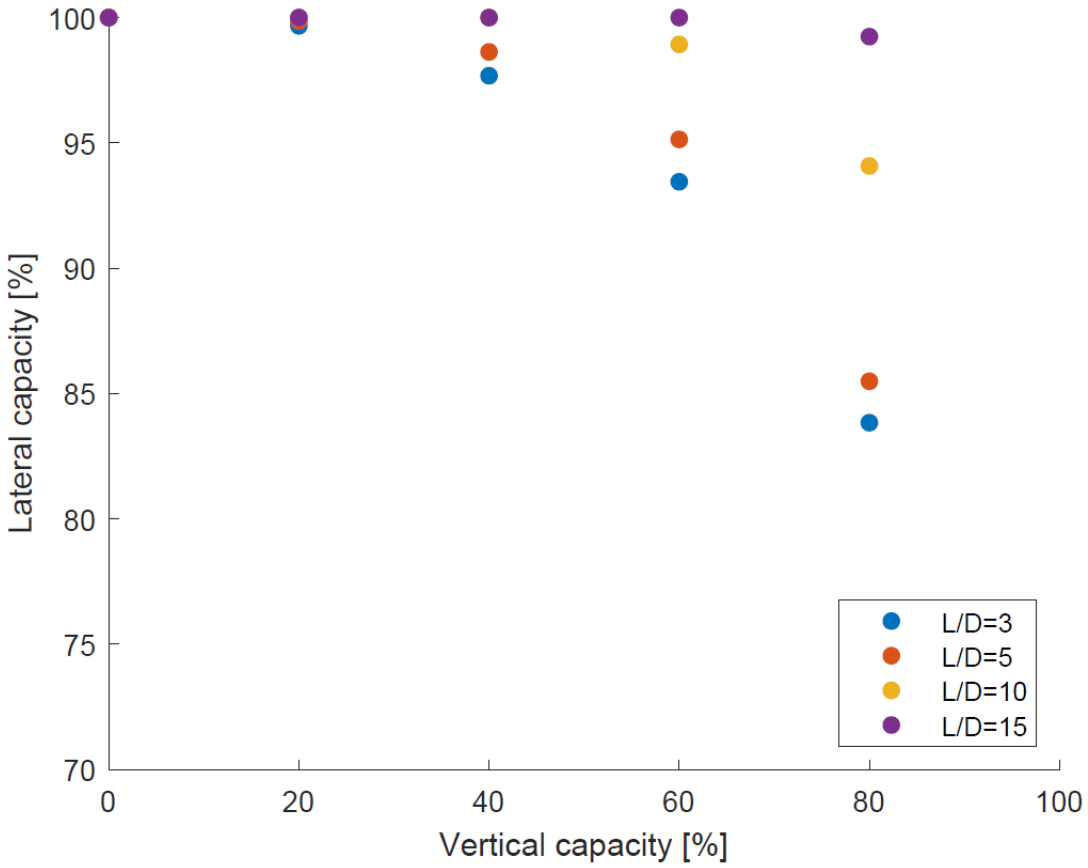

Figure 5.5: Reduced lateral capacity with vertical loading, for lateral deflection of 0.04D, for different slenderness ratios

From Figure 5.5 it is observed a similar trend for slenderness ratios of $L/D = 3$ and $L/D = 5$. For slenderness ratios of $L/D = 10$ and $L/D = 15$, a lower effect of vertical loading is observed. In Appendix B.3, the resulting graphs are presented. For the chosen lateral displacement of 0.04D, for higher slenderness ratios, the lateral force-displacement curves are further from a converged value. Due to numerical issues, the calculation phase in Plaxis ends before a converged value is reached. Therefore a larger effect might be observed for higher displacements. As it is not reaching a converged value, the lateral capacities for a fixed displacement of 0.04D are compared. The results indicate a lower effect of vertical loading for this displacement for higher slenderness ratios.

5.3 Discussion

Vertical capacity analyses

The vertical capacity calculations showed a deviation of up to 20% of the theoretical vertical capacity. A vertical capacity analysis is time-consuming, and a converged value is difficult to obtain with Plaxis 3D. Therefore, a displacement criterion is often used to define at what displacement the pile is considered to have failed. This is often

represented as a percentage of the pile diameter used in pile analyses. The ultimate vertical capacity coming from the pile base resistance might be mobilised after a high pile settlement. For this high pile settlement, the structure might already have suffered a catastrophic failure. Therefore, the vertical capacity is often defined by the mobilised resistance at an allowable settlement, such as 10% of the pile diameter (M. Randolph & Gourvenec, 2011). This was not done in this study. A consequence of this would be a slightly different estimated vertical capacity from the analyses done in this chapter. It affects the applied load in the analyses evaluating the effect of vertical loading on the lateral response. As the purpose of the analyses done in this chapter was to present the relative effect of vertical loading on the lateral pile behaviour for the full length of the pile, the small discrepancy in the applied vertical load compared to theoretical solutions is not considered to affect the results significantly.

Effect of slenderness ratio

The effect of the slenderness ratio on the reduction in the lateral capacities is evaluated by investigating the vertical load distribution with depth. The theoretical vertical capacity with the contribution from base and shaft resistance for the models with different slenderness ratio is compared. The theoretical capacities are calculated with a bearing capacity factor of $N_p = 9$, $r_s = 1$, for a 15m long pile, with soil unit weight equal to unit weight of pile and undrained shear strength of $s_u = 60kPa$. The results are presented in Table 5.10.

Table 5.10: Theoretical vertical capacity with contribution from the shaft and base resistance for different L/D-ratios

L/D - ratio	Shaft friction [kN]	Base resistance [kN]	Total vertical capacity [kN]
L/D = 3	14 137	10 603	24 740
L/D = 5	8 482	3 817	12 299
L/D = 10	4 241	954	5 195
L/D = 15	2 827	424	3 252

As can be observed from the table, for a slenderness ratio of $L/D = 3$, the contribution from base resistance is 42.9% of the vertical capacity. For increasing slenderness ratio, the contribution from base resistance decreases, and the vertical capacity is mainly coming from shaft friction.

In the output application of Plaxis 3D, it is possible to calculate the axial force distribution with depth. Volumetric forces in the pile volume are extracted through *Structural forces in volume piles*, and a centre line is created in the pile volume. The axial force along the length of the pile is then calculated. By evaluating the distribution of the axial load in the pile with depth from the FEA, the load taken by the side friction and base resistance in the models can be evaluated. The axial load distribution with depth for slenderness ratios of $L/D = 3$ and $L/D = 10$ is calculated. The purpose is to compare the vertical load distribution with depth. Figure 5.6 illustrates the axial load distribution with depth for 80% of the vertical capacity applied at the top of the pile. The axial force is normalised with the applied load.

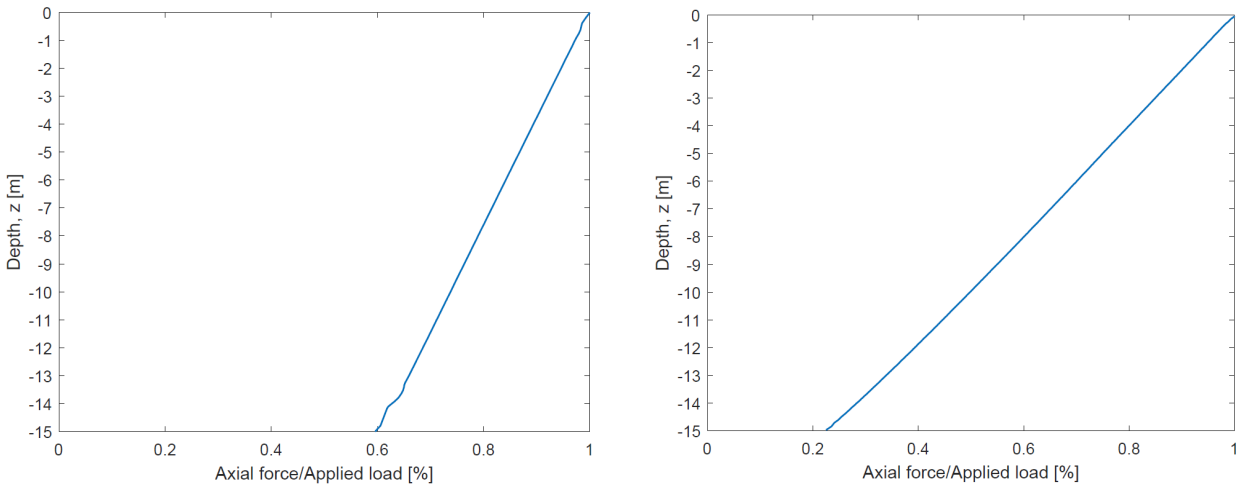

(a) $L/D = 3$ (b) $L/D = 10$

Figure 5.6: Normalised axial force distribution with depth in the pile

For a pile with a slenderness ratio of $L/D = 3$, the average axial load along the shaft is 81% of the applied load. However, for a pile with a slenderness ratio of $L/D = 10$, the average axial load along the shaft is 62% of the applied load. With higher axial load along the shaft, higher shear stresses in the surrounding soil are mobilised. Hence, the remaining capacity for lateral loading is reduced depending on the axial load along the shaft. This illustrates the more significant effect of the vertical load on the lateral capacities for piles with a lower pile slenderness ratio compared to the larger pile slenderness ratios.

5.3.1 Comparison to similar studies

Similar to findings reported by Hazzar et al. (2017), the capacity is reduced with vertical loading in clayey soil. Hazzar et al. (2017) also reported a s_u dependency, for lower s_u values, the reduced capacity was not that significant. However, in this study, the results did not show a dependency on s_u. A model with an undrained shear strength of $s_u = 10kPa$ was tested to confirm these results. The results are presented in Appendix B.4. The results show a similar decrease in lateral capacities due to vertical load to the analyses with higher undrained shear strength. However, for 0.8Vc, the lateral capacity was reduced by 10.09%. This is a smaller reduction then the other undrained shear strengths tested. Nevertheless, the reduction will affect the behaviour of the pile and should be taken into consideration. It should be noted, however, that Hazzar et al. (2017) tested for an increasing shear modulus of $G = 300s_u$. This was not studied here.

According to Karthigeyan et al. (2007), for piles installed in clayey soils, the effect of vertical loads on the lateral response is marginal for vertical loads up to 60% of the vertical capacity. However, for higher vertical loads, the lateral capacity is reduced as much as 20% for lateral displacement of 0.1D. The slenderness ratios tested in the study were down to $L/D = 8.3$. In this study, a pile with a slenderness ratio of $L/D = 3$ resulted in a reduction up to 17% for loads above 60% of the vertical capacity for lateral displacement of 0.04D. The analyses in this chapter was only performed for lateral displacements of 0.04D, and hence higher reductions might also have been observed if

the analyses were done for larger lateral displacements. Furthermore, Karthigeyan et al. (2007) suggested that the effect of vertical load on the lateral response on L/D-ratios above 16 is marginal and constant. As observed from analysing the effect of the pile slenderness ratio, for a pile with a slenderness ratio of $L/D = 15$ for 0.04D lateral displacement, it was observed a minimal effect of vertical loading. The analyses showed a decreasing effect of vertical load on the lateral response, similar to results reported by Karthigeyan et al. (2007).

Anagnostopoulos and Georgiadis (1993) reported a limited effect of vertical loading on the lateral pile behaviour. They studied a pile with a slenderness ratio of $L/D = 26$. As illustrated in this study, the effect of vertical loading on the lateral response is marginal for higher slenderness ratios. This might be the reason for the limited effect observed by the laboratory investigations reported by Anagnostopoulos and Georgiadis (1993).

Chapter 6

Deriving p-y curves from 3D slice models

6.1 Introduction

The p-y curves are derived from discretising the pile into a number of structural elements. The failure mechanism occurring in the soil during lateral loading of the pile is divided into wedge failure mechanism and flow-around failure mechanism. The plane strain flow-around failure mechanism can be modelled in Plaxis 3D by modelling only a slice of the pile. The pile elements are then represented by a slice with 1 m thickness. The pile is moved horizontally as a rigid body in the slice, and the p-y curves can be calculated with the soil resistance and displacement. The boundary conditions of the slice are preventing vertical movement, inducing a plane-strain condition and no breakaway of the soil is possible. Therefore, this method is only valid for the part of the pile where the horizontal flow-around failure mechanism is governed. A great benefit of creating a slice is the reduced calculation time compared to modelling the full length of the pile. Figure 6.1 illustrates a slice modelled in Plaxis 3D.

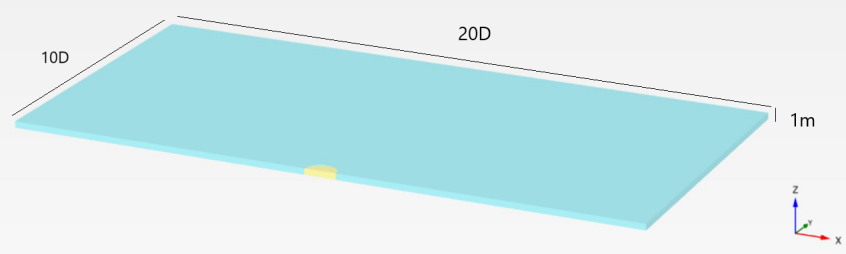

Figure 6.1: Illustration of a slice model

As this method is used in the industry, it would be beneficial to be able to include the vertical load on a slice in Plaxis 3D. With this method, it would be possible to analyse the effect of vertical load on the p-y curves, and possibly propose a correction factor to account for the effect of the vertical loading. Two methods are proposed for including vertical loading in the slice model in Plaxis 3D in this chapter. Both methods consist of modelling the full length of the pile as explained in Chapter 4. Since the vertical boundary conditions induce a plane-strain condition it is difficult to apply a vertical load directly on the slice. Therefore, the full length of the pile is used to load the pile

vertically before creating a slice. The purpose is to mobilise shear stresses along the pile shaft from vertical loading to see the effect on the p-y curves generated with the 3D slice models. The same soil and pile properties as used for modelling the full length of the pile, presented in Chapter 4, Table 4.1 and Table 4.2, is used in this chapter.

6.2 Slice model 1

The first method consists of creating a slice by removing soil volume from the full model to represent a slice with 1m thickness. The model created will further in this study be referred to as Slice model 1. Figure 6.2 illustrates the process of creating Slice model 1.

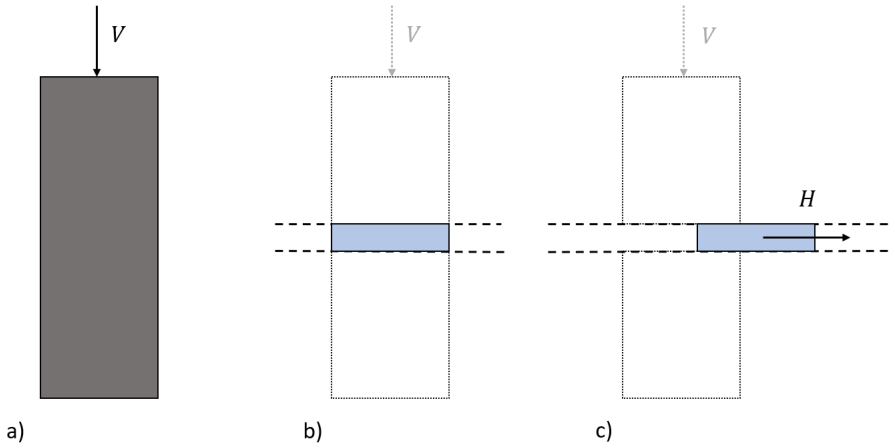

Figure 6.2: Illustration of creating Slice model 1, a) vertical loading of the pile, b) creating the slice by removing soil volume above and below the slice, c) lateral loading of the slice

The full length of the pile is used for vertical loading of the pile. After the vertical load is applied at the pile head, a slice is created by removing soil volume. New boundary conditions for the top and bottom of the pile are introduced, preventing vertical movement. The lateral load is applied by creating a surface in the middle of the slice and applying a prescribed displacement in the lateral direction. Figure 6.3 presents the slice after removing the soil volume and introducing new boundary conditions in Plaxis 3D. An arbitrary depth of 9 m to 10 m below the surface is chosen for creating a slice. The script used for creating Slice model 1 is presented in Appendix D.2.

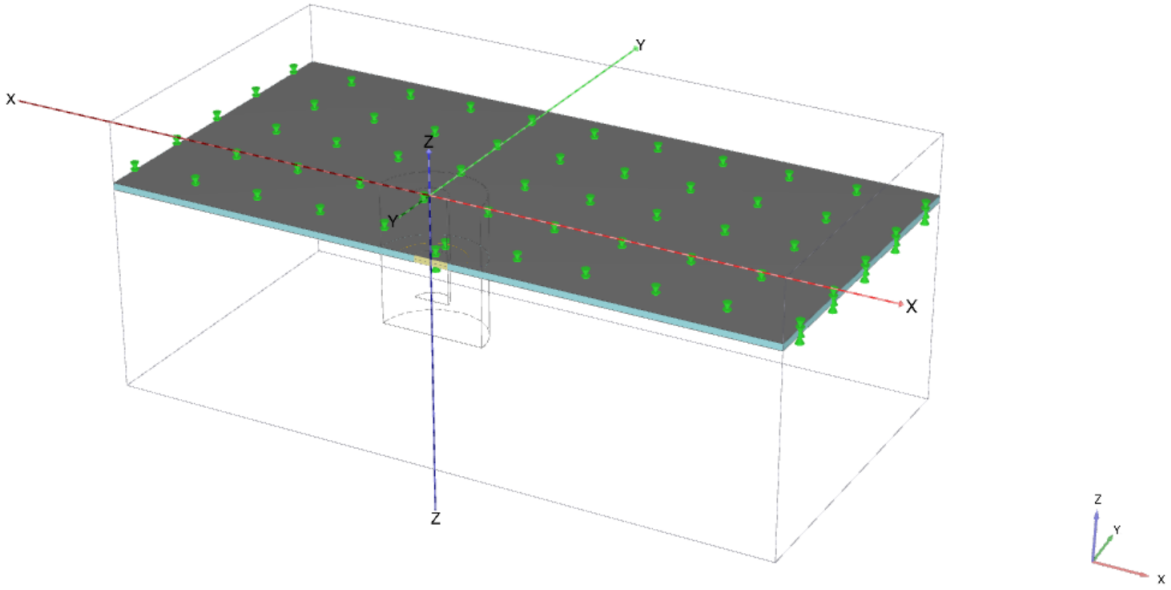

Figure 6.3: Illustration of Slice model 1 in Plaxis 3D- created by removing soil volume

The calculation phases used for creating Slice model 1 is listed below,

- **Phase 0**: Initial phase, the K0 calculation procedure is used to calculate the initial stress state of the soil material.
- **Phase 1**: Installation of the pile, the pile and interfaces are activated.
- **Phase 2**: Vertical loading, a vertical load is activated.
- **Phase 3**: Slice model, deactivating the volume above and below a 1m thick slice. New boundary conditions are introduced, and the displacements are reset.
- **Phase 4**: Lateral loading, lateral loading of the pile slice introduced in the model as prescribed lateral displacement.

6.3 Slice model 2

In Plaxis 3D interfaces are used to model the soil-structure interaction. In this study, interface elements are not only used for modelling the soil-structure interaction. With an interface, node pairs are created instead of single nodes, allowing the volume to move independently of each other. In this section a slice model is created by modelling a slice with interfaces, at the top and bottom of the slice, to allow the slice to move independently from the rest of the model. Using an interface with $R_{inter} = 0$, a smooth surface is created between the slice and the rest of the model, allowing the slice to move independently. This model will further in this study be referred to as Slice model 2. The process of creating Slice model 2 is illustrated in Figure 6.4.

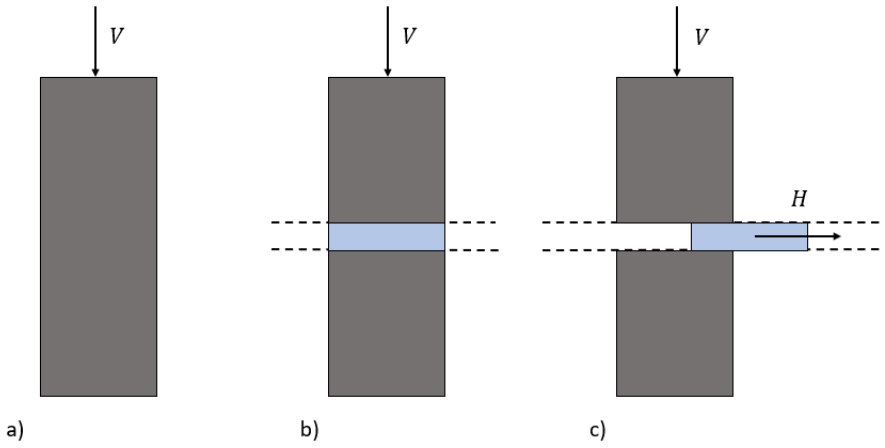

Figure 6.4: Illustration of creating Slice model 2, a) vertical loading of the pile, b) creating the slice by activating interfaces and additional boundary conditions, c) lateral loading of the slice

The full length of the pile is used for vertical loading of the pile. The slice model is created by using an interface along the top and bottom of the slice. The boundary conditions are the same as in the full model, with additionally boundary conditions including a vertically fixed boundary at the top and bottom of the slice. The purpose is to keep the soil volume and vertical load at the pile head and allow for lateral displacement of the slice. The script used for creating Slice model 2 is presented in Appendix D.3.

The interface is modelled with very low stiffness, and the parameter R_{inter} is set to the lowest possible, $R_{inter} = 0.01$. R_{inter} relates the strength of the interface to the strength of the surround soil material. The interfaces are allowing the pile and soil within the slice to move independently of the surrounding material. Slice model 2 modelled in Plaxis 3D is presented in Figure 6.5.

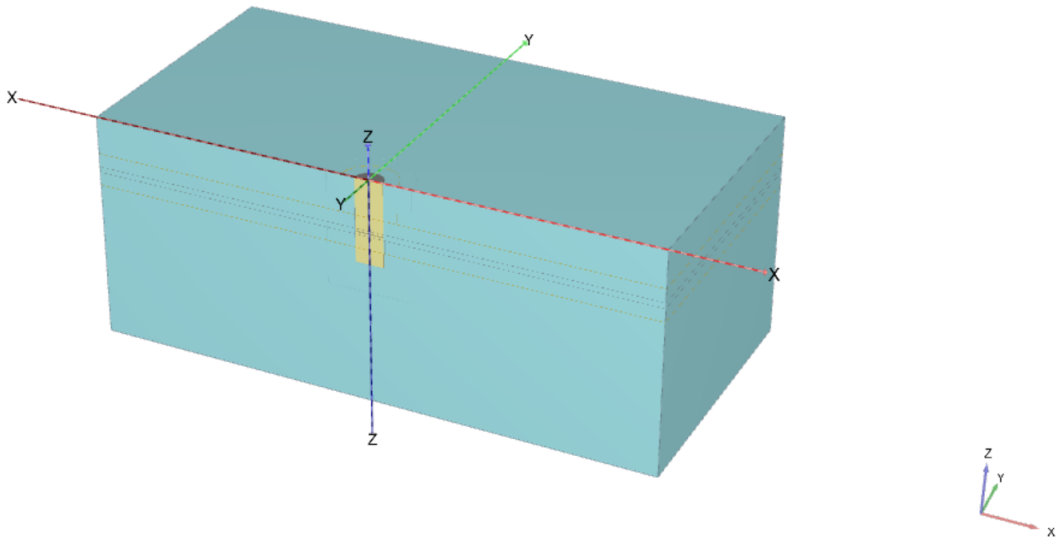

Figure 6.5: Illustration of Slice model 2 in Plaxis 3D- created by introducing additional interfaces

The calculation phases used for Slice model 2 are listed below,

- **Phase 0**: Initial phase, the K0 calculation procedure is used to calculate the initial stress state of the soil material.
- **Phase 1**: Installation of the pile, the pile and interfaces are activated.
- **Phase 2**: Vertical loading, a vertical load is activated.
- **Phase 3**: Slice model, activating an interface at the top and bottom of a 1m thick slice. New boundary conditions are introduced, and the displacements are reset.
- **Phase 4**: Lateral loading, lateral loading of the pile slice introduced in the model as prescribed lateral displacement.

6.3.1 Effect of interface properties

The strength properties used for the interface is presented in Table 6.1. A linear elastic soil model is used, and the interface is modelled with as low stiffness as possible, to allow for independent horizontal displacement of the slice. Lower strength properties are tested, and as it does not affect the results, the strength properties used are small enough to not affect the results.

Table 6.1: The interface properties used for creating Slice model 2

Linear elastic model		Interface
Unit weight [kN/m^3]	γ	20
Young's modulus [kPa]	E_{ref}	300
Drainage Type		Undrained (A)
R_{inter}		0.01

6.3.2 Plaxis numerical control parameters

The stage construction phase where the interfaces are activated, with $R_{inter} = 0.01$, results in numerical issues with the default calculation parameters set in Plaxis 3D. Numerical issues also occur during vertical loading of the pile, even though the horizontal interfaces creating the slice is not activated. Therefore, the interfaces are activated with the same properties as the surrounding material. The resulting vertical displacement field is controlled to confirm that the presence of the interfaces during vertical loading does not affect the results, and this is presented in Appendix C.1. When the slice is to be created, the material properties are changed to the properties of the interfaces with low strength and $R_{inter} = 0.01$.

The solver type in Plaxis defines the solver calculating the system of equations. The possible alternatives are given from Brinkgreve (2019), (a) Picos (multicore iterative), which is an iterative solver that solves the system of equations in parallel on multi-core processors, and is considered to be the fastest solver. (b) Pardiso (multicore direct), which is a direct solver that solves the system of equations in parallel on multi-core processors. It is the most robust way of solving the equations, and it has the highest memory consumption. (c) Classic (single core iterative), which is an iterative solver similar to the Picos solver, but solves the system of equations using a single core on the processor.

The default solver set by Plaxis is the Picos (multicore iterative), this results in numerical issues when activating the interface with $R_{inter} = 0.01$. The interface stiffness has a quadratic dependency on R_{inter}. Using very low values of R_{inter}, may result in unrealistic slipping or gapping between the soil and structure (*Plaxis | Modelling soil-structure interaction: interfaces*, 2012). For calculating the stage construction phase with an interface $R_{inter} = 0.01$, using the solver Pardiso (multicore iterative) is necessary. The numerical control parameters used are presented in Table 6.2.

Table 6.2: Numerical control parameters

Solver type	Pardiso (multicore direct)
Max cores to use	256
Max steps	1000
Tolerated error	0.01
Max unloading steps	50
Max load fraction per step	0.005
Max number of iterations	60
Desired min number of iterations	10
Desired max number of iterations	10
Use gradual error reduction	x

These settings are more time-consuming, and with the Paradiso solver, it has the highest memory consumption of the solver types.

6.4 Parametric study

A parametric study is to be performed on one of the slice models presented in this chapter. The parameters investigated are

- The effect of the undrained shear strength

$$s_u \text{ [kPa]} : 40, 60, 80$$

- The effect of the pile slenderness ratio

$$L/D : 3, 5, 10$$

Chapter 7

Effect of axial load on p-y curves

The results from the two slice models introduced in Chapter 6 will be presented. Only one model will be used for further parametric study.

7.1 Slice model 1

Slice model 1 was created by removing soil volume above and below the slice. This was testes for a model with an undrained shear strength of $s_u = 60kPa$ and a slenderness ratio of $L/D = 3$. The slice depth was chosen arbitrarily to represent a slice, $z_{top} = -9m$ and $z_{bottom} = -10m$ below the surface.

7.1.1 Verification of Slice model 1

The applicability of Slice model 1 is verified by comparing the ultimate lateral capacity calculated from FEA and theoretical ultimate lateral capacity. For pure lateral loading, the ultimate lateral capacity calculated from FEA for the slice is $p_{ult} = 3643kN$, as presented in Figure 7.1. Compared to p-y curve formulations given by M. F. Randolph and Houlsby (1984), the ultimate capacity in soft clay is given by $p_{ult} = N_p s_u D$, and for a fully rough pile-soil interface, a limiting bearing capacity factor of $N_p = 12$ is recommended. The soil-structure interface in the model is modelled with $R_{inter} = 1$, corresponding to a rough pile. The results from Slice model 1 for the ultimate lateral capacity corresponds to a bearing capacity factor of $N_p = 12.14$. This is close to the limiting bearing capacity factor given for a fully rough pile. The study presented by Zhang and Andersen (2017), revealed an over-estimation of 5-7% compared to the theoretical values.

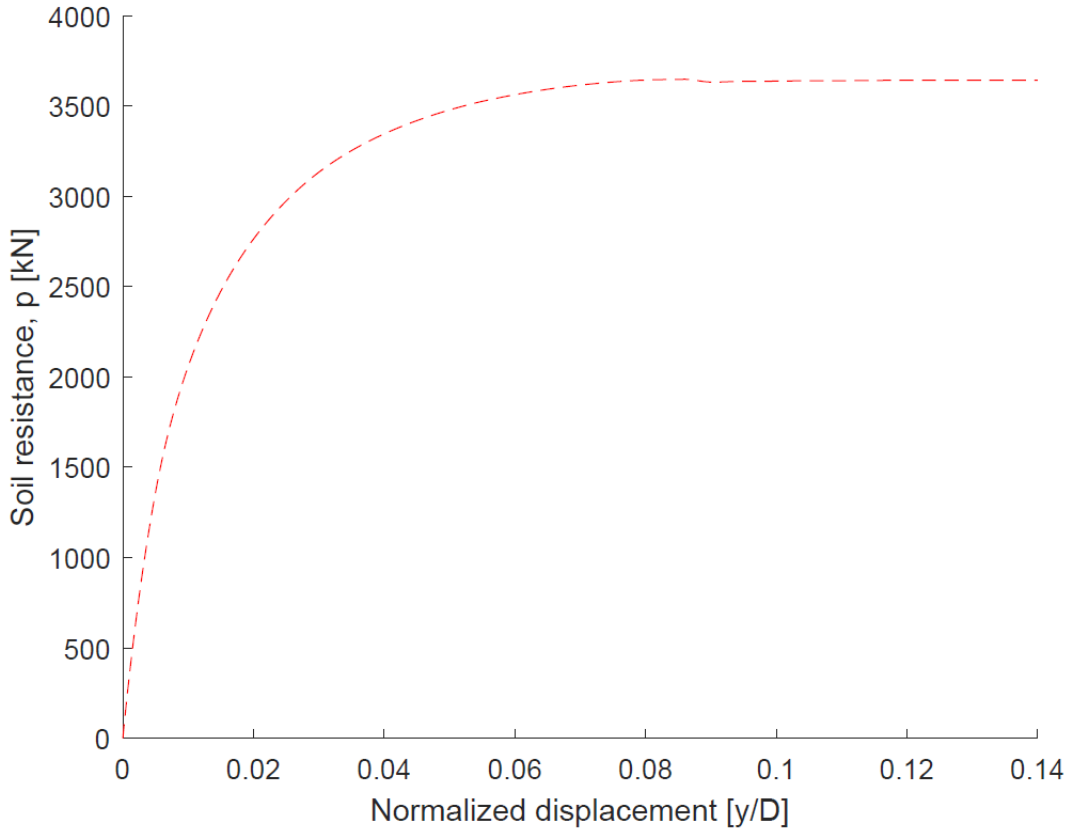

Figure 7.1: p-y curve for pure lateral loading

A deviation in the bearing capacity factor of 1.9% is observed between FEA and the theoretical solution proposed by M. F. Randolph and Houlsby (1984). As the deviation is marginal, Slice model 1 is applicable to the ultimate lateral capacity, p_{ult}, in the p-y curve formulations representing the flow-around soil failure mechanism.

7.1.2 Lateral capacities

Based on a vertical capacity analysis given in Chapter 5, the effect of the vertical load on the lateral response was evaluated. Figure 7.2 presents the lateral response of the model for vertical loads of 20%, 40%, 60%, 80%, and 100% of the vertical capacity. During lateral loading, the strain increases in the soil and the stiffness decreases, as observed in the figure. The results are presented for lateral displacement of 0.14D to illustrate the converged values indicating that the ultimate lateral capacity is reached.

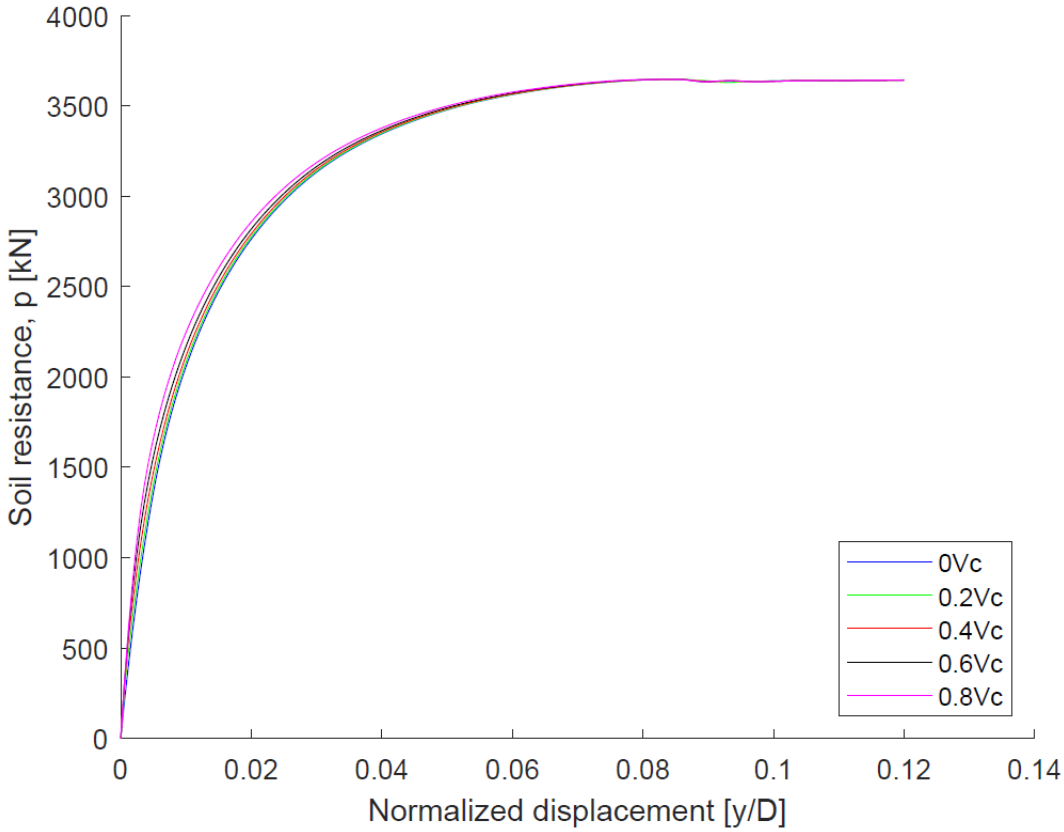

Figure 7.2: Comparison of p-y curves with combined vertical and lateral loading

The slope of the curves indicates a higher reaction modulus, E_{py}, at the beginning of the curves for the models with vertical loads present. This was also observed from the model of the full length of the pile. Furthermore, as can be observed from the figure, the lateral capacities for the different vertical loads reach the same value.

From Plaxis output, the calculation phases were investigated. It was observed that several plastic failure points were created during vertical loading. A plastic failure point illustrates a point in the material that is currently on the failure envelope. The failure envelope in a total stress analysis is defined by the Tresca yield surface. The Tresca yield surface is defined by $\tau_{max} = \frac{\sigma_1 - \sigma_3}{2} = s_u$.

After the vertical load was applied, the soil above and below the slice was removed. During lateral loading, the plastic failure points created by the vertical load was no longer a plastic failure point. The stresses creating plastic failure points during vertical loading was remobilised during lateral loading. Consequently, Slice model 1 with vertical loading reaches the same ultimate lateral capacity as for pure lateral loading.

From these analyses, it was concluded that the vertical load needs to be present at the top of the pile to prevent the stress change in the slice. Therefore this slice method is not able to capture the effect of a combined vertical and lateral load on the p-y curve response.

7.2 Slice model 2

Slice model 2 was created by introducing interfaces above and below the slice, in addition to introducing additional boundary conditions to prevent vertical motion. The slice depth was the same as Slice model 1, $z_{top} = -9m$ and $z_{bottom} = -10m$ below the surface.

7.2.1 Verification of Slice model 2

Slice model 2 is modelled with the full length of the pile, with interfaces and boundary conditions to create a slice model. As the model is not only representing a slice, several analyses were done to evaluate the applicability of the results obtained from the model. The results are presented in Appendix C.1, and the results are summarised in the following.

The lateral displacement field was evaluated from Plaxis output, and the total displacement field is presented in Figure 7.3. The results show that the slice is moving laterally without a visible effect from the rest of the model, and the symmetrical displacement field is observed for lateral loading in the slice.

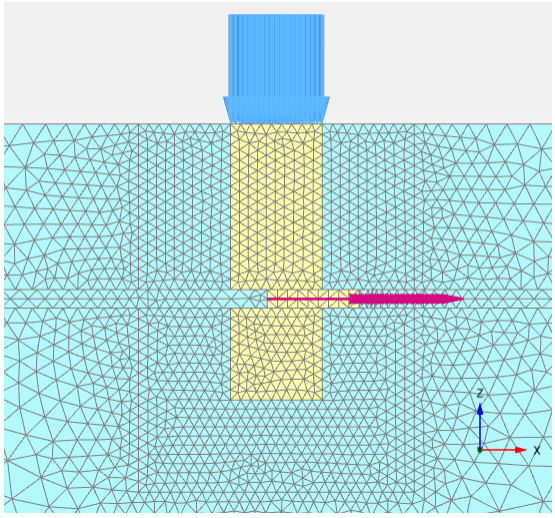

Figure 7.3: The total displacement field for a prescribed lateral displacement with vertical loading

For pure lateral loading, the ultimate lateral capacity for Slice model 2 is $p_{ult} = 3646kN$, resulting in a bearing capacity factor of $N_p = 12.15$. This results in an over-estimation of 1.3% compared to the theoretical solution of $N_p = 12$.

The effect of the initial stresses was evaluated by creating a model with zero-unit weight. As the analysis is based on the Tresca yield criteria, the results should not depend on the initial stresses in the soil. The results indicate a marginal effect of the initial stresses in the soil. This confirms that the analyses are only depending on the undrained shear strength of the soil.

In addition, only a slice was created with no unit weight, similar to the approach presented in Zhang and Andersen (2017). This is illustrated in Figure 7.4. The models give similar results with deviation in the bearing capacity

factor of 0.2%. This confirms that Slice model 2 is moving independently from the rest of the model. The interface is modelled with low enough strength properties allowing the soil volume in the slice to move independently from the surrounding soil.

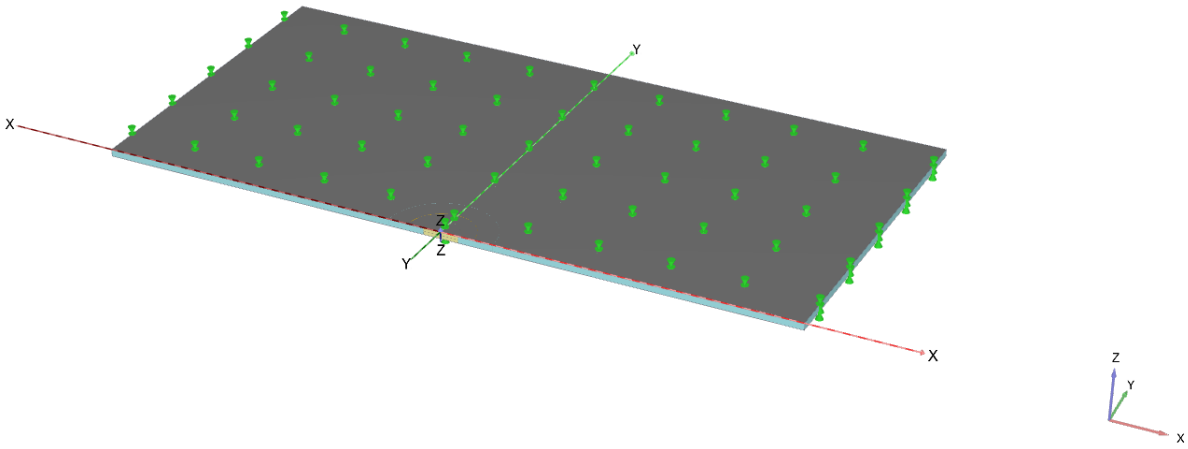

Figure 7.4: A slice model

The effect of creating the slice with interfaces and additional boundary conditions were evaluated from the vertical stresses in the slice. The vertical stress change is observed to be marginal.

The validity of the Slice model 2 is verified by the analyses described above. As the analyses showed marginal effect of the interfaces, the initial stresses and the results are in agreement with theory, Slice model 2 is applicable to the ultimate lateral capacity in the p-y curve formulations representing the flow-around soil failure mechanism.

7.2.2 Lateral capacities

The full length of the pile was exposed to vertical loads of 20%, 40%, 60% and 80% of the vertical capacity before a slice was created. The results are presented in Figure 7.5 for lateral deflection of 0.14D.

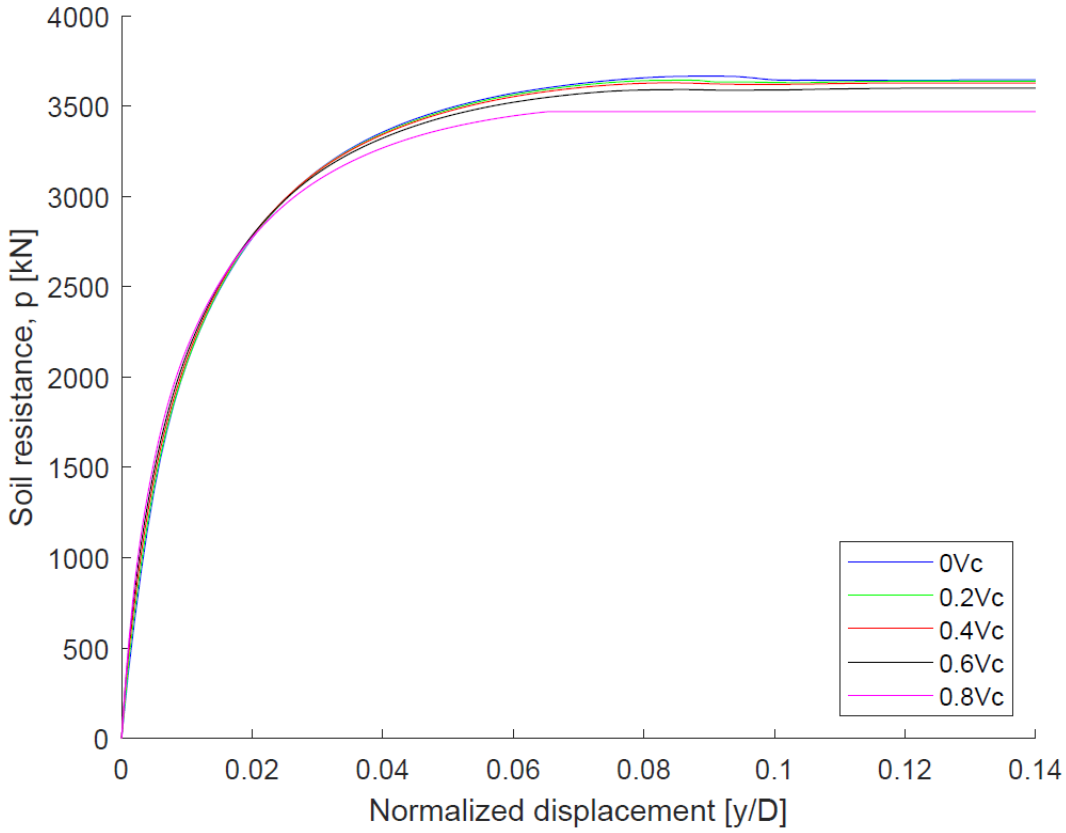

Figure 7.5: Comparison of p-y curves with combined vertical and lateral loading

As can be observed from the figure, the initial stiffness of the slopes indicates a stiffer behaviour for higher vertical loads. This is similar results obtained from Slice model 1. However, the lateral capacity reached, indicate a reduced capacity for vertical loading compared to a case with pure lateral loading. The reduced capacities are presented in Table 7.1.

Table 7.1: Reduced ultimate lateral capacities with combined vertical and lateral loading

	Reduced ultimate lateral capacity [%]				
Model	0Vc	0.2Vc	0.4Vc	0.6Vc	0.8Vc
Slice model 1	100	99.8	99.5	98.7	95.2

It is observed a reduced ultimate lateral capacity of 1.3% and 4.8% for vertical loading of 0.6Vc and 0.8Vc respectively. For vertical loading below 0.6Vc, the reduced ultimate lateral capacity is below 1%. Furthermore, as can be observed, the slope of the model exposed to vertical loads has a stiffer slope at the beginning. This was also observed from Slice model 1, and from the model of the full length of the pile. The higher stiffness at the beginning for higher vertical loads comes from the mobilised shear stresses in the soil surrounding the pile from vertical loading. When the lateral load is applied, shear stresses are already mobilised along the length of the pile, inducing a stiffer behaviour to lateral loading. This is confirmed by evaluating the stress paths later in this chapter.

7.2.3 Comparison to another soil model

The NGI-ADP soil model was used to confirm the results obtained with the HS soil model. For comparison to the HS soil model, the vertical capacity for the NGI-ADP soil model was calculated from M_{stage}, for the same vertical displacement as the HS-model. This resulted in a vertical capacity for the NGI-ADP soil model of $F_z = 19360kN$. The soil parameters used are presented in Appendix C.2. As the results show, the NGI-ADP soil model gives similar results to the HS soil model, higher initial stiffness at the beginning and a reduced capacity for the lateral load. The purpose of using the NGI-ADP soil model was to confirm the behaviour of the p-y curves obtained from the HS model. The resulting lateral load - lateral deflection is presented in Figure 7.6 and Table 7.2.

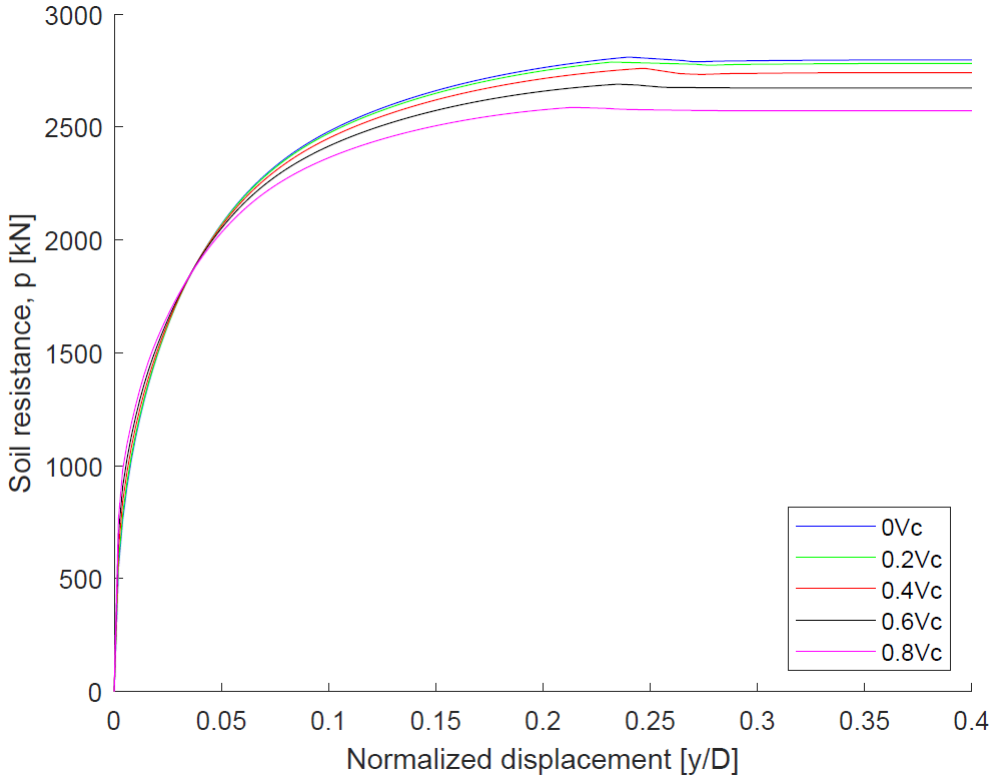

Figure 7.6: Comparison of p-y curves with combined vertical and lateral loading - NGI-ADP soil model

Table 7.2: The ultimate lateral capacities with combined vertical and lateral loading for NGI-ADP soil model

	Ultimate lateral capacity				
Model	0Vc	0.2Vc	0.4Vc	0.6Vc	0.8Vc
NGI-ADP soil model	2 797kN	2 782kN	2 740kN	2 673kN	2 572kN

The reduced lateral capacities are presented in Table 7.3.

Table 7.3: Reduced ultimate lateral capacities with combined vertical and lateral loading for NGI-ADP soil model

	Reduced ultimate lateral capacity [%]				
Model	$0Vc$	$0.2Vc$	$0.4Vc$	$0.6Vc$	$0.8Vc$
NGI-ADP soil model	100	99.5	98.0	95.6	92.0

As can be observed from Table 7.3, the results indicate an 8% reduction in the lateral capacity with a vertical load of 0.8Vc. This is a 3% higher reduction compared to the results of the HS model for a vertical load of $0.8Vc$. Furthermore, a higher lateral deflection is observed before the model reaches an ultimate lateral capacity.

The discrepancy between the two soil models could come from the soil parameters used for the NGI-ADP soil model is not directly comparable to the parameters used for the HS model. However, the results from the NGI- ADP soil model show a similar decrease in the ultimate lateral capacity as the HS model.

7.2.4 Parametric study

A parametric study was performed on Slice model 2 as this model showed an effect of vertical loading on the lateral response. The parameters to investigate was,

- Effect of undrained shear strength
- Effect of pile slenderness ratio on the lateral response

Effect of undrained shear strength

The effect of undrained shear strength is tested. Three different undrained shear strengths are analysed and compared,

$$s_u \text{ [kPa]: } 40, 60, 80$$

The results are presented in Table 7.4, and the reduced capacities are presented in Table 7.5.

Table 7.4: The ultimate lateral capacities with combined vertical and lateral load for different undrained shear strengths

	Ultimate lateral capacity				
Undrained shear strength	0Vc	0.2Vc	0.4Vc	0.6Vc	0.8Vc
$s_u = 40kPa$	2 431	2 428	2 417	2 398	2 331
$s_u = 60kPa$	3 646	3 639	3 628	3 600	3 470
$s_u = 80kPa$	4 854	4 847	4 834	4 798	4 677

Table 7.5: The reduced ultimate lateral capacities with combined vertical and lateral loading for different undrained shear strengths

	Reduced ultimate lateral capacity[%]				
Undrained shear strength	0Vc	0.2Vc	0.4Vc	0.6Vc	0.8Vc
$s_u = 40kPa$	100	99.9	99.4	98.6	95.9
$s_u = 60kPa$	100	99.8	99.5	98.7	95.2
$s_u = 80kPa$	100	99.9	99.6	98.8	96.4

For vertical loading of 0.6Vc and 0.8Vc, the reduction in the ultimate lateral capacity is observed to be close to 1% and 4-5% respectively. Similar to the results obtained from the full length of the pile, Slice model 2 does not show a significant effect of the undrained shear strength. The p-y curves are presented in Figure 7.7 for comparison.

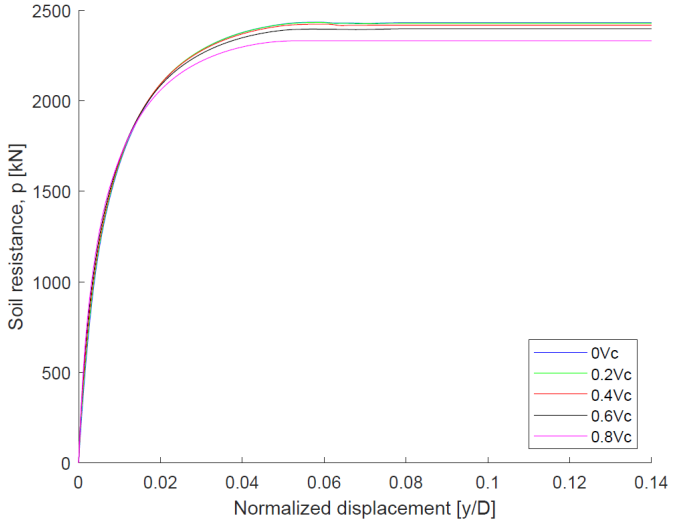

(a) $s_u = 40kPa$

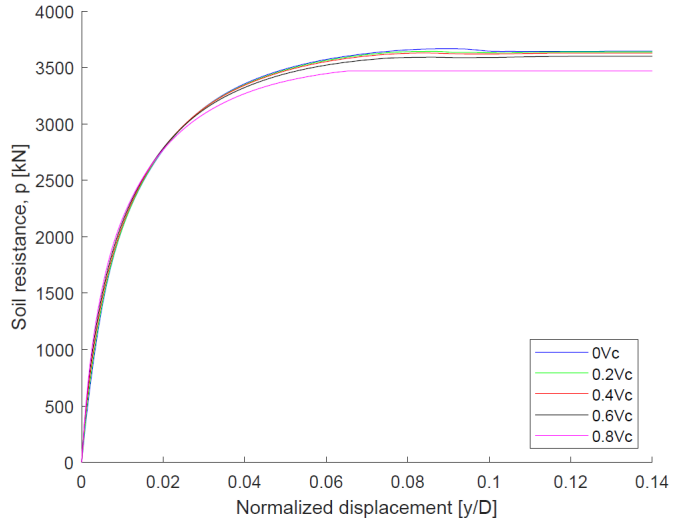

(b) $s_u = 60kPa$

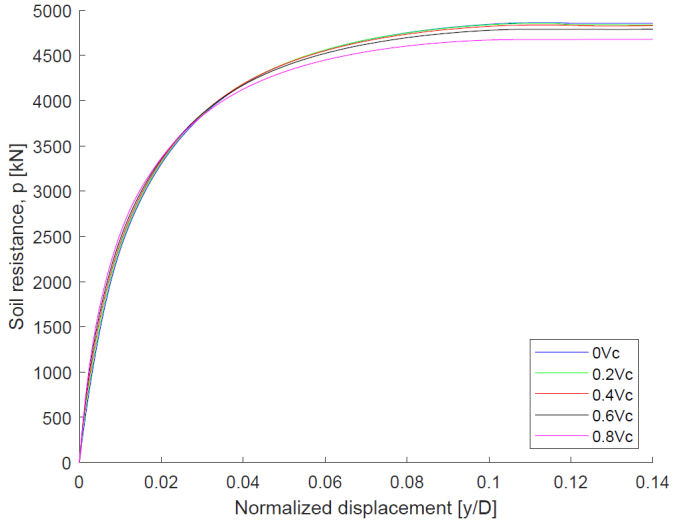

(c) $s_u = 80kPa$

Figure 7.7: Comparison of p-y curves with combined vertical and lateral loading for different undrained shear strengths

Effect of L/D - ratio

The effect of the slenderness ratio is tested for three different L/D-ratios. The results are analysed and compared for slenderness ratios of

$$L/D : 3, 5, 10$$

The slenderness ratios are chosen for values up to $L/D = 10$ as this is representing a larger diameter pile. The vertical capacities for the slenderness ratios evaluated in this section are presented in Chapter 5. Based on the vertical capacity analysis, the lateral response to vertical loading is analysed. The ultimate lateral capacities are presented in Table 7.6, and the reduced ultimate lateral capacities are presented in Table 7.7.

Table 7.6: The ultimate lateral capacities with combined vertical and lateral load for different L/D - ratios

	Ultimate lateral Capacity				
Slenderness ratio	0Vc	0.2Vc	0.4Vc	0.6Vc	0.8Vc
$L/D = 3$	3 646	3 639	3 628	3 600	3 470
$L/D = 5$	2 194	2 193	2 189	2 181	2 167
$L/D = 10$	1 109	1 109	1 108	1 105	1 094

Table 7.7: Reduced ultimate lateral capacities with combined vertical and lateral loading for different L/D - ratios

	Reduced ultimate lateral capacity [%]				
Slenderness ratio	0Vc	0.2Vc	0.4Vc	0.6Vc	0.8Vc
$L/D = 3$	100	99.8	99.5	98.7	95.2
$L/D = 5$	100	99.9	99.8	99.4	98.8
$L/D = 10$	100	100	99.9	99.7	98.7

As observed from Table 7.7, the reduction in the ultimate lateral capacity is lower for higher slenderness ratios. For a vertical load of 0.8Vc, the reduction in the ultimate lateral capacities are close to 1% for $L/D = 5$ and $L/D = 10$. This is close to 4% lower effect compared to $L/D = 3$. Similar to the results obtained from the full length of the pile, a lower effect of vertical loading is observed for higher slenderness ratios. The p-y curves are presented in Figure 7.8 for comparison.

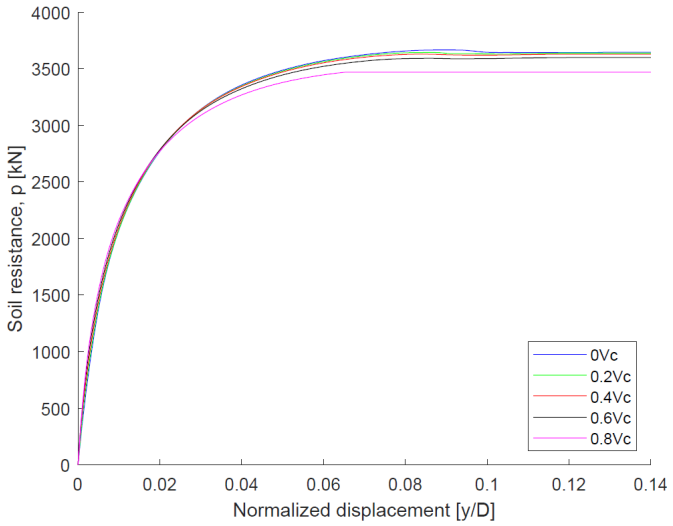

(a) $L/D = 3$

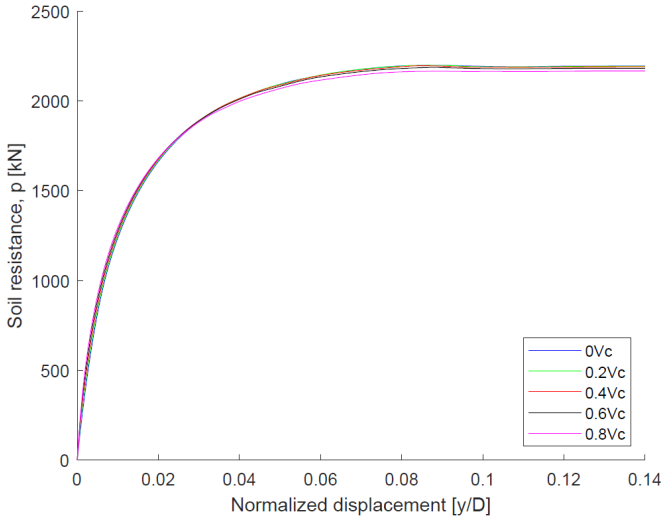

(b) $L/D = 5$

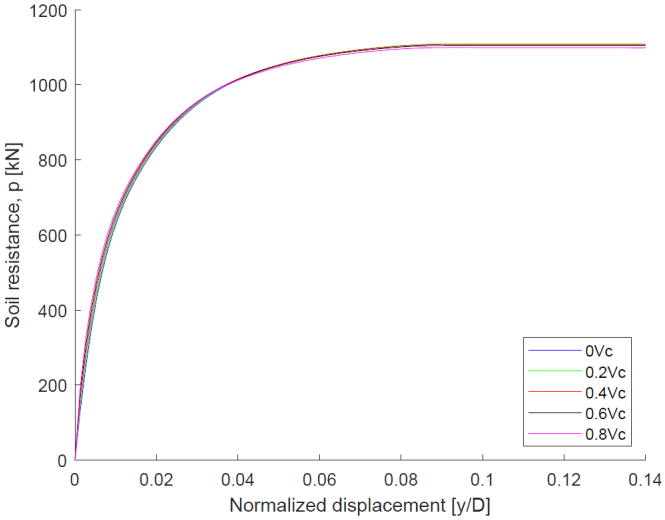

(c) $L/D = 10$

Figure 7.8: Comparison of p-y curves with combined vertical and lateral loading for different slenderness ratios

7.2.5 Effect of the depth chosen for the slice

The depth of the slice chosen is at the lower part of the monopile, from 9 m to 10 m below the surface. As the vertical load decreases with depth, as illustrated in Chapter 5, higher shear stresses are mobilised in the soil surrounding the pile closer to the surface. A slice taken from a depth of 2 m to 3 m below the surface was chosen to evaluate the effect of the higher shear stresses in the slice. The results are given in Appendix C.3, and the reduced capacities are summarised in Table 7.8.

Table 7.8: Reduced ultimate lateral capacities with combined vertical and lateral loading for a new slice at depth 2 m to 3 m below the surface

	Reduced ultimate lateral capacity [%]				
Model	0Vc	0.2Vc	0.4Vc	0.6Vc	0.8Vc
New slice	100	99.9	99.6	98.6	95.5

From Table 7.8, it is observed a reduction of close to 1% and 4% for vertical loading of 0.6Vc and 0.8Vc respectively. As the results show, there is no significant effect compared to the slice taken at a deeper depth. This indicates that the reduces capacities are independent of the depth chosen for the slice.

Axial force in the pile slice

Vertical loads are applied at the top of the pile depending on the calculated vertical capacity of the pile. As the load is taken by side friction along the length of the pile, it will vary with depth.

In Chapter 5, the axial force distribution along the length of the pile was calculated. Similar to this approach, it was attempted to extract the axial force acting in the pile slice. The purpose of investigating the structural forces is to be able to evaluate the effect of vertical loading on the lateral response depending on the amount of vertical load taken by the slice. As the vertical load is decreasing with depth, the soil closer to the surface is taking more of the vertical load.

However, due to the horizontal interface created above and below the slice, the volumetric forces calculated by Plaxis indicated no force taken by the slice. From observing both the vertical displacement and vertical stresses in the slice during the phase of vertical loading and activating the interfaces, the results indicated an even stress distribution with depth. Thus, the numerical issue occurring when calculating the volumetric forces in the slice is not considered to have an impact on the results presented in this study.

As it was not possible to extract the axial force in the slice from the volumetric forces in the pile, the axial force in the slice has to be evaluated from the axial force distribution with depth, for 0.8Vc, from the full model from Chapter 5. For a slice taken from depth 9m to 10m, the average axial force in the slice is 75% of the applied vertical load. Compared to the average axial force in the slice at depth 2m to 3m, the axial force in the slice is 93% of the applied vertical load. This is illustrated in Figure 7.9.

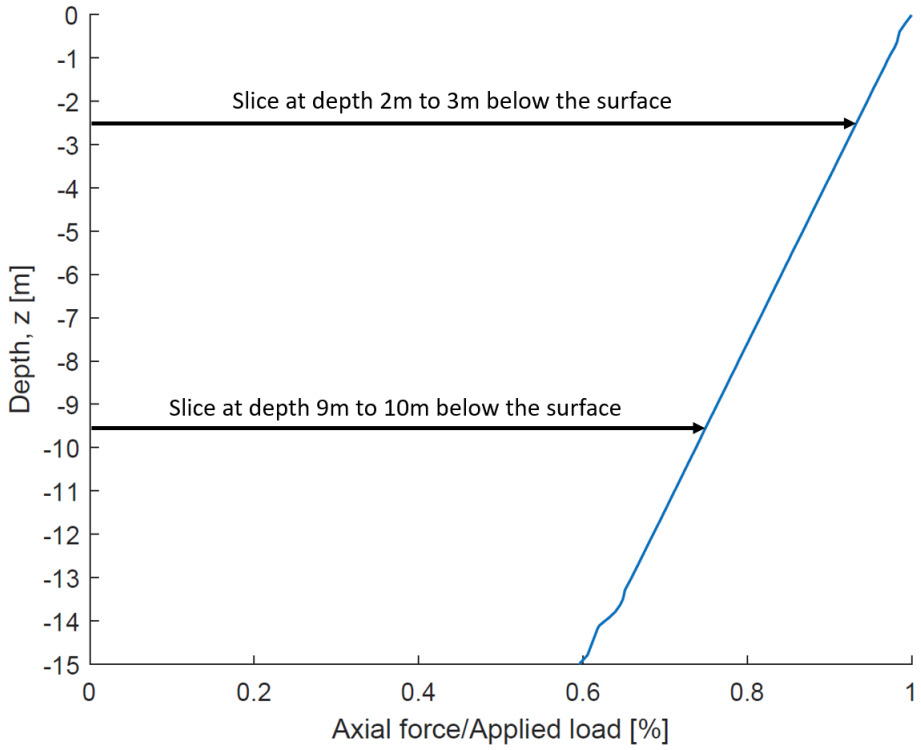

Figure 7.9: Illustration of the normalised axial force acting along the length of the pile for a slice at depth 2m to 3m and a slice at depth 9m to 10m

Based on this, the effect of vertical loading on the lateral capacity should indicate a larger effect for the slice taken at 2m to 3m compared to the slice at 9m to 10m.

7.2.6 Effect of fully mobilised side friction

The vertical loading applied will mobilise both base resistance and shear resistance along the shaft. As illustrated in Chapter 5, for the large diameter pile used in this project, a large part of the vertical load is taken by the pile base resistance. The effect of only mobilised shear resistance along the shaft is evaluated in this section.

Assuming no resistance at the pile tip, an interface, similar to the interface used for creating the slice with $R_{inter} = 0.01$ and low strength, is modelled at the bottom of the pile. As the pile tip is not able to take any load, the load will only be taken by side friction. The purpose of the interface is to evaluate the effect of larger mobilised side friction along the length of the pile.

The vertical stress field was evaluated to confirm that the model is only mobilising shear forces along the shaft. This is illustrated in Figure 7.10 for a vertical load of 80% of the vertical capacity. The model presented is for a unit weight of zero, to illustrate only the effect of vertical loading on the vertical stress field. As can be observed from the vertical stresses, σ_z, the stresses decrease along the length of the pile.

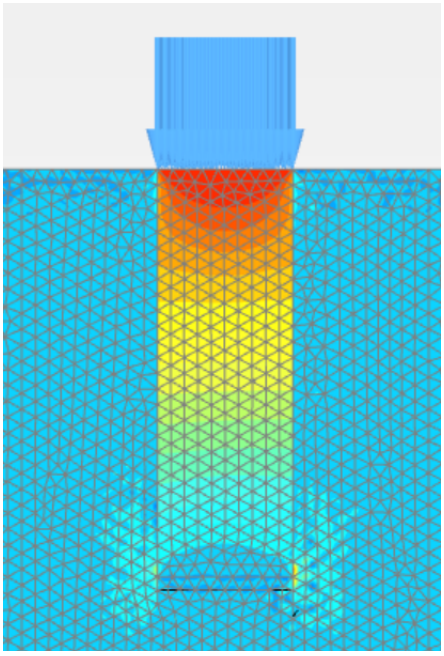

Figure 7.10: Vertical stress field, σ_z, to evaluate the effect of only mobilised side friction

A vertical capacity analysis was performed. The vertical capacity was calculated to $F_z = 14137kPa$, which is in agreement with the theoretical value of the side friction along the length of the pile, based on the equation, $Q_s = \pi DLs_u$. As the side friction is depending on the undrained shear strength of the material alone, the capacity calculated by Plaxis and the theoretical capacity obtain the same value.

Close to the pile tip, it is observed stress singularities in the soil surrounding the pile. These singularities could come from the interface is only modelled at the cross-sectional area of the pile, without extensions. These singularities are not considered to affect the results, and as observed at the pile tip, the vertical stresses are close to zero.

Based on the vertical capacity analysis, a vertical load of 80% of the vertical capacity was applied at the pile head, before creating the slice, and compared to a case of pure lateral loading. The results from the lateral capacity analysis are presented in Appendix C.4. A marginal reduction of 1% for the lateral capacity was observed for 0.8Vc compared to pure lateral loading. This is a smaller reduction compared to Slice model 2. A slice at depth 2m to 3m was also tested, but it showed similar results as the slice taken from 9m to 10m.

The purpose of this analysis was to evaluate if a larger mobilised shear resistance could have an impact on the effect of the vertical load on the p-y curves. To only mobilise side friction, the base resistance is neglected. This is a simplification which is not representative of the real situation of a pile with a slenderness ratio of $L/D = 3$. As illustrated from theoretical calculations, almost 50% of the vertical capacity is a result of base resistance. As a smaller reduction was observed for this model compared to Slice model 2, the effect of higher mobilised shear resistance is not affecting the results obtained with Slice model 2.

7.2.7 The stress paths

The stress path for soil elements close to the slice for combined vertical and lateral loading is presented in this section. As there was not observed a change in the reduced lateral capacity for the slice closer to the surface, the effect of applying a vertical load is evaluated in the soil surrounding the pile. Stress nodes are chosen at a distance of 0.5D, 1D, 2D, 3D and 4D from the pile as illustrated in Figure 7.11. The results are presented in p-q plots from the selected stress points at the centre of the slice for pure lateral loading and lateral loading with a vertical load of 0.8Vc. Stress nodes are chosen prior to calculating the phases in Plaxis 3D, and the results are extracted through Plaxis output.

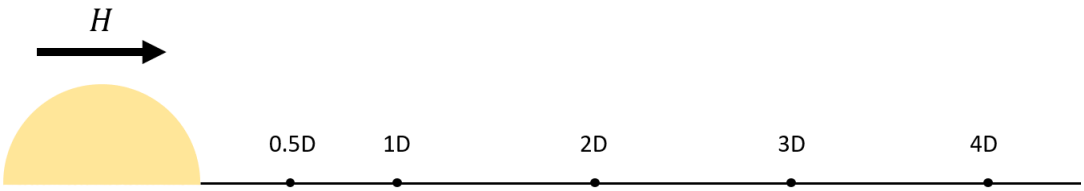

Figure 7.11: Illustration of the selected stress nodes for evaluating the effect of vertical loading on the stress paths in the soil

A p-q plot is illustrating the mean total stress and deviatoric total stress state in the soil during loading. The mean total stress and deviatoric total stress is defined by Equation 7.1 and Equation 7.2 respectively.

$$p = \frac{\sigma_1 + \sigma_2 + \sigma_3}{3} \tag{7.1}$$

$$q = \sigma_1 - \sigma_3 \tag{7.2}$$

The Tresca yield criterion is equal to $\tau_c = \frac{\sigma_1 - \sigma_3}{2} = s_u$. Introducing this into Equation 7.2, the failure criterion is defined by,

$$q = \sigma_1 - \sigma_3 = 2\tau_c = 2s_u \tag{7.3}$$

The effect of vertical loading is illustrated by evaluating the model with a vertical loading of 80% of the vertical capacity. The stress path for a point at a distance 0.5D from the pile is presented in Figure 7.12.

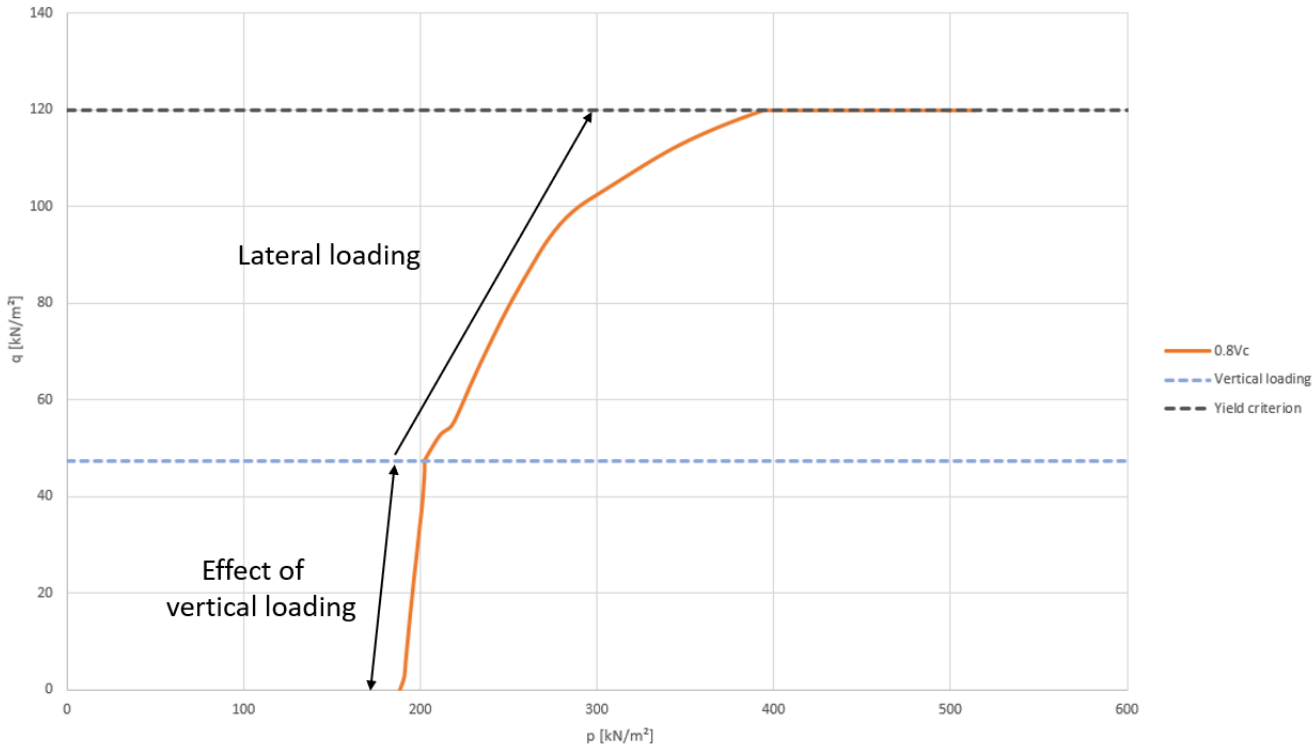

Figure 7.12: The effect of vertical loading of 0.8Vc illustrated in a p-q plot in a stress point 0.5D from the pile

The initial starting point of the curve is from an isotropic stress condition with $\sigma_x = \sigma_y = \sigma_z$, at a depth of $z = -9m$ to $z = -10m$, resulting in $p = 190kPa$, and no mobilised deviatoric stress in the soil, $q = 0kPa$. In the figure, the initial part of the slope is illustrating the effect of vertical loading on the lateral response. The deviatoric stress increases with vertical loading, and the effect of vertical loading is observed to be significant. With deviatoric stress after vertical loading of $q = 47.5kPa$, the remaining capacity is $q = 72.5kPa$.

The stress path for pure lateral loading and vertical loading of 0.8Vc is presented in Figure 7.13, 7.14, 7.15, 7.16, and 7.17, at a distance 0.5D, 1D, 2D, 3D, and 4D from the pile. As can be observed from the figures, all the stress points do not reach the Tresca failure criterion of $q = 2s_u = 120kPa$. This is because the points in the FE analyses have not reached failure, but it is presented to illustrate the stress paths in the soil material surrounding the pile.

Distance 0.5D

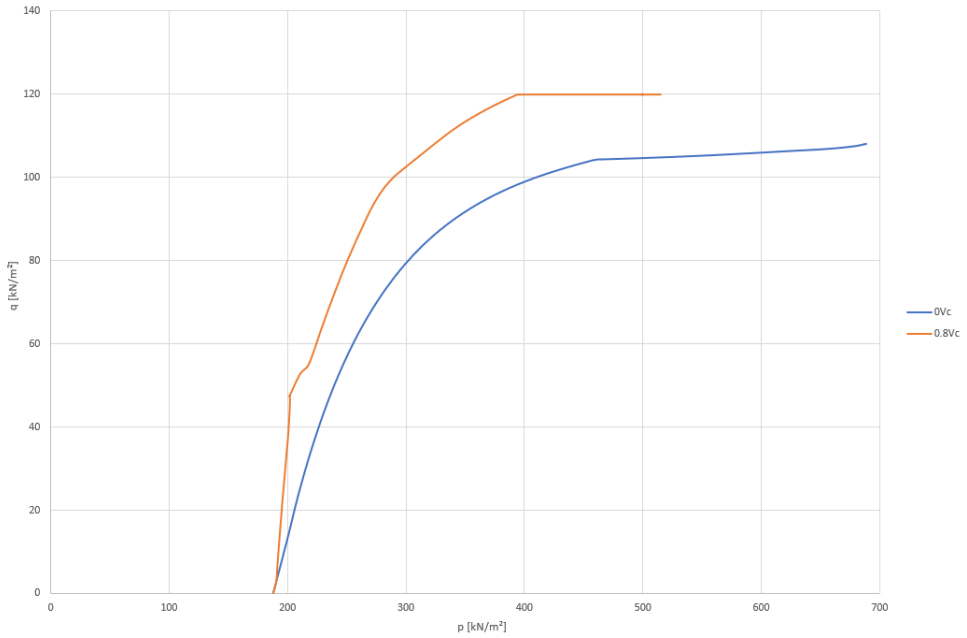

Figure 7.13: The stress path from a stress point at a distance of 0.5D from the pile

As observed from the lateral loading of the pile, a stiffer behaviour was observed for higher vertical loads compared to pure lateral loading. This can be observed from the stress path presented in the p-q plot in Figure 7.13, a stiffer response in the soil material close to the pile, after a vertical load is applied.

Distance 1D

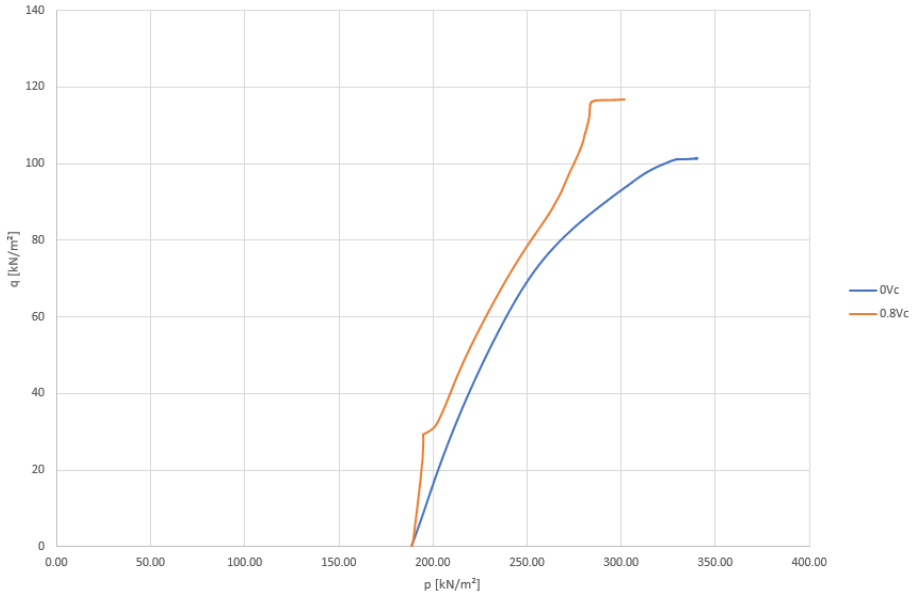

Figure 7.14: The stress path from a stress point at a distance of 1D from the pile

Distance 2D

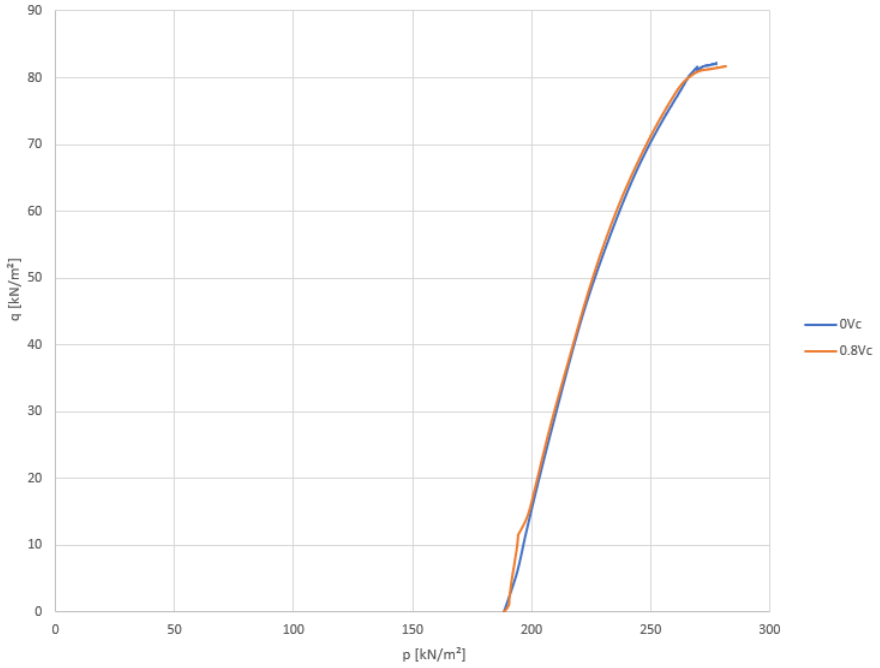

Figure 7.15: The stress path from a stress point at a distance of 2D from the pile

Distance 3D

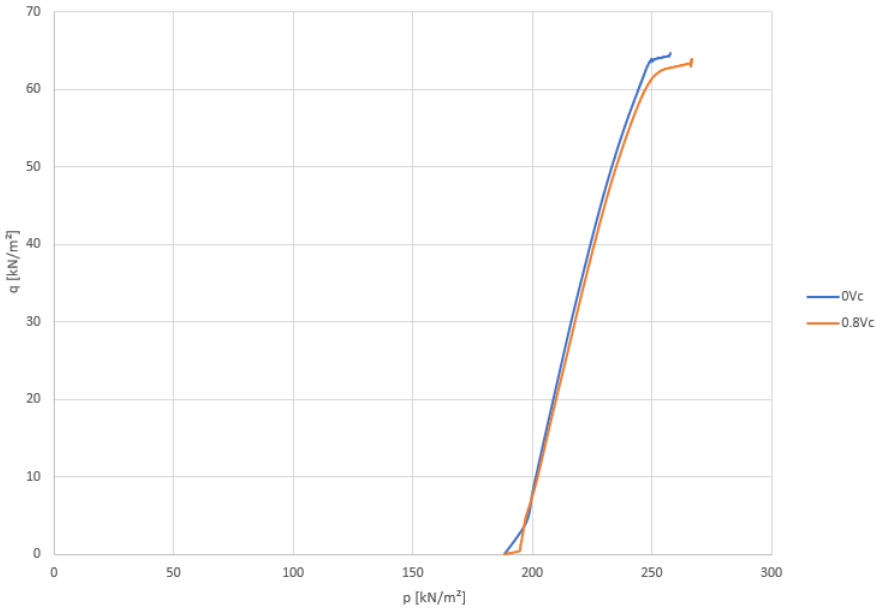

Figure 7.16: The stress path from a stress point at a distance of 3D from the pile

Distance 4D

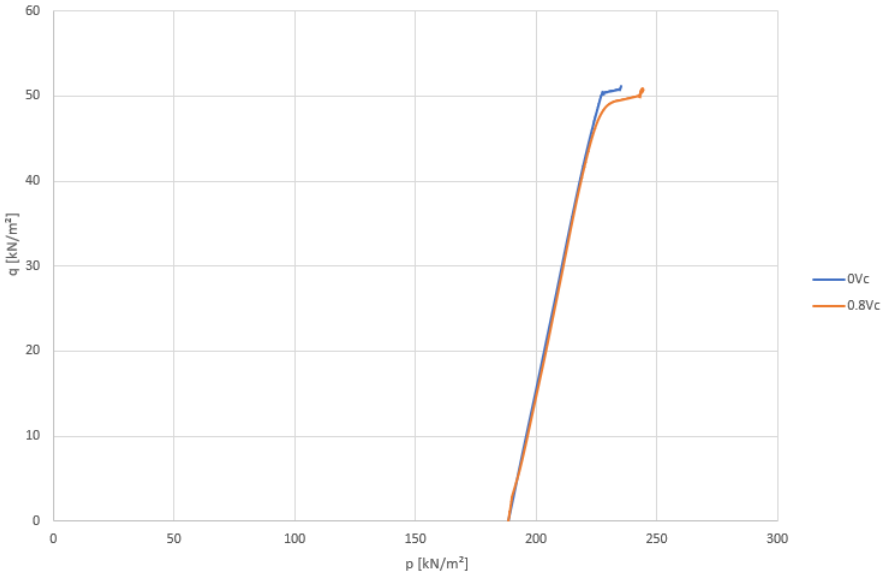

Figure 7.17: The stress path from a stress point at a distance of 4D from the pile

For points with increasing distance from the pile, the effect of vertical loading decreases. For the point at a distance 4D from the pile, the effect of vertical loading is only mobilising marginal deviatoric stress of $q = 2.87kPa$. As can be observed from the p-q plot, lateral loading mobilises nearly the same deviatoric stresses in this stress point.

7.3 Discussion

Two methods of including vertical loading on a pile slice in Plaxis 3D were tested in this chapter. The purpose was to evaluate the effect of vertical loading on the p-y curves governing the flow-around failure mechanism and to evaluate if it is possible to propose a correction factor to account for vertical loading. The ultimate lateral capacity was verified with theory, and the applicability of the results to the p-y curve formulations is limited to the ultimate lateral capacity.

Slice model 1 was created by using the full length of the pile for vertical loading, and the slice was created by removing soil volume. The results indicate no effect of vertical loading on the ultimate lateral capacity. The shear stresses from vertical loading were remobilised during lateral loading, and as a result, the obtained ultimate lateral capacity was the same for pure lateral loading and combined vertical and lateral loading.

Slice model 2 was also created using the full length of the pile for vertical loading, and a slice was created by introducing two horizontal interfaces. This model results in a reduced ultimate lateral capacity for vertical loading. Similar to the model of the full length of the pile, the model does not depend on the undrained shear strength of the soil material, and for higher slenderness ratios, the effect of vertical loading decreases. However, the effect of vertical loading does not depend on depth. As the vertical load decreases with depth, it should have an effect on

the reduction in the ultimate lateral capacities. A larger reduction is expected for a slice taken closer to the surface, then for a slice taken at deeper depths. By evaluating the stress path, there is observed a significant effect of vertical loading on the soil elements close to the pile. However, observing the effect of vertical loading on the ultimate lateral capacity, the effect is small. As the effect of vertical loading is only affecting the soil relatively close to the pile, there is only observed a marginal effect on the soil elements at a distance from the pile. For lateral loading, shear stresses are mobilised in the soil at a larger distance from the pile. Therefore, the soil effected by vertical loading is small compared to the soil effected by lateral loading. This can be observed by observing the mobilised shear stress field τ_{mob} from Plaxis output. In Figure 7.18 and Figure 7.19, for pure vertical loading, and with the same vertical loading and additionally with applying lateral loading until failure in the slice. As can be observed from the figures, a significantly larger area of soil is affected by the lateral loading.

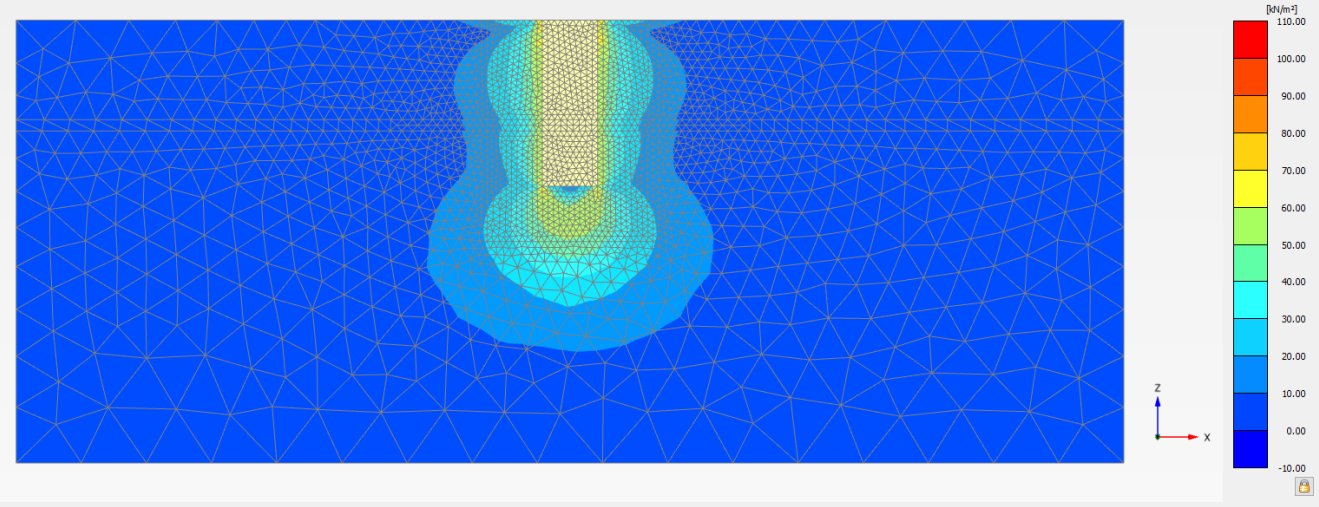

Figure 7.18: Mobilised shear strength field, τ_{mob}, for vertical loading of 80% of the vertical capacity

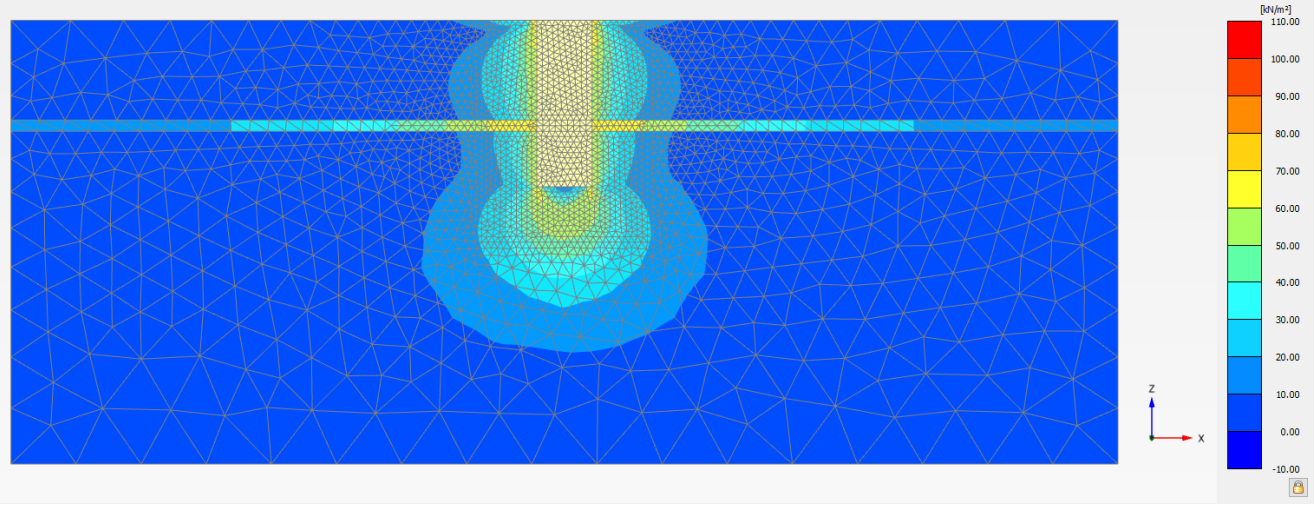

Figure 7.19: Mobilised shear strength field, τ_{mob}, for combined vertical and lateral loading, the vertical load applied is 80% of the vertical capacity

For vertical loading of the pile, a circular failure mechanism is forming at the pile tip. This is observed from the mobilised shear stress field presented in Figure 7.18 and Figure 7.19. This is due to the rupture failure mechanism is characterised by failure planes with 45° angles. This activates larger shear surfaces, and as a result, the pile has a higher resistance to failure.

In Figure 7.20 and Figure 7.21, the mobilised shear stress field in the slice for pure vertical loading and for combined vertical and lateral loading is presented.

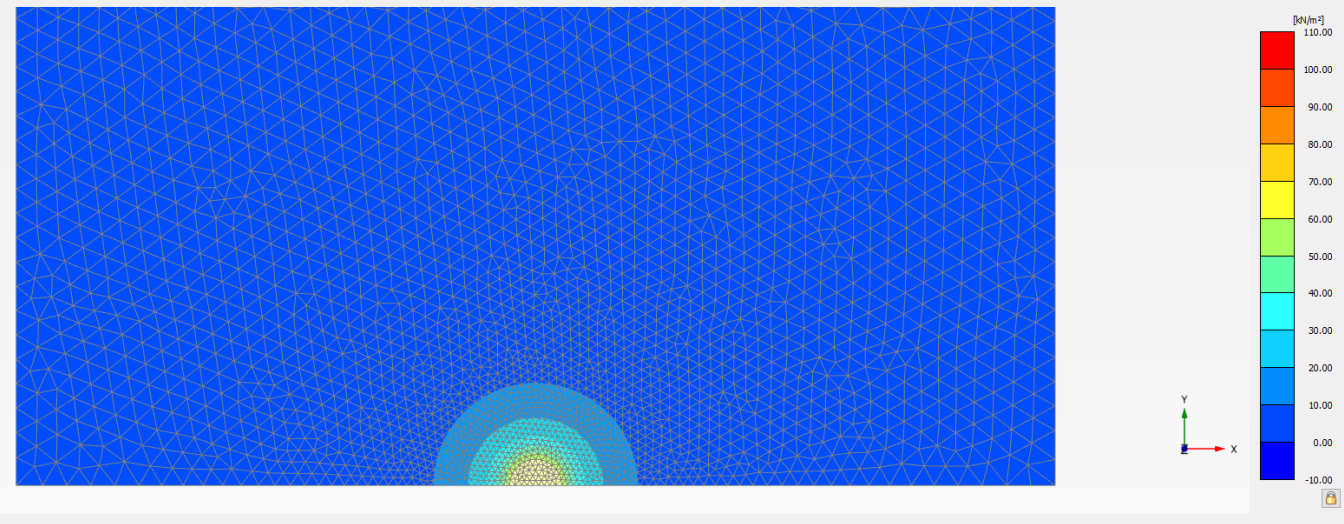

Figure 7.20: Mobilised shear strength field, τ_{mob}, in the slice for vertical loading of 80% of the vertical capacity

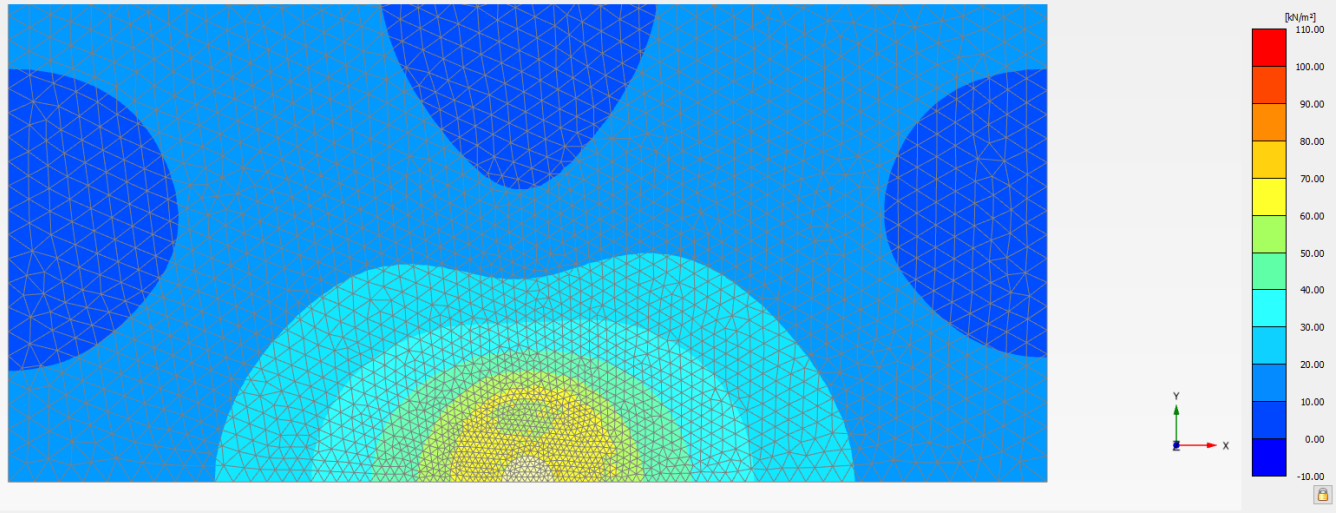

Figure 7.21: Mobilised shear strength field, τ_{mob}, in the slice for combined vertical and lateral loading, the vertical load applied is 80% of the vertical capacity

As observed from the mobilised shear stress field in the slice, the vertical loading mobilised shear stresses in a small area compared to the mobilised shear stress field for lateral loading. Compared to the results from the model of the full length of the pile as presented in Chapter 5, the reduction in the lateral capacity is marginal. The pile slice is

not able to represent the effect of vertical loading on the lateral response. The lateral capacity is dominated by the large part of the soil material not affected by the vertical loading.

7.4 Correction factor for the ultimate lateral capacity p_{ult}

The slice model was to be used for proposing a correction factor for p-y curves representing the flow-around failure mechanism. It would be a great benefit to be able to propose a correction factor to be used in p-y curve formulations. This would give practising engineers the possibility of including this in the p-y curves used for design, without the need for advanced numerical analyses. The p-y curves consist of three parts, the initial small-strain stiffness, the yielding section of the curve, and the ultimate lateral resistance. As the ultimate lateral resistance, p_{ult} is verified by theory for the slice models, proposing a correction factor for p_{ult} would have been possible.

A method of proposing a correction factor could be to introduce a term, α, in the equation for the ultimate lateral capacity for p-y curves representing the flow-around failure mechanism in cohesive soils. As observed from this study, the term would be depending on the pile slenderness ratio, L/D, in addition to the vertical load acting at the pile head. The corrected ultimate lateral capacity, p^*_{ult}, could then be written,

$$p^*_{ult} = \alpha(Vc, L/D) \quad p_{ult} \tag{7.4}$$

Several attempts were performed to create a slice in Plaxis 3D. Slice model 2 was able to represent an effect of vertical loading on the lateral capacity, however, the effect was limited. From the analyses of the full length of the pile, significantly higher reductions in the lateral capacities were observed for lateral deflections of 0.04D, then for the model only representing the flow-around failure mechanism. Slice model 2 is not able to capture the effect of vertical loading on the lateral response, and the model can not be used for proposing a correction factor to account for vertical loading on the lateral p-y curves.

Chapter 8

Conclusion

In the p-y curve methodology, interaction effects between vertical and lateral loading are neglected. The purpose of this study was to investigate the effect of vertical loading on the lateral pile behaviour and to see if it was possible to propose a correction factor to account for the effect of vertical load on the lateral p-y curves. Deriving p-y curves based on a full three-dimensional finite element analysis is a time-consuming process, as a large number of analyses is required to test for different loads, and load combinations. Therefore, it would be a great benefit to use simplified methods to investigate the effect of vertical loading on the lateral p-y curves. A method of representing the flow-around failure mechanism governed at deeper depths was used to derive p-y curves in this study.

In this study, a large diameter pile installed in an isotropic homogeneous cohesive soil was analysed. The full length of the pile was modelled to investigate the effect of vertical loading on the lateral response of the pile. This resulted in a reduction in the lateral capacity of up to 17% for static vertical loads of 80% of the vertical capacity. The presence of vertical loads decreases the lateral capacity of the pile. In addition, the effect of the undrained shear strength and the pile slenderness ratio were investigated. The undrained shear strength was not observed to affect the obtained results. However, for higher slenderness ratios, the effect of vertical loading on the lateral response decreased, and for a slenderness ratio of $L/D = 15$ only marginal reductions in the lateral capacity was observed for the prescribed displacement evaluated.

The p-y curves were derived from a pile slice representing the flow-around failure mechanism. Two methods of creating a pile slice with both static vertical and lateral loading simultaneously were tested in Plaxis 3D. This was done by modelling the full length of the pile for vertical loading before creating a slice. For both models, the ultimate lateral capacity for pure lateral loading was verified with theory. One of the models was able to represent an effect on the ultimate lateral capacity for combined static vertical and lateral loading. The effect of vertical loading on the lateral p-y curves appeared to be limited, and a reduction of up to 5% was observed for vertical loads of 80% of the vertical capacity. Although the effect was limited, a decreasing effect of the vertical loading was observed for higher slenderness ratios, similar to the results obtained from the model of the full length of the pile. Several analyses were conducted to evaluate the results obtained from the slice model. The findings from the study indicate that the flow-around failure mechanism represented by a slice in Plaxis 3D is dominated by the soil not

affected by vertical loading.

The p-y curves derived from the slice method is used in a Winkler-spring model, where Euler-Bernoulli beam theory is used for the pile. It is questioned whether this theory is applicable to large diameter piles as studied in this project. Nevertheless, the horizontal flow-around soil failure mechanism represented by a slice in Plaxis 3D is not able to represent the effect of vertical loading on the lateral p-y curves.

From the FE analyses of the full length of the pile, the reduction in the lateral capacity is only observed to be significant for vertical loads above 60% of the vertical capacity. For offshore wind turbines, the static vertical load is coming from the weight of the turbine and the structure itself. Hence, offshore wind turbines are lightweight structures compared to other offshore structures. The vertical load is low compared to the vertical capacity of the foundation, and the vertical load is not expected to exceed 60% of the vertical capacity. Therefore, a correction factor for the ultimate lateral capacity might not be necessary for offshore wind turbines. Furthermore, as illustrated from the results of the full model, the effect of vertical loading decreases for higher slenderness ratios. Therefore, it might not be necessary with a correction factor for slender piles used for other offshore structures, although the piles are exposed to significantly higher vertical loads.

Nevertheless, the results of this study indicate that the vertical and lateral behaviour for slender piles is nearly uncoupled. For non-slender piles, however, the vertical and lateral behaviour appears to be highly coupled for vertical loads above 60% of the vertical capacity, and neglecting the effect of vertical loading on the lateral behaviour leads to an erroneous representation of the pile behaviour.

Chapter 9

Recommendations for further work

The results from this study indicates that effect of vertical loading on lateral p-y curves needs to be assessed from a full three-dimensional finite element analysis. Due to the coronavirus outbreak during the spring of 2020, this semester provided some challenges and set some constraints on the work. The aim of this study was to be able to provide a correction factor to account for the effect of vertical loading on the lateral p-y curves. However, the p-y curves derived in this study was not able to represent the effect of vertical loading. The existing studies on the subject are rather limited and inconsistent. This empathises the importance of investigating the effect of vertical loading on the lateral response further.

9.1 Further work

The following is recommended for further work

- For higher slenderness ratios, the effect of vertical loading on the lateral response is limited. A further study of different slenderness ratios is recommended to evaluate when the effect of vertical loading on the lateral response is of importance.
- The effect of vertical loading should be evaluated by deriving p-y curves from the full length of the pile. Furthermore, investigate if it is possible to propose a correction factor to account for vertical loading on the lateral response.
- If p-y curves are derived from the full length of the pile, the effect of the vertical load on the lateral p-y curves should be employed in integrated analysis, to see the impact on the structural behaviour of offshore wind turbines. As the offshore wind turbines are dynamically sensitive structures, the sensitivity to a potential reduction in the lateral capacity and changes in the initial stiffness should be investigated. RIFLEX, as mentioned in Chapter 2, could be used for this purpose. It would be interesting to investigate the effect on the natural frequency of the support structure. A change in the foundation stiffness could lead to significant

changes in the natural frequency of the offshore wind turbine. A change in the natural frequency could bring the natural frequency of the structures closer to the excitation frequency.

References

Anagnostopoulos, C., & Georgiadis, M. (1993). Interaction of Axial and Lateral Pile Response. *Journal of Geotechnical Engineering*, *119*(4), 793–798.

Bell, K. (2014). *An engineering approach to FINITE ELEMENT ANALYSIS of linear structural mechanics problems*. Fagbokforlaget.

Brinkgreve, R. (2019). PLAXIS 3D CONNECT Edition V20.

De Vries, W. (2011). *Final Report WP 4.2: Support Structure Concepts for Deep Water Sites* (Tech. Rep.). Delft University of Technology.

DNV. (2014). *DNV-OS-J101 Design of Offshore Wind Turbine Structures*. Det Norske Veritas AS.

Dogger Bank Wind Farm. (2020). Accessed: 2020-04-15. Retrieved from `https://doggerbank.com/`

Equinor. (2018). *Arkona offshore windfarm*. Accessed: 2020-04-15. Retrieved from `https://www.equinor.com/en/news/arkona-offshore-windfarm-online.html`

Hazzar, L., Hussien, M. N., & Karray, M. (2017). Influence of vertical loads on lateral response of pile foundations in sands and clays. *Journal of Rock Mechanics and Geotechnical Engineering*, *9*, 291–304.

Karthigeyan, S., Ramakrishna, V. V. G. S. T., & Rajagopal, K. (2007). Numerical Investigation of the Effect of Vertical Load on the Lateral Response of Piles. *Journal of Geotechnical and Geoenvironmental Engineering*, *133*(5), 512–521.

Matlock, H. (1970). Correlations for Design of Laterally Loaded Piles in Soft Clay. In *Proceedings of the second annual offshore technology conference* (pp. 577–594). Offshore Technology Conference.

Nordal, S., Eiksund, G. R., & Grimstad, G. (2016). *TBA 5100 Theoretical Soil Mechanics*. Geotechnical Division - NTNU.

Page, A. M., Schafhirt, S., Eiksund, G. R., Skau, K. S., Jostad, H. P., & Sturm, H. (2016). Alternative Numerical Pile Foundation Models for Integrated Analyses of Monopile-based Offshore Wind Turbines. In *Proceedings of the twenty-sixth international offshore and polar engineering conference* (pp. 111–119). International Society of Offshore and Polar Engineers (ISOPE).

Plaxis | Modelling soil-structure interaction: interfaces. (2012). Accessed: 2020-05-10. Retrieved from `https://www.plaxis.com/support/tips-and-tricks/modelling-soil-structure-interaction-interfaces/`

Poulos, H. G., & Hull, T. S. (1989). The Role of Analytical Geomechanics in Foundation Engineering. In *Proceedings of congress on foundation engineering: Current principles and practices* (pp. 1578–1606). ASCE.

Ramirez, L., Fraile, D., & Brindley, G. (2020). *Offshore wind in Europe - Key trend and statistics 2019*. Accessed: 2020-04-25. Retrieved from https://windeurope.org/wp-content/uploads/files/about-wind/statistics/WindEurope-Annual-Offshore-Statistics-2019.pdf

Randolph, M., & Gourvenec, S. (2011). *Offshore Geotechnical Engineering*. Spon Press.

Randolph, M. F., & Houlsby, G. T. (1984). Limiting Pressure on a Cricular Pile Loaded Laterally in Cohesive Soil. *Geotechnique*, *34*(4), 613–623.

Reese, L. C., Cox, W. R., & Koop, F. D. (1975). Field Testing and Analysis of Laterally Loaded Piles in Stiff Clay. In *Proceedings of the seventh annual offshore technology conference* (pp. 671–690). Offshore Technology Conference.

Reese, L. C., & Van Impe, W. F. (2011). *Single Piles and Pile Groups Under Lateral Loading* (2nd ed.). CRC Press/Balkema.

Renewable energy directive. (2020). Accessed: 2020-04-15. Retrieved from https://ec.europa.eu/energy/topics/renewable-energy/renewable-energy-directive/overview_en

SINTEF-Ocean. (2019). RIFLEX 4.17.0 User Guide.

Skau, K. S., Page, A. M., Kaynia, A. M., Løvholt, F., Norén-Cosgriff, K., Sturm, H., … Eichler, D. (2018). *REDWIN - REDucing cost in offshore WINd by integrated structural and geotechnical design* (Tech. Rep.). NGI.

Sørensen, S. P. H., Brødbaek, K. T., Møller, M., & Augustesen, A. H. (2012). *Review of laterally loaded monopiles employed as the foundation for offshore wind turbines* (Tech. Rep.). Aalborg University.

Spyder. (2020). *Spyder Website*. Accessed: 2020-05-09. Retrieved from https://www.spyder-ide.org/

Tomlinson, M. J. (2001). *Foundation Design and Construction* (7th ed.). Prentice Hall.

WindEurope. (2020). *History of Europe's Wind Industry*. Accessed: 2020-04-25. Retrieved from https://windeurope.org/about-wind/history/

Zhang, Y., & Andersen, K. H. (2017). Scaling of lateral pile p-y response in clay from laboratory stress-strain curves. *Marine Structures*, *53*, 124–135.

Appendices

The appendices include the following

- Appendix A: Vertical capacity analyses
- Appendix B: Lateral response to axial loading
- Appendix C: Slice model 2
- Appendix D: Scripts for modelling in Plaxis 3D

Appendix A

Vertical capacity analyses

The vertical capacities are calculated from applying a surface load at the top of the pile in Plaxis 3D. The purpose of using a surface load is to distribute the stresses at the top of the pile evenly. As the loading type is *Stage construction*, the stage construction calculation is controlled by the total multiplier $\sum M_{stage}$. This multiplier starts from zero at the beginning of the phase, and stepwise increase to the ultimate level. The ultimate level is generally equal to $\sum M_{stage} = 1$, as this indicates that the current stage construction phase is finished. If a stage construction phase has not reached the ultimate level, failure of the soil body has occurred during the calculation. This is used for calculating the vertical capacity of the pile. The maximum load taken by the pile is extracted by using the output of the reached $\sum M_{stage}$ and multiplying by the added load.

The vertical capacity is calculated based on the following equation,

$$F_z = 2 \sum M_{stage} \sigma_z A_{load} \tag{A.1}$$

where F_z is the vertical capacity of the pile, σ_z is the stress applied, and the A_{load} is the area where the stress is applied, here $A_{load} = A_{pile}/2 = \frac{\pi}{4} D^2/2$, and D is the diameter of the pile. The total force is multiplied by two as only half of the pile is modelled. If multiple load steps, n, are applied, Plaxis 3D will apply the difference between the load steps, and the vertical capacity is calculated based on the following equation,

$$F_z = 2[M_{stage,1} \sigma_{z,1} + \sum_{i=2}^{n} M_{stage,i} (\sigma_{z,i} - \sigma_{z,i-1}] A_{load} \tag{A.2}$$

Appendix B

Lateral response to axial loading

B.1 Effect of undrained shear strength

The lateral capacities for lateral deflection of 0.04D with combined vertical and lateral loading for different undrained shear strengths are presented in Table B.1.

Table B.1: The lateral capacities for lateral deflection of 0.04D with combined vertical and lateral load

	Lateral capacity				
Undrained shear strength	0Vc	0.2Vc	0.4Vc	0.6Vc	0.8Vc
$s_u = 20kPa$	6 342	6 306	6 186	5 928	5 318
$s_u = 40kPa$	12 190	12 128	11 916	11 386	10 258
$s_u = 60kPa$	17 470	17 412	17 064	16 325	14 648
$s_u = 80kPa$	22 228	22 170	21 823	20 789	18 619
$s_u = 100kPa$	26 784	26 784	26 089	24 945	22 323

Figure B.1, B.2, B.3, B.4, and B.5 presents the lateral force - displacement for undrained shear strength of $s_u = 20kPa$, $s_u = 40kPa$, $s_u = 60kPa$, $s_u = 80kPa$, $s_u = 100kPa$ for lateral deflection of 0.04D.

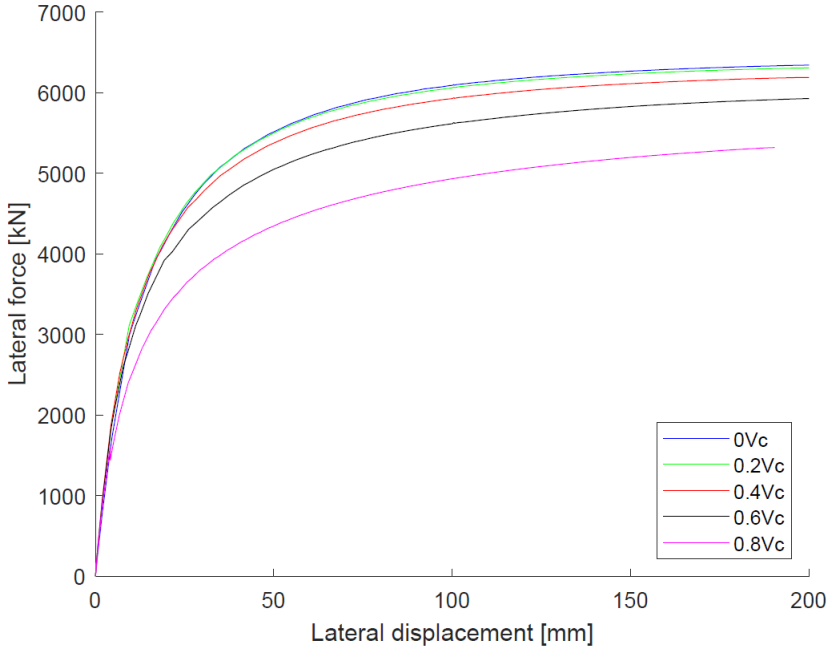

Figure B.1: Lateral force-displacement for $s_u = 20kPa$

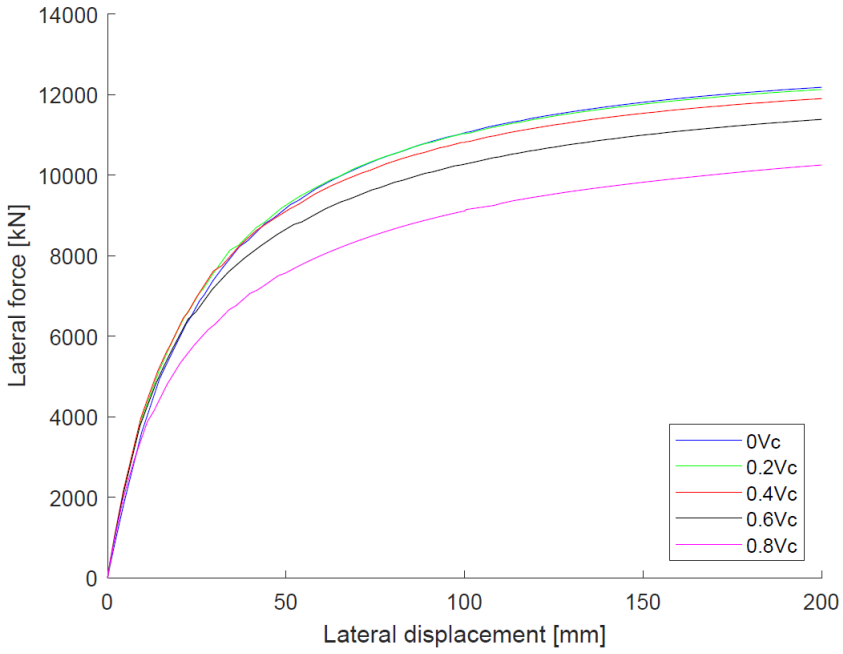

Figure B.2: Lateral force-displacement for $s_u = 40kPa$

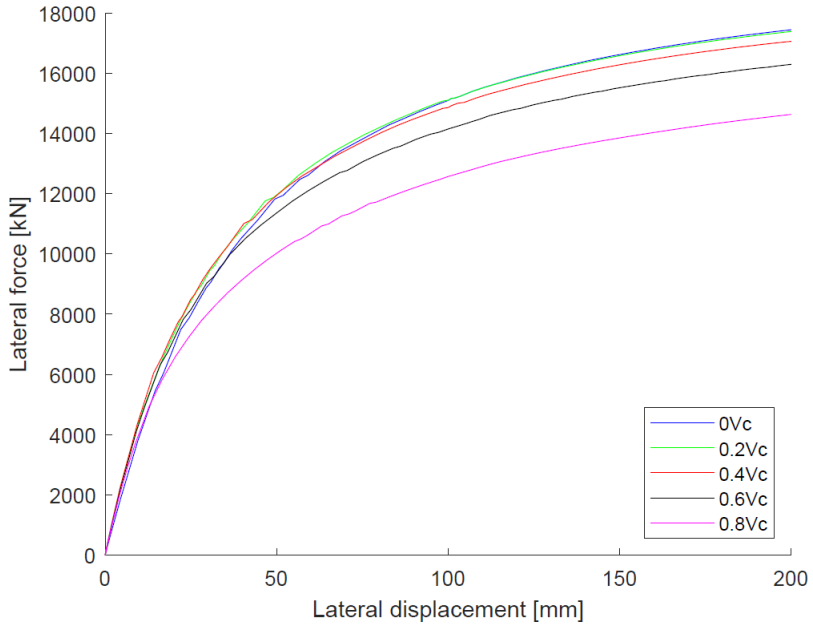

Figure B.3: Lateral force-displacement for $s_u = 60kPa$

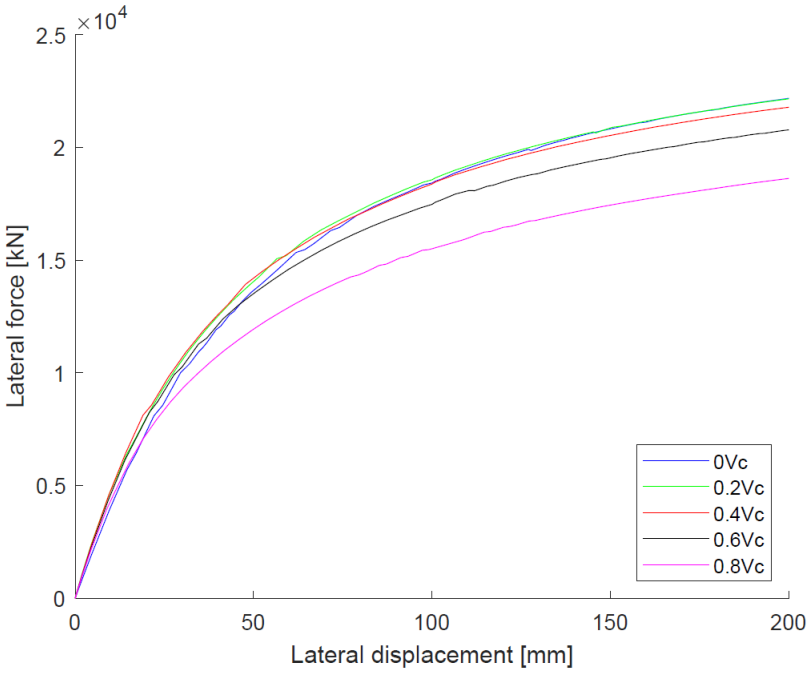

Figure B.4: Lateral force-displacement for $s_u = 80kPa$

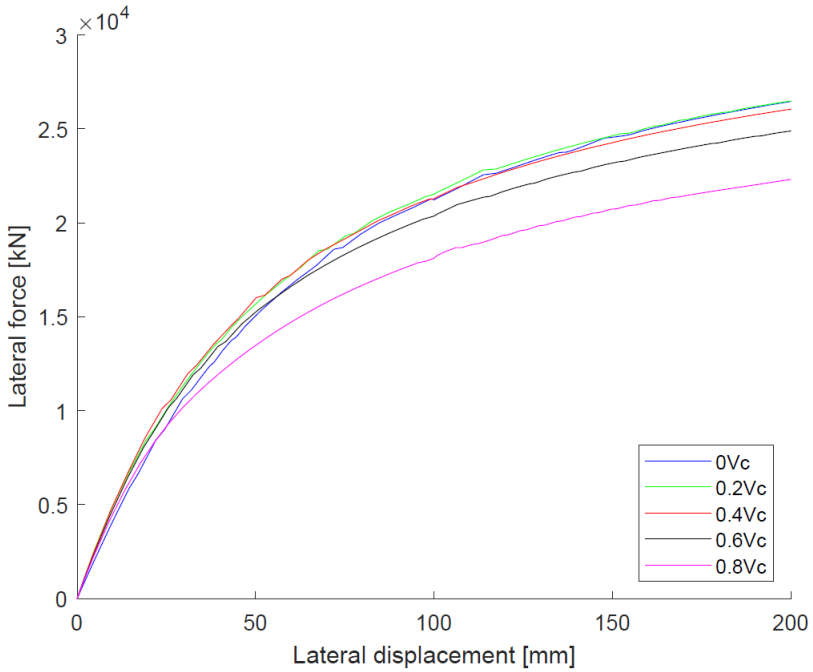

Figure B.5: Lateral force-displacement for $s_u = 100kPa$

B.2 Effect of increasing undrained shear strength

A vertical capacity analysis was performed for a model with increasing undrained shear strength. The vertical capacity calculated is presented in Table B.2 with the theoretical lower and upper limit.

Table B.2: The vertical capacity for increasing undrained shear strength of $s_u = 30kPa + 4kN/m^3 * z$

		Theoretical vertical capacity [kN]	
Model	Vertical capacity [kN]	Low	High
$s_u = 30kPa + 4kN/m^3 * z$	32 936	30 041	35 343

The lateral capacities for lateral deflection of 0.04D with combined vertical and lateral loading is presented in Table B.3 and Figure B.6.

Table B.3: The lateral capacities for lateral deflection of 0.04D with combined vertical and lateral load for $s_u = 30kPa + 4kN/m^3 * z$

	Lateral capacity				
Model	0Vc	0.2Vc	0.4Vc	0.6Vc	0.8Vc
$s_u = 30kPa + 4kN/m^3 * z$	14 866kN	14 854kN	14 549kN	13 764kN	12 416kN

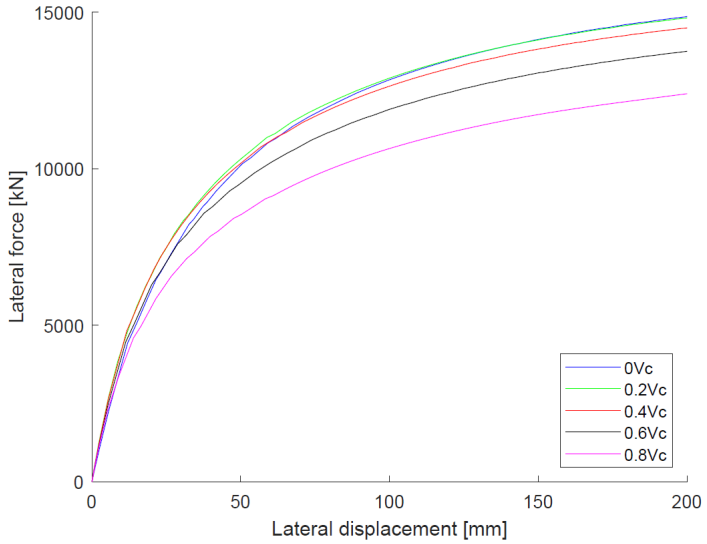

Figure B.6: Lateral force-displacement for increasing undrained shear strength

B.3 Effect of L/D-ratio

The lateral capacities for lateral deflection of 0.04D with combined vertical and lateral loading for different slenderness ratios are presented in Table B.4. The lateral force-displacement is presented in Figure B.7, B.8, B.9, and B.10 for $L/D = 3$, $L/D = 5$, $L/D = 10$, and $L/D = 15$ respectively.

Table B.4: The lateral capacities for lateral deflection of 0.04D with combined vertical and lateral load

	Lateral capacity				
Slenderness ratio	0Vc	0.2Vc	0.4Vc	0.6Vc	0.8Vc
$L/D = 3$	17 470	17 412	17 064	16 325	14 648
$L/D = 5$	10 077	10 064	9 939	9 588	8 615
$L/D = 10$	4 853	4 868	4 870	4 801	4 566
$L/D = 15$	2 754	2 766	2 794	2 783	2 733

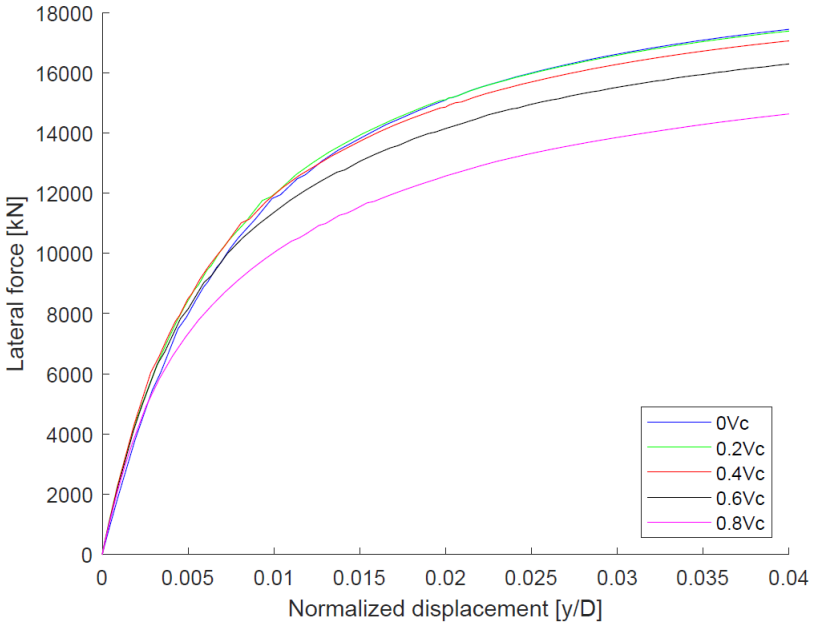

Figure B.7: Lateral force - displacement for $L/D = 3$

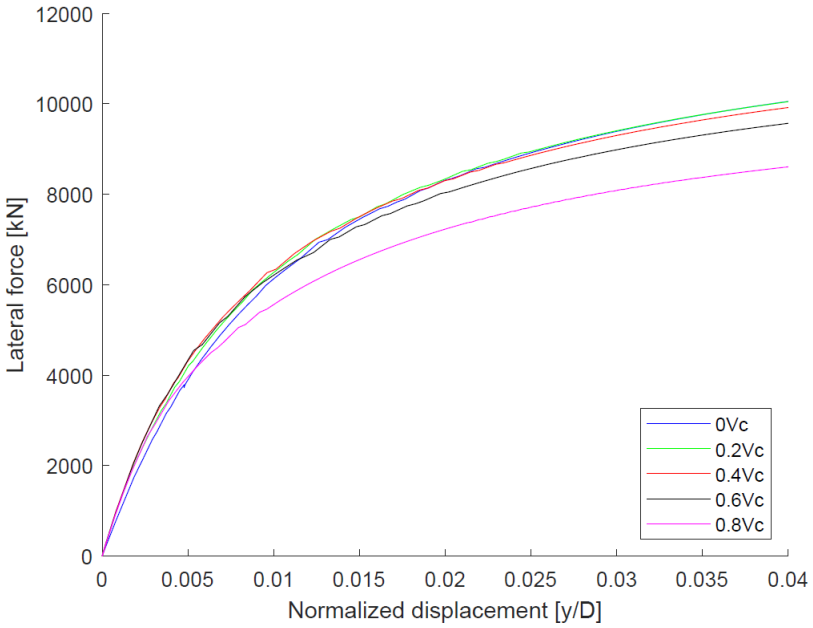

Figure B.8: Lateral force - displacement for $L/D = 5$

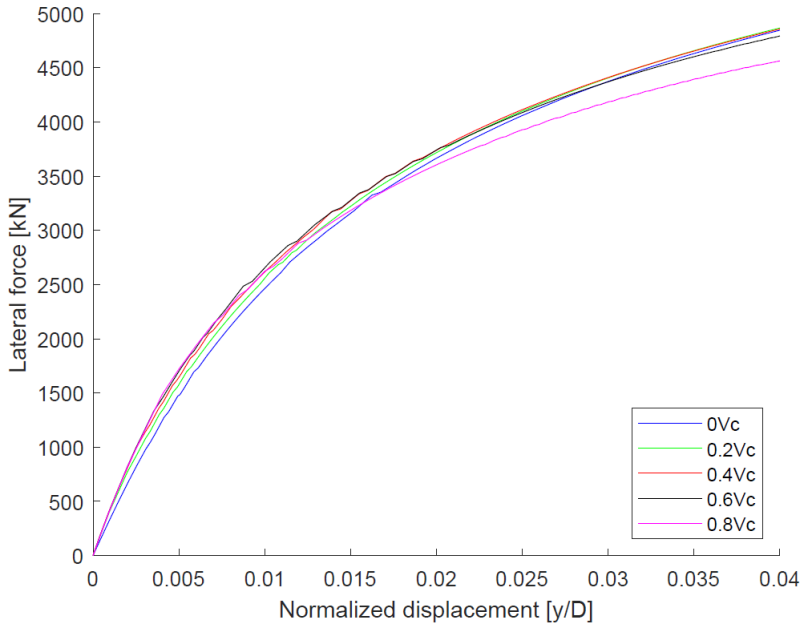

Figure B.9: Lateral force - displacement for $L/D = 10$

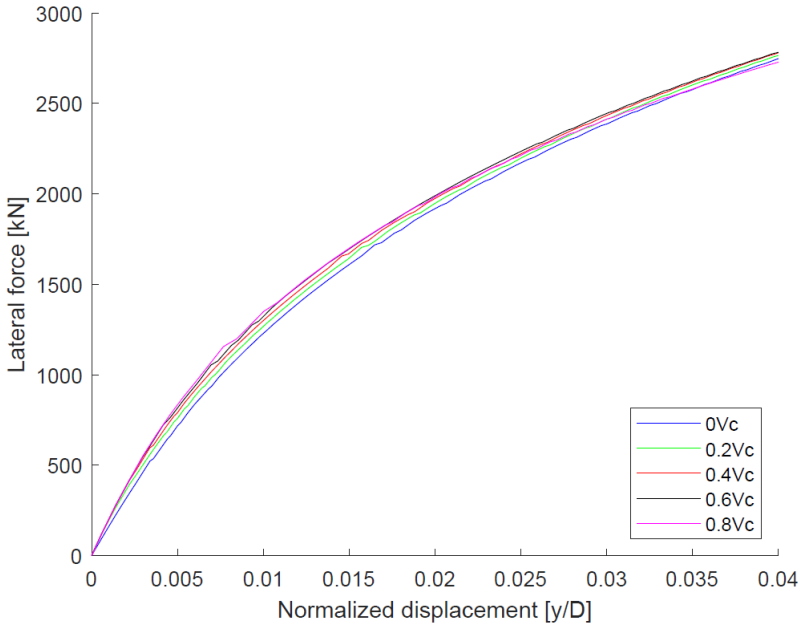

Figure B.10: Lateral force - displacement for $L/D = 15$

B.4 A model with an undrained shear strength of $s_u = 10kPa$

A vertical capacity analysis was performed for a model with an undrained shear strength of $s_u = 10kPa$. A vertical capacity of $F_z = 4398kN$ was calculated. Table B.5 and Figure B.11 present the lateral capacities for lateral deflection of 0.04D with combined vertical and lateral loading. The reduced capacity is presented in Table B.6.

Table B.5: The lateral capacity for lateral deflection of 0.04D with combined vertical and lateral load for $s_u = 10kPa$

	Lateral capacity				
Model	0Vc	0.2Vc	0.4Vc	0.6Vc	0.8Vc
$s_u = 10kPa$	3 214kN	3 203kN	3 162kN	3 073kN	2 890kN

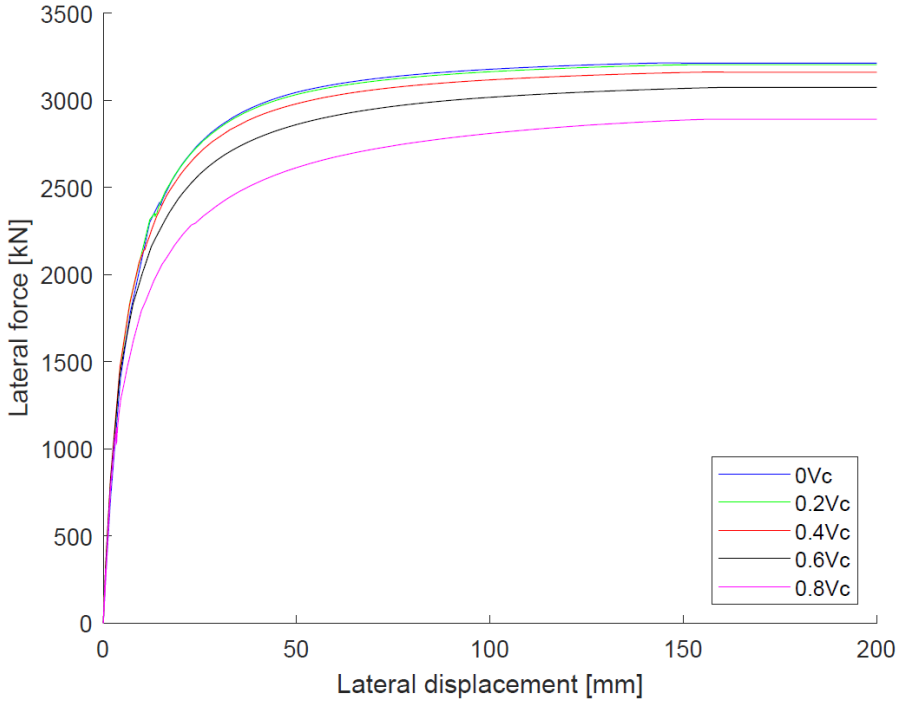

Figure B.11: Lateral force-displacement for $s_u = 10kPa$

Table B.6: The reduced lateral capacity for lateral deflection of 0.04D with combined vertical and lateral load for $s_u = 10kPa$

	Reduced lateral capacity [%]				
Model	0Vc	0.2Vc	0.4Vc	0.6Vc	0.8Vc
$s_u = 10kPa$	100	99.66	98.36	95.62	89.91

Appendix C

Slice model 2

C.1 Verification of Slice model 2

Slice model 2 is modelled with interfaces to allow for independent lateral displacement from the rest of the model. As this model is not only represented by a slice, several analyses were done to confirm the results obtained from the model.

Vertical displacement field

The vertical displacement field is presented in Figure C.1 for vertical loading. The vertical displacement field is presented with horizontal interfaces activated with material properties same as adjacent soil during vertical loading of the pile. This was done as the presence of the horizontal interfaces resulted in numerical issues. Therefore activating the interfaces with same material properties as the adjacent soil was done, and controlled by evaluating the displacement field. As can be observed from the figure, the interfaces does not affect the results.

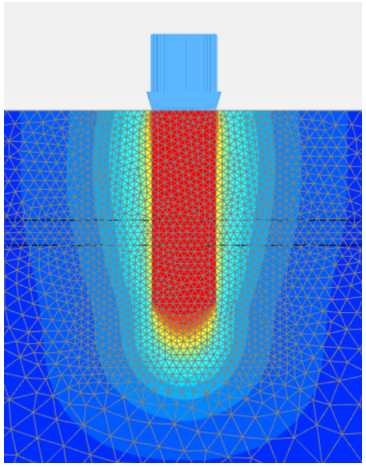

Figure C.1: Vertical displacement field, u_z, for vertical loading

Lateral displacement field

The lateral displacement field for a prescribed displacement of $u_x = 0.4m$ is illustrated in Figure C.2. The lateral displacement field is presented for only the slice to illustrate the symmetrical displacement field for the flow-around soil failure mechanism in Figure C.3.

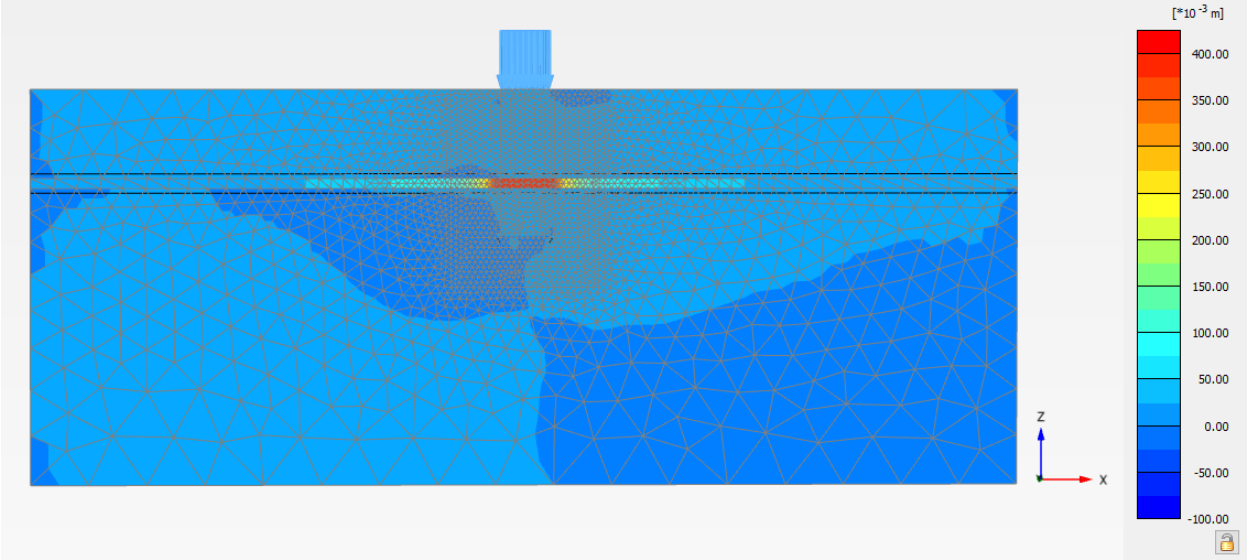

Figure C.2: The lateral displacement field for a prescribed displacement with vertical loading

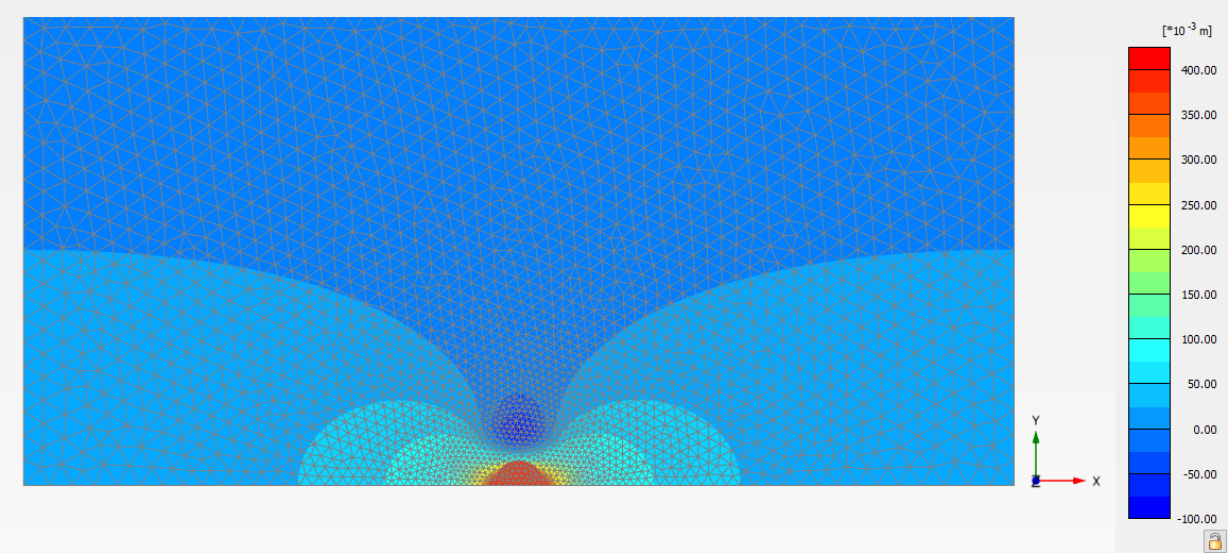

Figure C.3: The lateral displacement field for the slice with vertical loading

Comparison to Slice model 1

The p-y curves for pure lateral loading from Slice model 2 and Slice model 1 are compared. The purpose is to evaluate the effect of the interfaces used to create Slice model 2, on the ultimate lateral capacity. The results are presented in Figure C.4, and the resulting bearing capacity factors are presented in Table C.1.

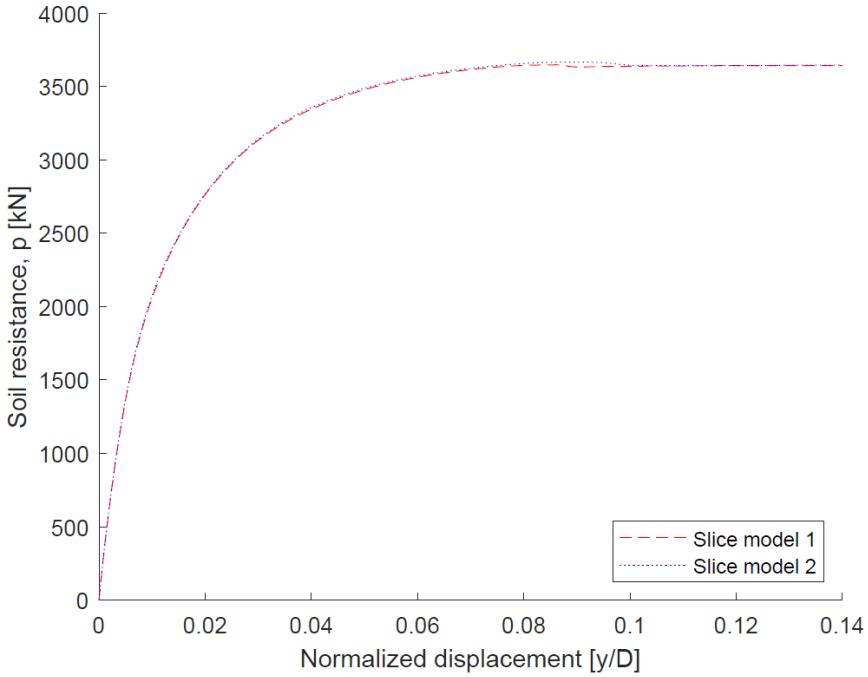

Figure C.4: Comparison of p-y curves from Slice model 1 and Slice model 2

Table C.1: Bearing capacity factor, N_p, for Slice model 1 and Slice model 2

Model	Bearing capacity factor, N_p
Slice model 1	12.14
Slice model 2	12.15

As can be observed, both models result in the same limiting bearing capacity factor with only marginal discrepancy.

Effect of initial stresses

The results obtained by Slice model 2 were controlled by analysing a model with zero-unit weight. The purpose of this was to evaluate if the initial stresses in the soil are affecting the results. The results are presented in Figure C.5, and the resulting bearing capacity factor is presented in Table C.2.

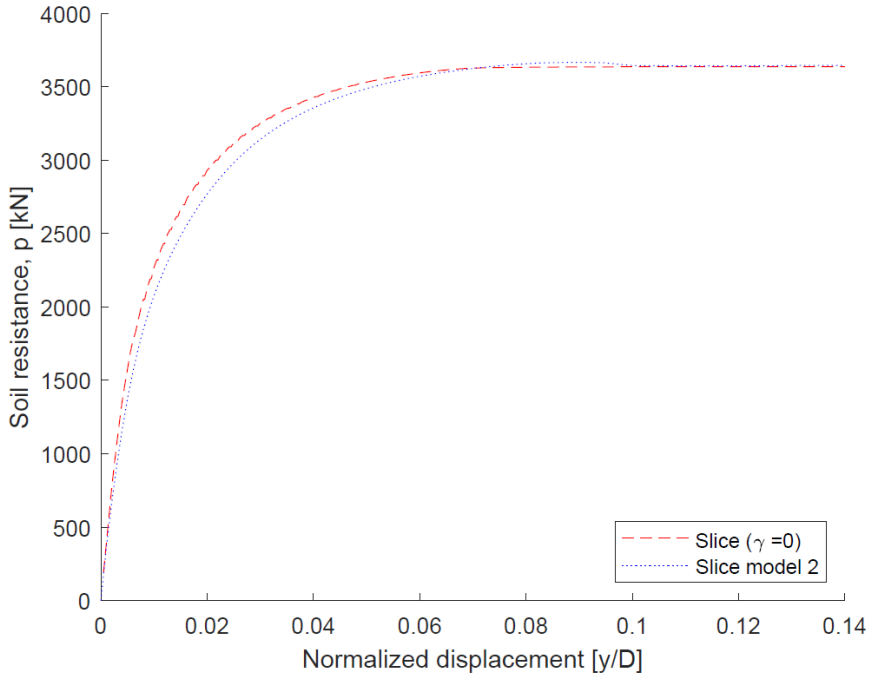

Figure C.5: Effect of initial stresses on the p-y curves

Table C.2: Bearing capacity factor, N_p, for Slice model 2 with a unit weight and with zero-unit weight

Model	Bearing capacity factor, N_p
Slice model 2 ($\gamma = 0$)	12.16
Slice model 2	12.15

As can be observed from Table C.2, the initial stresses are not affecting the obtained results from Slice model 2.

Only a slice model

In addition, only a slice with no unit wight was modelled to control the results. The results are given in Figure C.6 and Table C.3.

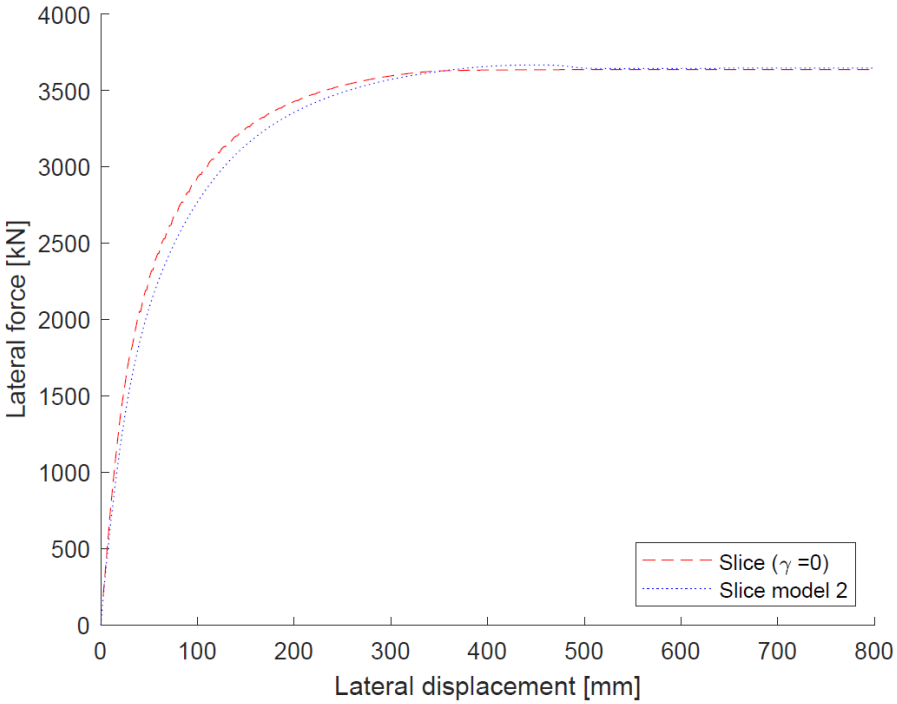

Figure C.6: Comparison of p-y curves from Slice model 2 and a slice model

Table C.3: Bearing capacity factor, N_p, for a slice model and Slice model 2

Model	Bearing capacity factor, N_p
Slice model ($\gamma = 0$)	12.12
Slice model 2	12.15

The slice model results in a numerical over-estimation of 1% compared to the theoretical solution of $N_p = 12$, and a 0.24% lower bearing capacity factor compared to Slice model 2.

Stress change

The vertical stress change for creating the slice, with activating interfaces and resetting displacements, is presented in this section. The results are extracted from Plaxis output. The results presented are from calculation Phases 2 and 3, as presented in Chapter 6. In Phase 2, a load is applied at the top of the pile, and in Phase 3 the displacements are reset and the interfaces are activated.

It should be noted that the phase name indicated at the top of the figures, does not necessarily mean that a load has been applied. The script is created for generating phases with vertical loading of 0Vc, 0.2Vc, 0.4Vc, 0.6Vc, and 0.8Vc. The calculation phases are presented in Figure C.7.

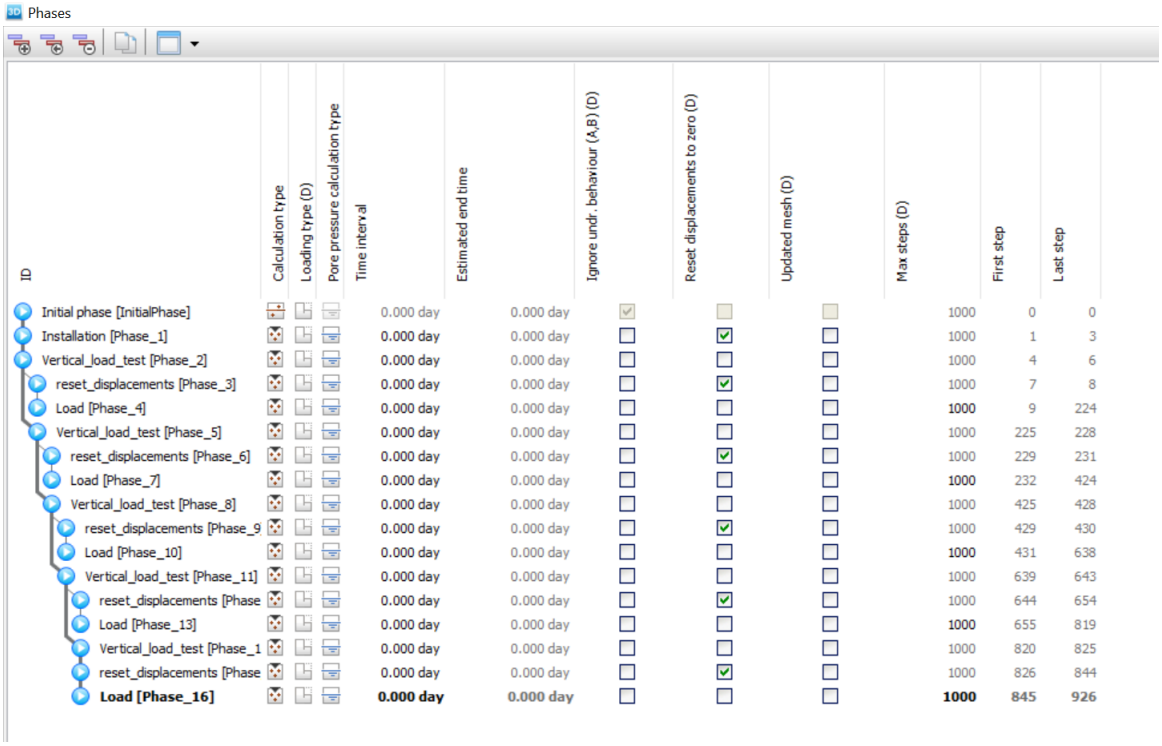

Figure C.7: Calculation phases in the model

The figures in this section are only presenting the stress change in the slice. The soil above and below is not shown, as the effect of activating the interfaces and resetting the displacements in the slice are of interest. By observing the maximum and minimum value indicated at the bottom of the figures, a marginal stress change is observed. It should be noted that for 0Vc the scale used is to illustrate the stress change over the slice created by the unit weight of the soil. As the slice is taken for depth 9 m to 10 m below the surface, the theoretical vertical stress, given by $\sigma_z = \gamma * z$, acting in the slice should be from $\sigma_z = 190kPa$ to $\sigma_z = 200kPa$. As observed from the figures, this is in agreement with the initial stresses calculated from FEA. For 0.2Vc, 0.4Vc, 0.6Vc and 0.8Vc, the stress-scale is the same.

Pure lateral loading (0Vc)

For pure lateral loading, no stress change is observed in the slice. This is illustrated in Figure C.8, and Figure C.9.

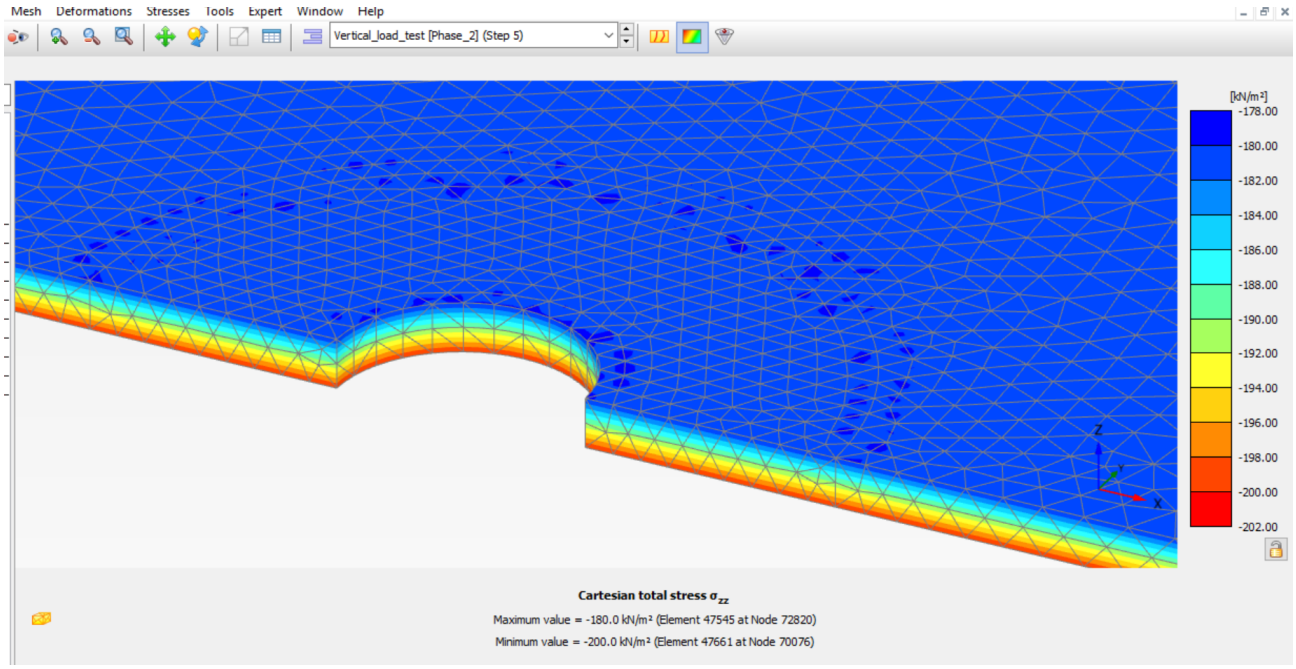

Figure C.8: Stresses in the slice for pure lateral loading

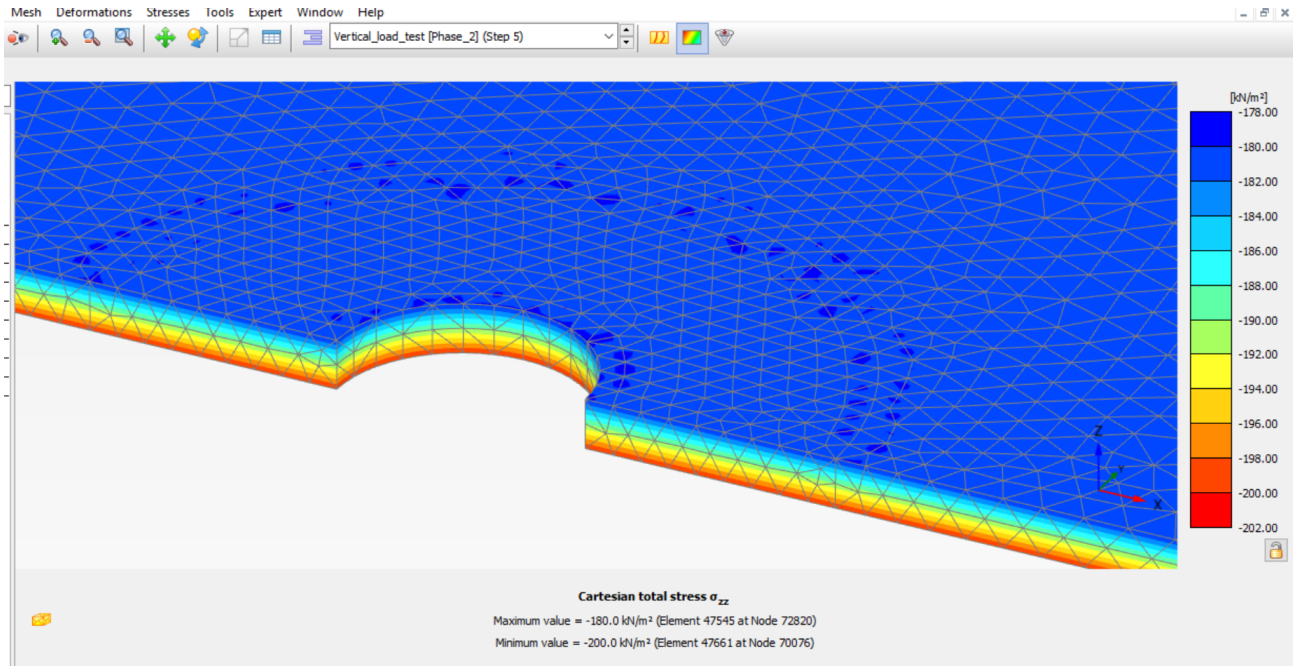

Figure C.9: Stresses in the slice for pure lateral loading, phase of resetting the displacement

0.2Vc lateral loading

For vertical loading of 0.2Vc, a marginal stress change is observed. This is illustrated in Figure C.10, and Figure C.11.

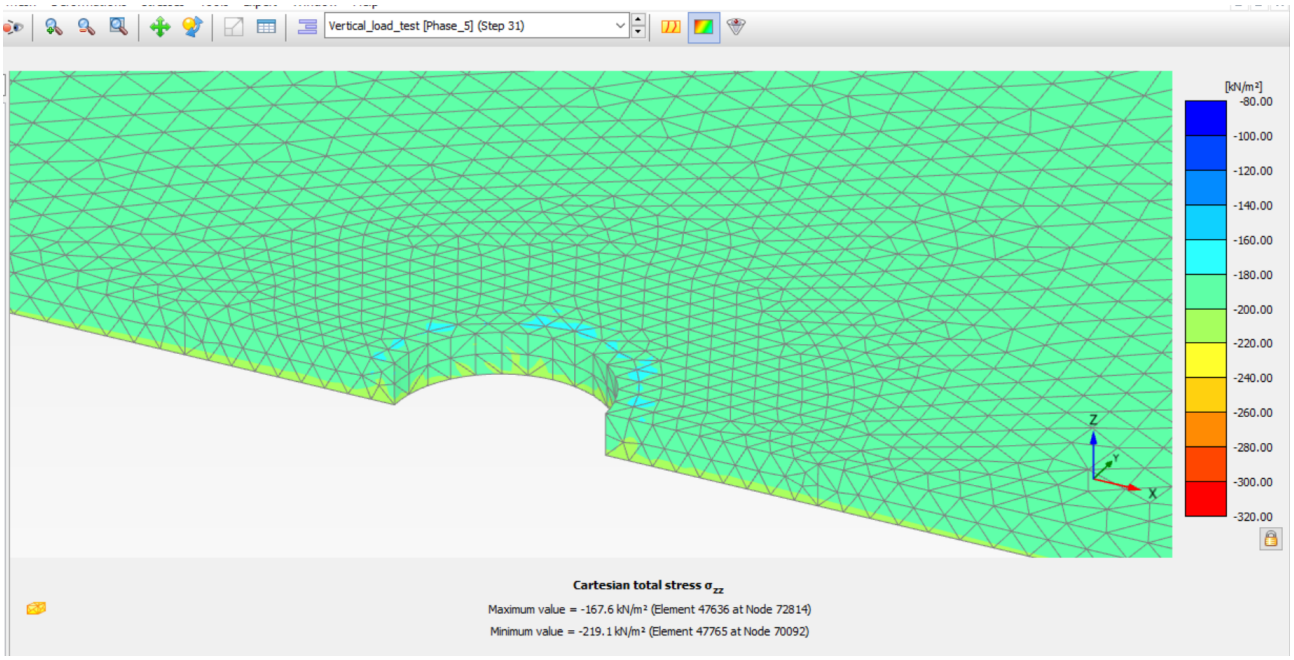

Figure C.10: Stresses in the slice for a vertical load of 0.2Vc

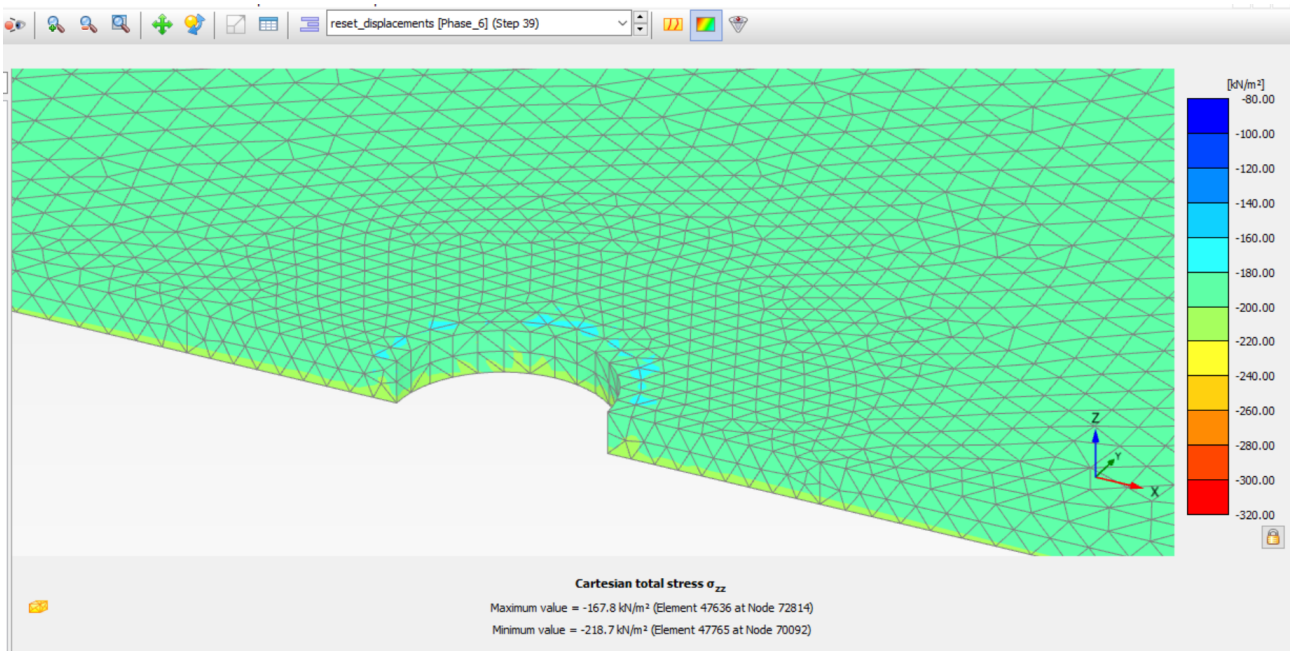

Figure C.11: Stresses in the slice for a vertical load of 0.2Vc, phase of resetting the displacement

0.4Vc lateral loading

For vertical loading of 0.4Vc, a marginal stress change is observed. This is illustrated in Figure C.12, and Figure C.13.

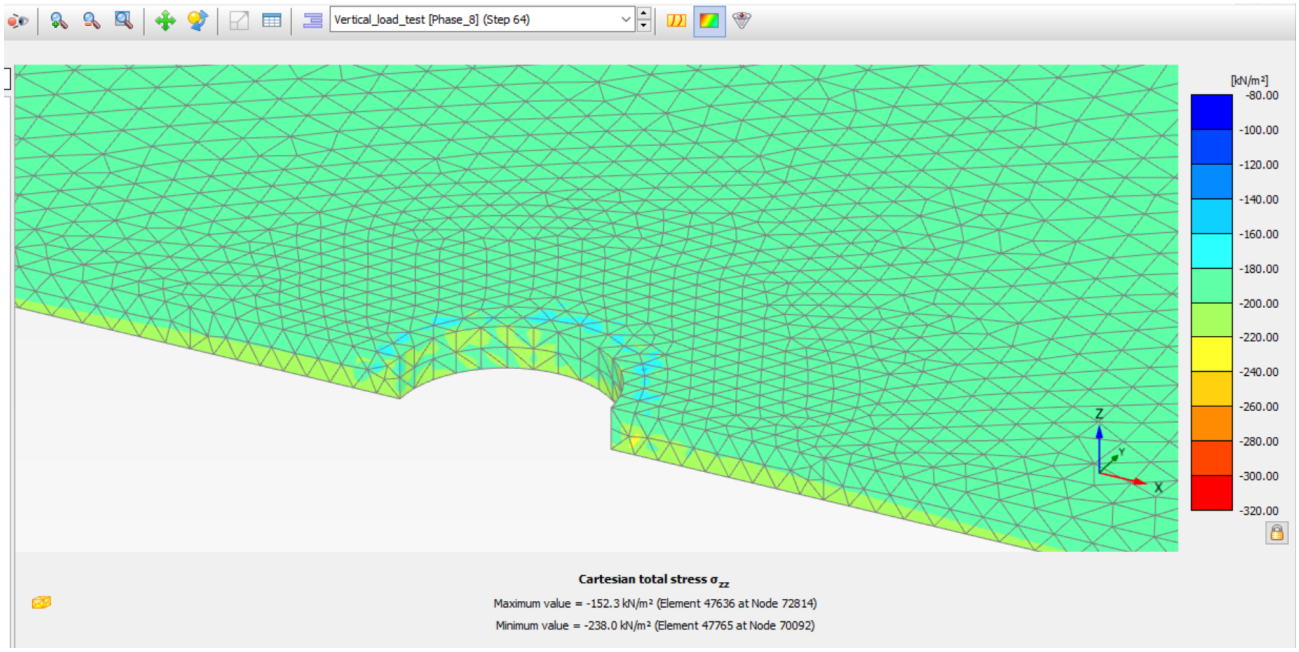

Figure C.12: Stresses in the slice for a vertical load of 0.4Vc

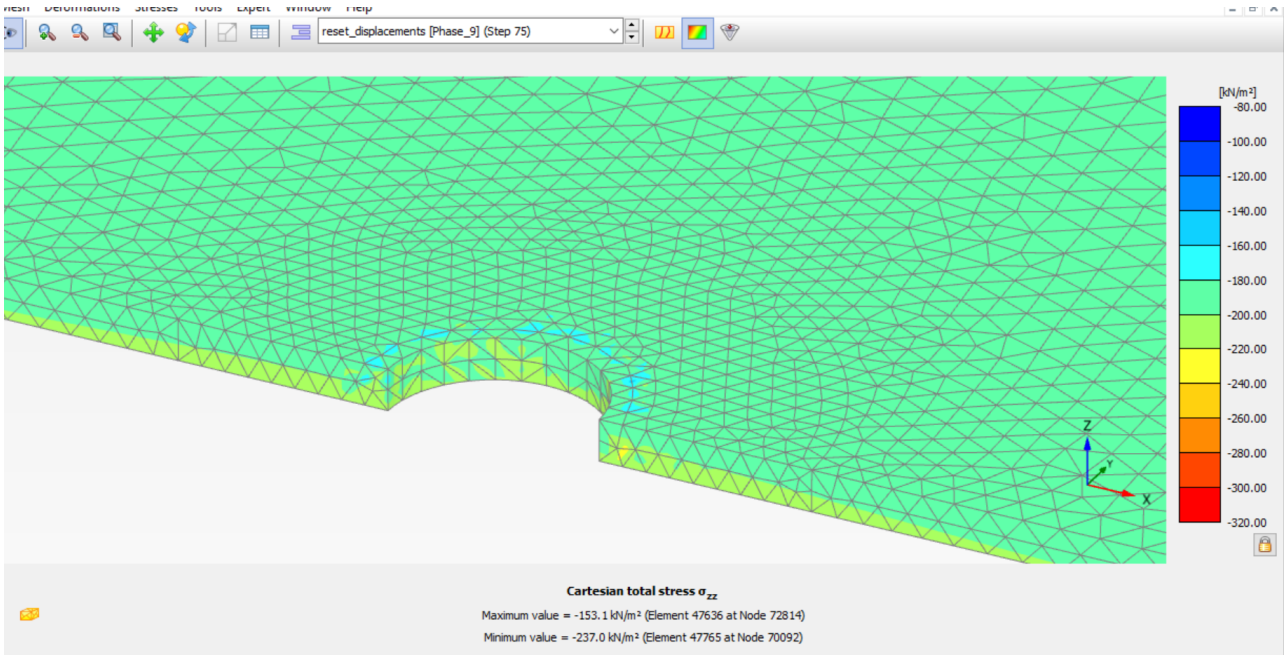

Figure C.13: Stresses in the slice for a vertical load of 0.4Vc, phase of resetting the displacement

0.6Vc lateral loading

For vertical loading of 0.6Vc, a marginal stress change is observed. This is illustrated in Figure C.14, and Figure C.15.

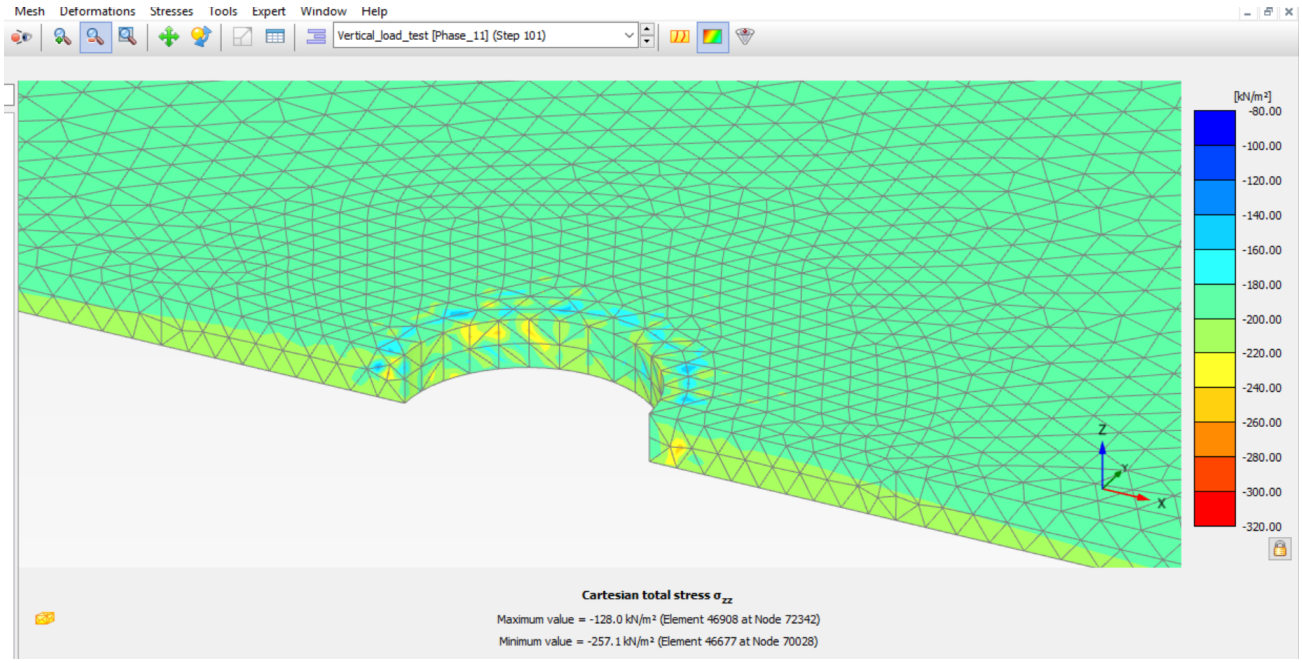

Figure C.14: Stresses in the slice for a vertical load of 0.6Vc

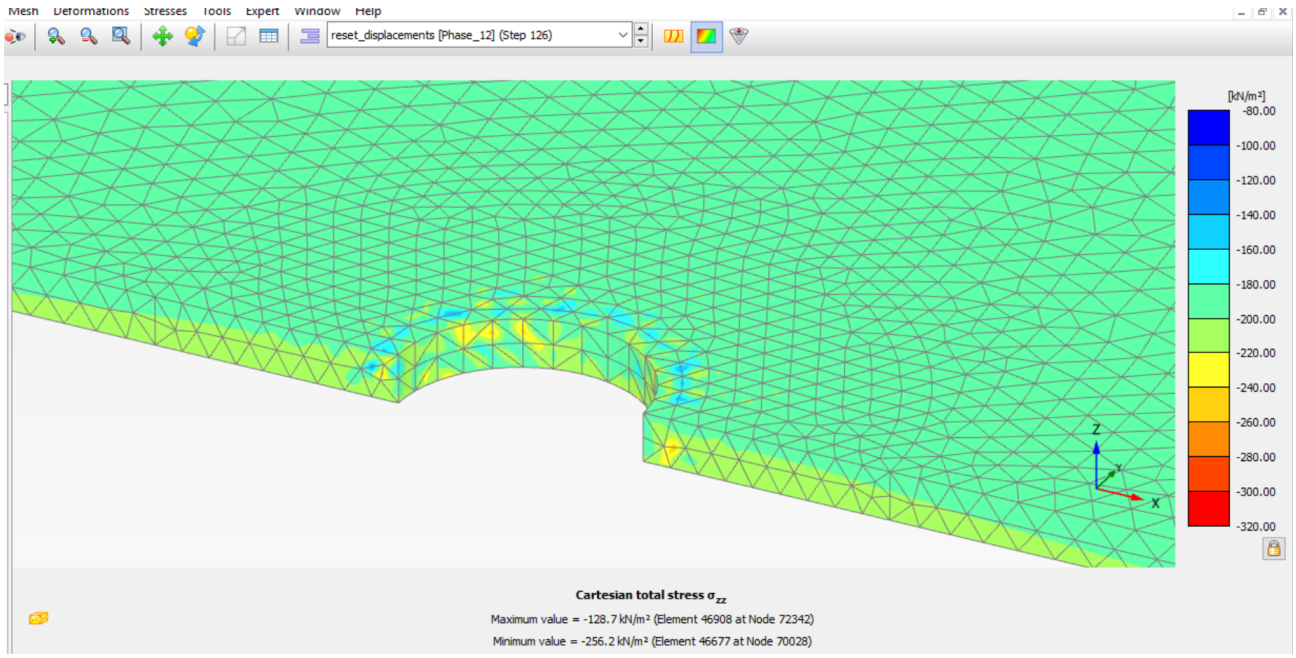

Figure C.15: Stresses in the slice for a vertical load of 0.6Vc, phase of resetting the displacement

0.8Vc lateral loading

For vertical loading of 0.8Vc, a marginal stress change is observed. This is illustrated in Figure C.16, and Figure C.17.

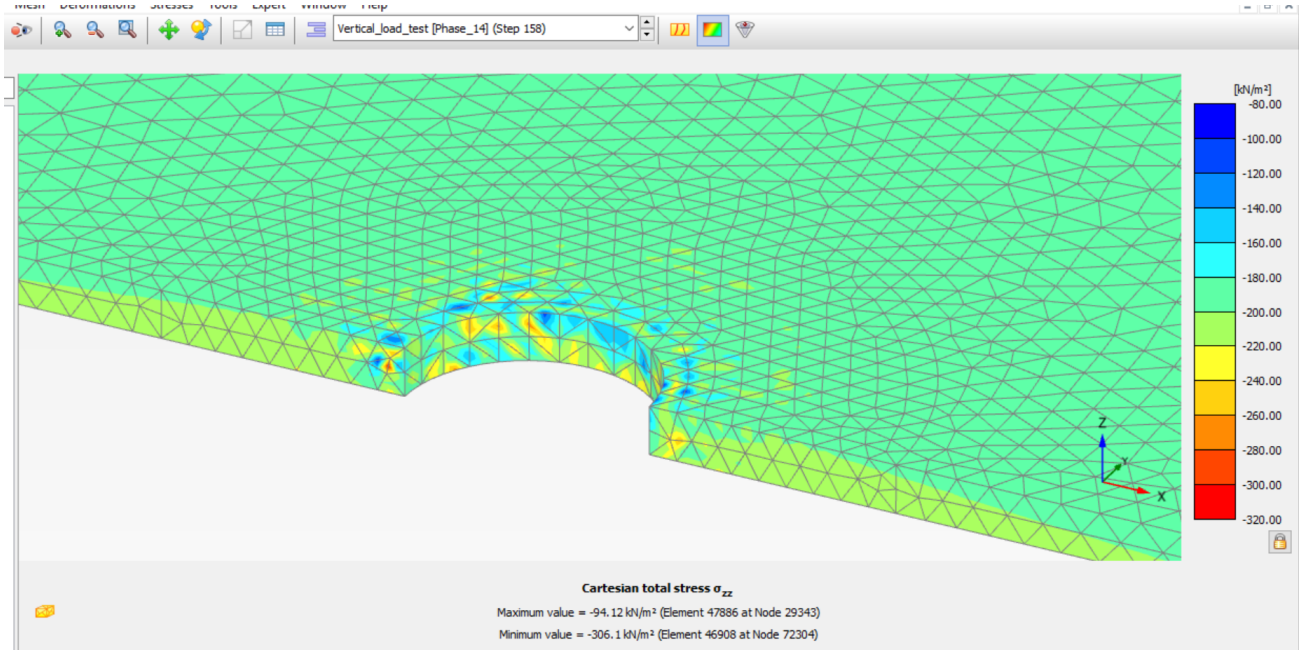

Figure C.16: Stresses in the slice for a vertical load of 0.8Vc

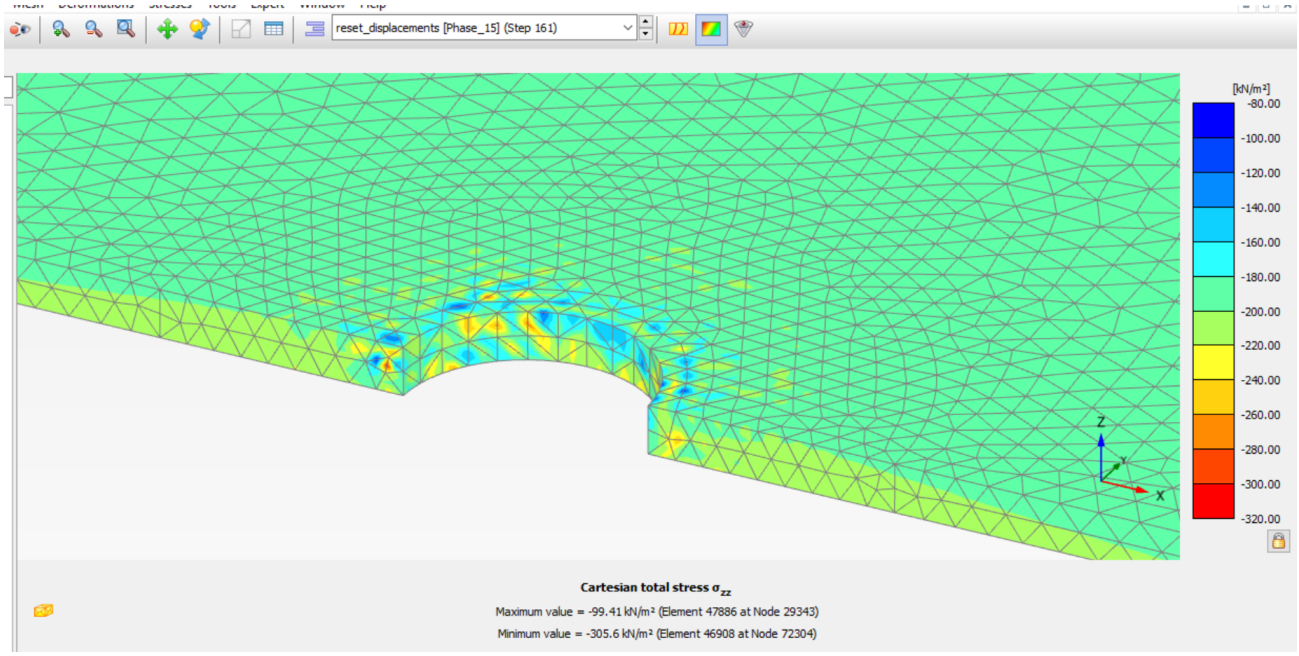

Figure C.17: Stresses in the slice for a vertical load of 0.8Vc, phase of resetting the displacement

C.2 NGI-ADP soil model

The soil parameters used for the NGI-ADP model is presented in Table C.4.

Table C.4: The stiffness parameters for the NGI-ADP model

NGI - ADP model		Clay
Unit weight of soil [kN/m^3]	γ	20
Ratio unloading/reloading shear modulus over (plane strain) active shear strength [−]	G_{ur}/Su^A	500
Shear strain at failure in triaxial compression [%]	γ_f^C	10
Shear strain at failure in triaxial extension [%]	γ_f^E	15
Shear strain at failure in direct simple shear [%]	γ_f^{DSS}	15
Reference (plane strain) active shear strength [$kN/m^2/m$]	$s_{u,ref}^A$	60
Reference depth [m]	y_{ref}	0
Increase of shear strength with depth [$kN/m^2/m$]	$s_{u,inc}^A$	0
Ratio of (plane strain) passive shear strength over (plane strain) active shear strength [−]	s_u^P/s_u^A	0,48
Initial mobilization [−]	τ_0/s_u^A	0
Ratio of direct simple shear strength over (plane strain) active shear strength [−]	s_u^{DSS}/s_u^A	0,67
Drainage Type		Undrained (C)

C.3 Slice from 2m to 3m below the surface

A slice at a depth of $z_{top} = -2m$ to $z_{bottom} = -3m$ was created to compare the results to the slice at depth $z_{top} = -9m$ to $z_{bottom} = -10m$. The results are presented in Table C.5 and Figure C.18.

Table C.5: The lateral capacity with combined vertical and lateral load for a new slice

	Lateral capacity				
Model	0Vc	0.2Vc	0.4Vc	0.6Vc	0.8Vc
New slice	3 639	3 633	3 622	3 587	3 475

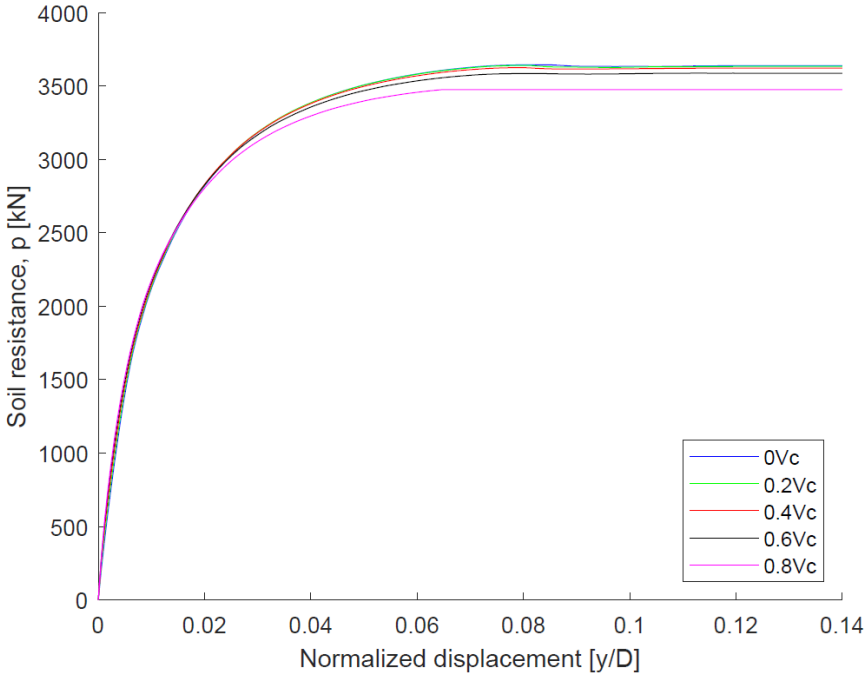

Figure C.18: Comparison of p-y curves with combined vertical and lateral loading for a new slice at depth 2 m to 3 m below the surface

C.4 Effect of higher mobilised side friction

Slice model 2 was used to evaluate the effect of higher mobilised side shear resistance. This was assessed by adding an interface with $R_{inter} = 0.01$ and low stiffness at the pile tip, to remove the base resistance during vertical loading. A vertical load of 80% of the vertical capacity was compared to a case of pure lateral loading. The results are presented in Table C.6 and Figure C.19.

Table C.6: The lateral capacity with combined vertical and lateral load for evaluating the effect of only mobilised side friction

	Ultimate lateral capacity	
Model	0Vc	0.8Vc
Only mobilised side resistance	3 645	3 612

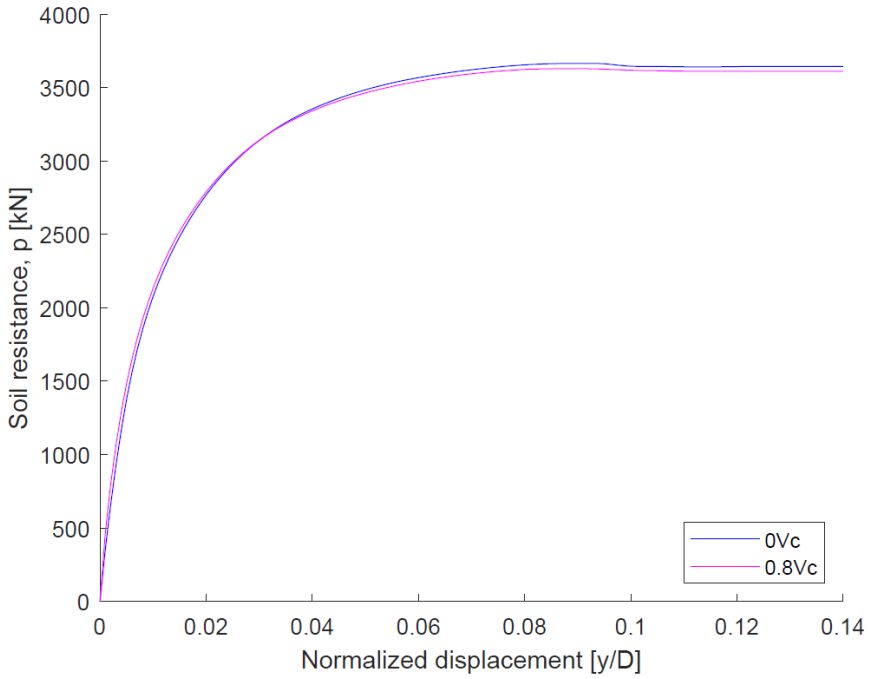

Figure C.19: Comparison of p-y curves with combined vertical and lateral loading for evaluating the effect of only mobilised side friction

Appendix D

Scripts for modelling in Plaxis 3D

This study is based on modelling of a large diameter pile in Plaxis 3D. The models are created through Python scripting, and the scripts are presented in this appendix. The scripts are designed as general as possible to change parameters for the analysis performed easily. The scripts included are:

- Script for modelling the full length of the pile in Appendix D.1.
- Script for modelling Slice model 1 in Appendix D.2.
- Script for modelling Slice model 2 in Appendix D.3.
- Script for modelling only a slice in Appendix D.4.
- Scripts for extracting results from Plaxis output in Appendix D.5.
  Including extracting M_{stage} vs u_z and F_x vs u_x.

The first part of every script involves connecting to the Plaxis application. The Plaxis 3D version used in this study is Plaxis 3D 2018.01. This is done through the *Configure remote scripting server* in Plaxis 3D. This is illustrated in Figure D.1. The served port and password needs to changes by the user to match the script.

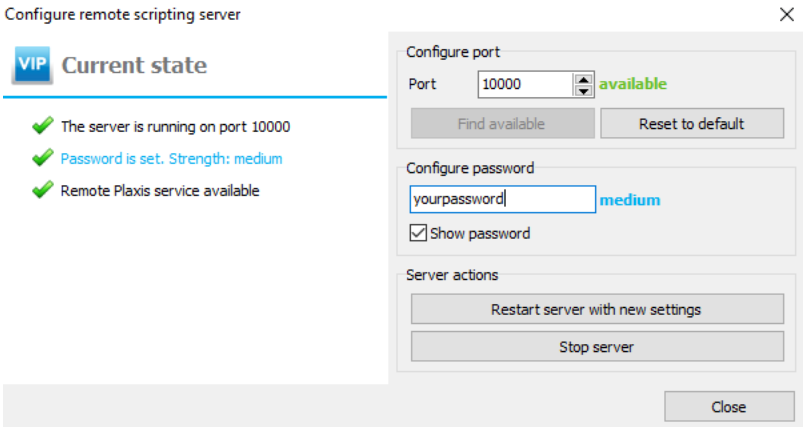

Figure D.1: Connecting to the Plaxis application through *Configure remote scripting server* in Plaxis 3D

D.1 Script for modelling the full length of the pile

```
################################################################################
############################## FULL MODEL ######################################

########## LIBRARIES AND CONNECTION TO PLAXIS APPLICATION ####################
import os
import imp

plaxis_path=r'C:\Program Files\Plaxis\PLAXIS 3D'
plaxis_python_path=r'python\Lib\site-packages'
port_num = 10000
port_num_output = 10001
pw = 'yourpassword'  #change for your password

plx_modules = ['plxscripting','encryption']

for plx_module in plx_modules:
    print('importing module %s'%plx_module)
    found_module = imp.find_module(plx_module,
                                   [os.path.join(plaxis_path,
                                                 plaxis_python_path)])
    plxscripting = imp.load_module(plx_module,*found_module)

from plxscripting.easy import *

s_i, g_i = new_server('localhost', port_num, password=pw)
s_o, g_o=new_server('localhost', port_num_output, password=pw)

################################################################################
################ Based on a vertical capacity analysis #########################

vc_60_ld3=1359 # [kPa]

#For vertial loading of the pile
vc=-vc_60_ld3 # Vertical capacity based on a vertical capacity analysis
su=60 # Undrained shear strength

# Variables created for prescribed lateral displacement in StageConstruction
verticalload=[0, 0.2*vc, 0.4*vc, 0.6*vc, 0.8*vc]
step=0.6 # Load step/displacement
numb=1 # Number of displacement steps

# Path and name for saving the project
save_path=r'C:\karianne\Full_model'

################################################################################
############################## INPUT ###########################################

# Creating a new project
s_i.new()

# Set model and elements properties
g_i.setproperties("ModelType", "Full", "ElementType", "10-Noded")

# Pile properties
LDratio=3
pile_length = 15
diameter=pile_length/LDratio
radius=diameter/2

# Model boundaries
xmin = -10*diameter
ymin = 0
zmin= -pile_length-(5*diameter)
xmax = 10*diameter
ymax = 10*diameter
zmax = 0
g_i.SoilContour.initializerectangular(xmin, ymin, xmax, ymax)

################################################################################
############### Soil model and properties ######################################

# Clay
clay = g_i.soilmat() # Create a soil material set
clay.setproperties("MaterialName", "clay",
                   "Colour", 15262369,
                   "SoilModel", 3,
                   "DrainageType", "Undrained (B)",

                   "gammaUnsat", 20,
                   "gammaSat", 20,

                   "E50ref", 20000,
                   "cref", su,

                   "K0Determination","Manual",
                   "K0Primary",1,
                   "K0Secondary",1,
```

```
                    "powerm",1)

# Soil-structure interface
inter = g_i.soilmat()
inter.setproperties("MaterialName", "inter",
                    "Colour", 964844,
                    "SoilModel", 3,
                    "DrainageType", "Undrained (B)",

                    "gammaUnsat", 20,
                    "gammaSat", 20,

                    "E50ref", 20000,
                    "cref", su,

                    "K0Determination","Manual",
                    "K0Primary",1,
                    "K0Secondary",1,
                    "powerm",1)

# Pile
pile = g_i.soilmat()
pile.setproperties("MaterialName", "pile",
                    "Colour",10283244,
                    "SoilModel", 1,
                    "DrainageType", 4,
                    "Gref", 76923076.9230769,
                    "cref", 0,
                    "gammaUnsat", 20,
                    "Eref", 200000000,
                    "nu", 0.3,
                    "K0Determination","Manual",
                    "K0Primary",1,
                    "K0Secondary",1)
################################################################################
############################## Borehole ########################################

borehole = g_i.borehole(0, 0) # x,y-coordinate of the borehole
borehole.setproperties("Head", 0) # z-coordinate of the water head
g_i.soillayer(-zmin) # Define a layer with z-coordinate of the lower boundary

################################################################################
############################## Structures ######################################
g_i.gotostructures()

#Create soil polygon
soil=g_i.surface((xmin,ymin,zmax),(ymax,ymin,zmax),
                 (xmax,ymax,zmax),(xmin,ymax,zmax))
g_i.extrude(soil,(0,0,zmin))
g_i.delete(soil)
g_i.Volume_1.Soil.Material=clay

# Create polycurve for the pile
p=g_i.polycurve(0, 0, 0, radius, 0, 0, 0, radius, 0)
p.Offset1=radius
p.Offset2=0
p.add()
p.Segments[-1].SegmentType = "Arc"
p.Segments[-1].ArcProperties.RelativeStartAngle1=90
p.Segments[-1].ArcProperties.Radius=radius
p.Segments[-1].ArcProperties.CentralAngle=180
s=p.close() # Close to create volume

# Create lines along polycurve
lin=g_i.extrude(p,(0,0,-pile_length))

# Create solid surface
sur=g_i.surface(p)

# Creating surface load for verical loading
g_i.surfload(sur)
g_i.SurfaceLoad_1.setproperties("sigx",0,"sigy",0,"sigz",0)

# Create volume for pile
g_i.extrude(sur,(0,0,-pile_length))
g_i.Volume_2.Soil.Material=pile

# Create intephase along lines
g_i.delete(s) #delete line along BC (closed curve), to avoide interface here
g_i.delete(lin) #delete surface created for volume
f=g_i.extrude(p,(0,0,-pile_length-1)) # create surface for interface

g_i.neginterface(f) #NegativeInterface_1, Default - from Adjacent soil
g_i.NegativeInterface_1.MaterialMode = "custom"
g_i.NegativeInterface_1.Material=inter # Assigning material

################ Creating volume for refined mesh
```

```
# Create polycurve
v8=g_i.polycurve(0, 0, 0, 3*radius, 0, 0, 0, 3*radius, 0)
v8.Offset1=3*radius
v8.Offset2=0
v8.add()
v8.Segments[-1].SegmentType = "Arc"
v8.Segments[-1].ArcProperties.RelativeStartAngle1=90
v8.Segments[-1].ArcProperties.Radius=3*radius
v8.Segments[-1].ArcProperties.CentralAngle=180
v9=v8.close() # Close to create volume

# Create solid surface
v10=g_i.surface(v8)

# Create volume
g_i.extrude(v10,(0,0,-pile_length-(2*radius)))

g_i.delete(v10)
g_i.delete(v8)

################ Interface at the bottom
vb=g_i.polycurve(0, 0, -pile_length,
                 radius+1, 0, -pile_length,
                 0, radius+1, -pile_length)
vb.Offset1=radius+1
vb.Offset2=0
vb.OrientationAxis1X=1
vb.OrientationAxis1Y=0
vb.OrientationAxis1Z=0
vb.OrientationAxis2X=0
vb.OrientationAxis2Y=1
vb.OrientationAxis2Z=0
vb.add()
vb.Segments[-1].SegmentType = "Arc"
vb.Segments[-1].ArcProperties.RelativeStartAngle1=90
vb.Segments[-1].ArcProperties.Radius=radius+1
vb.Segments[-1].ArcProperties.CentralAngle=180
vs=vb.close() # Close to create volume

# Create solid surface
vd=g_i.surface(vb)
g_i.neginterface(vd)
g_i.NegativeInterface_2.MaterialMode = "custom" # Notice: general interface ref
g_i.NegativeInterface_2.Material=inter # Assigning material

# Surface displacement for lateral load
g_i.surfdispl(sur)
g_i.SurfaceDisplacement_1.setproperties("Displacement_x","Free",
                                        "Displacement_y","Free",
                                        "Displacement_z","Free")

#############################################################################
###################### GroundWaterFlow ######################################

#Set as default if not changed

#############################################################################
########################### Mesh#############################################

g_i.gotomesh()

# Soil volume outside
g_i.BoreholeVolume_1_Volume_1_1.CoarsenessFactor=1
#Pile and soil volume with finer mesh
g_i.BoreholeVolume_1_Volume_1_Volume_2_Volume_3_1.CoarsenessFactor=0.1
g_i.BoreholeVolume_1_Volume_1_Volume_3_1.CoarsenessFactor=0.1

g_i.mesh() # Generating mesh

# Selecting nodes and stress points in the output server
# NB: generating mesh will cleare all prior curve points
# It will select a node A and stress point K closes to the point
# (numbering A,B,C... for nodes, K,L,M... for stress ponints)

g_i.selectmeshpoints() #Opening the output

g_o.addcurvepoint("Node", (0,radius/2,0))

g_o.update()

#############################################################################
######################### StageConstruction #################################

g_i.gotostages()

##### Initial phase, do not need to enter the phase
```

```
# Assigning material
g_i.set(g_i.Soil_1_Soil_2_1.Material,(g_i.InitialPhase),clay)
g_i.set(g_i.Soil_1_Soil_2_Soil_3_Soil_4_1.Material,(g_i.InitialPhase),clay)
g_i.set(g_i.Soil_1_Soil_2_Soil_4_1.Material,(g_i.InitialPhase),clay)

######## Phase 1: Installation of pile + interface
g_i.phase(g_i.InitialPhase) #Add Initial phase
g_i.setcurrentphase(g_i.Phase_1) # Make Phase 1 current

g_i.Phase_1.Identification = "Installation" # IDENTIFICATION

#Pile material assigned to soil volume
g_i.set(g_i.Soil_1_Soil_2_Soil_3_Soil_4_1.Material,(g_i.Phase_1),pile)

g_i.Surface_2.activate(g_i.Phase_1)
g_i.Interfaces.activate(g_i.Phase_1) # Activating interface

######## Vertical loading
# Applying vertical loads equal to [0, 0.2, 0.4, 0.6, 0.8]*Vertical capacity

nr=2 # start of phases
lastnr=1

# Creating a loop for applying the vertical load, creating the slice
# and loading the slice laterally by assigning a prescribed displacement (ux)

for x in verticalload:
    #VERTICAL LOADING
    g_i.phase(g_i.Phases[lastnr])
    g_i.setcurrentphase(g_i.Phases[nr])
    g_i.Phases[nr].Identification = "Vertical_load_test"
    g_i.SurfaceLoads[0].activate(g_i.Phases[nr])
    g_i.set(g_i.SurfaceLoad_1_1.sigz,g_i.Phases[nr],x)

    # Resetting displacements
    g_i.phase(g_i.Phases[nr])
    g_i.setcurrentphase(g_i.Phases[nr+1])
    g_i.Phases[nr+1].Identification = "reset_displacements"
    g_i.Phases[nr+1].Deform.ResetDisplacementsToZero=True

    # LATERAL LOADING (PRESCRIBED DISPLACEMENT u_x)
    s=nr+1 # nr last phase, "start from"
    vec=[x*step for x in range(-s+1,numb+1)] # List with displacements
    list1=list(range(s,s+numb)) # List starting from last phase, here phase 1
    for b in list1:
        g_i.phase(g_i.Phases[int(b)])
        g_i.setcurrentphase(g_i.Phases[int(b+1)])
        g_i.Phases[int(b+1)].Identification = "Load"

        # Activating the prescribed lateral displacement
        g_i.SurfaceDisplacement_1.activate(g_i.Phases[int(b+1)])
        g_i.set(g_i.SurfaceDisplacement_1_1.Displacement_x,
                (g_i.Phases[int(b+1)]),"Prescribed")
        g_i.set(g_i.SurfaceDisplacement_1_1.ux,(g_i.Phases[int(b+1)]),vec[b])

        # Changing the numerical control parameters
        g_i.Phases[int(b+1)].MaxStepsStored=30
        g_i.Phases[int(b+1)].Deform.UseDefaultIterationParams=False
        g_i.Phases[int(b+1)].Deform.MaxLoadFractionPerStep=0.05
        g_i.Phases[int(b+1)].Deform.MaxUnloadingSteps=50
        g_i.Phases[int(b+1)].Deform.DesiredMinIterations=5
        g_i.Phases[int(b+1)].Deform.DesiredMaxIterations=5

    if lastnr==1:
        lastnr=2
    else:
        lastnr=nr

    nr=nr+2+numb


################################## CALCULATE ###################################
g_i.calculate()
############################ Saving the project ################################
g_i.save(save_path)
```

D.2 Script for modelling Slice model 1

```
################################################################################
######################### SLICE MODEL 1 ########################################

########## LIBRARIES AND CONNECTION TO PLAXIS APPLICATION ######################
import os
import imp

plaxis_path=r'C:\Program Files\Plaxis\PLAXIS 3D'
plaxis_python_path=r'python\Lib\site-packages'
port_num = 10000
port_num_output = 10001
pw = 'yourpassword'  #change for your password

plx_modules = ['plxscripting','encryption']

for plx_module in plx_modules:
    print('importing module %s'%plx_module)
    found_module = imp.find_module(plx_module,
                                   [os.path.join(plaxis_path,
                                                 plaxis_python_path)])
    plxscripting = imp.load_module(plx_module,*found_module)

from plxscripting.easy import *

s_i, g_i = new_server('localhost', port_num, password=pw)
s_o, g_o=new_server('localhost', port_num_output, password=pw)

################################################################################
################ Based on a vertical capacity analysis ########################

vc_60_ld3=1359 # [kPa]

#For vertial loading of the pile
vc=-vc_60_ld3 # vertical capacity
su=60
verticalload=[0, 0.2*vc, 0.4*vc, 0.6*vc, 0.8*vc]

step=0.6 # Load step/displacement
numb=1 # Number of displacement steps

# Path and name for saving the project
save_path=r'C:\karianne\Slice_model_1'

################################################################################
############################## INPUT ###########################################

# Creating a new project
s_i.new()

# Set model and elements properties
g_i.setproperties("ModelType", "Full", "ElementType", "10-Noded")

LDratio=3
pile_length = 15
diameter=pile_length/LDratio
radius=diameter/2

# Model boundaries
xmin = -10*diameter
ymin = 0
zmin= -pile_length-(5*diameter)
xmax = 10*diameter
ymax = 10*diameter
zmax = 0
g_i.SoilContour.initializerectangular(xmin, ymin, xmax, ymax)

# The chosen depth of the slice
slice_top=-9
slice_bot=-10

################################################################################
############### Soil model and properties ######################################

# Clay
clay = g_i.soilmat() # Create a soil material set
clay.setproperties("MaterialName", "clay",
                   "Colour", 15262369,
                   "SoilModel", 3,
                   "DrainageType", "Undrained (B)",

                   "gammaUnsat", 20,
                   "gammaSat", 20,

                   "E50ref", 20000,
                   "cref", su,

                   "K0Determination","Manual",
```

```
                    "K0Primary",1,
                    "K0Secondary",1,
                    "powerm",1)

# Soil-structure interface
inter = g_i.soilmat()
inter.setproperties("MaterialName", "inter",
                    "Colour", 964844,
                    "SoilModel", 3,
                    "DrainageType", "Undrained (B)",

                    "gammaUnsat", 20,
                    "gammaSat", 20,

                    "E50ref", 20000,
                    "cref", su,

                    "K0Determination","Manual",
                    "K0Primary",1,
                    "K0Secondary",1,
                    "powerm",1)

# Pile
pile = g_i.soilmat()
pile.setproperties("MaterialName", "pile",
                    "Colour",10283244,
                    "SoilModel", 1,
                    "DrainageType", 4,
                    "Gref", 76923076.9230769,
                    "cref", 0,
                    "gammaUnsat", 20,
                    "Eref", 200000000,
                    "nu", 0.3,
                    "K0Determination","Manual",
                    "K0Primary",1,
                    "K0Secondary",1)

################################################################################
############################## Borehole ########################################

borehole = g_i.borehole(0, 0) # x,y-coordinate of the borehole
borehole.setproperties("Head", 0) # z-coordinate of the water head
g_i.soillayer(-zmin) # Define a layer with z-coordinate of the lower boundary

################################################################################
############################ Structures ########################################

g_i.gotostructures()

# Create soil polygon for the clay
soil=g_i.surface((xmin,ymin,zmax),(ymax,ymin,zmax),
                 (xmax,ymax,zmax),(xmin,ymax,zmax))
g_i.extrude(soil,(0,0,zmin))
g_i.delete(soil)
g_i.Volume_1.Soil.Material=clay

# Create polycurve for the pile
p=g_i.polycurve(0, 0, 0, radius, 0, 0, 0, radius, 0)
p.Offset1=radius
p.Offset2=0
p.add()
p.Segments[-1].SegmentType = "Arc"
p.Segments[-1].ArcProperties.RelativeStartAngle1=90
p.Segments[-1].ArcProperties.Radius=radius
p.Segments[-1].ArcProperties.CentralAngle=180
s=p.close() # Close to create volume

# Create lines along polycurve
lin=g_i.extrude(p,(0,0,-pile_length))

# Create solid surface
sur=g_i.surface(p)

# Creating surface load for verical loading
g_i.surfload(sur)
g_i.SurfaceLoad_1.setproperties("sigx",0,"sigy",0,"sigz",0)

# Create volume for pile
g_i.extrude(sur,(0,0,-pile_length))
g_i.Volume_2.Soil.Material=pile

# Create inteface along lines
g_i.delete(s) #delete line along BC (closed curve), to avoide interface
g_i.delete(lin) #delete surface created for volume
f=g_i.extrude(p,(0,0,-pile_length))

g_i.neginterface(f) #NegativeInterface_1, Default - from Adjacent soil
```

```
g_i.NegativeInterface_1.MaterialMode = "custom"
g_i.NegativeInterface_1.Material=inter # Assigning material


################## Creating volume for mesh

# Create polycurve
v8=g_i.polycurve(0, 0, 0, 3*radius, 0, 0, 0, 3*radius, 0)
v8.Offset1=3*radius
v8.Offset2=0
v8.add()
v8.Segments[-1].SegmentType = "Arc"
v8.Segments[-1].ArcProperties.RelativeStartAngle1=90
v8.Segments[-1].ArcProperties.Radius=3*radius
v8.Segments[-1].ArcProperties.CentralAngle=180
v9=v8.close() # Close to create volume

# Create solid surface
v10=g_i.surface(v8)

# Create volume
g_i.extrude(v10,(0,0,-pile_length-(2*radius)))

g_i.delete(v10)
g_i.delete(v8)

################## CREATE A SOIL SLICE
# creating volumes to be removed during phase construction of the slice
soil1=g_i.surface((xmin,ymin,zmax),(xmax,ymin,zmax),
                  (xmax,ymax,zmax),(xmin,ymax,zmax))

g_i.extrude(soil1,(0,0,slice_top))

soil2=g_i.surface((xmin,ymin,slice_bot),(xmax,ymin,slice_bot),
                  (xmax,ymax,slice_bot),(xmin,ymax,slice_bot))

g_i.extrude(soil2,(0,0,(zmin-slice_bot)))


################## CREATE SURFACE FOR LOAD, CENTER OF SLICE

# Create polycurve
v5=g_i.polycurve((xmax+xmin)/2, ymin, (slice_top+slice_bot)/2,
                 radius, ymin, (slice_top+slice_bot)/2,
                 (xmax+xmin)/2, radius, (slice_top+slice_bot)/2)
v5.Offset1=radius
v5.Offset2=0
v5.OrientationAxis1X=1
v5.OrientationAxis1Y=0
v5.OrientationAxis1Z=0
v5.OrientationAxis2X=0
v5.OrientationAxis2Y=1
v5.OrientationAxis2Z=0
v5.add()
v5.Segments[-1].SegmentType = "Arc"
v5.Segments[-1].ArcProperties.RelativeStartAngle1=90
v5.Segments[-1].ArcProperties.Radius=radius
v5.Segments[-1].ArcProperties.CentralAngle=180
v6=v5.close() # Close to create volume

# Create solid surface
v7=g_i.surface(v5)

################## Boundary conditions for slice model

# top
g_i.surfdispl((xmin,ymin,slice_top),(xmax,ymin,slice_top),
              (xmax,ymax,slice_top),(xmin,ymax,slice_top))
g_i.SurfaceDisplacement_1.setproperties("Displacement_x","Free",
                                        "Displacement_y","Free",
                                        "Displacement_z","Fixed")

# bottom
g_i.surfdispl((xmin,ymin,slice_bot),(xmax,ymin,slice_bot),
              (xmax,ymax,slice_bot),(xmin,ymax,slice_bot))
g_i.SurfaceDisplacement_2.setproperties("Displacement_x","Free",
                                        "Displacement_y","Free",
                                        "Displacement_z","Fixed")

# Surface displacement for lateral load
g_i.surfdispl(v7)
g_i.SurfaceDisplacement_3.setproperties("Displacement_x","Free",
                                        "Displacement_y","Free",
                                        "Displacement_z","Free")


###############################################################################
```

```
###################### GroundWaterFlow ######################################

#Set as default if not changed

#############################################################################
########################### Mesh#############################################

g_i.gotomesh()

# Soil volume outside
g_i.BoreholeVolume_1_Volume_1_Volume_4_1.CoarsenessFactor=1
g_i.BoreholeVolume_1_Volume_1_1.CoarsenessFactor=1
g_i.BoreholeVolume_1_Volume_1_Volume_5_1.CoarsenessFactor=1

#Pile and soil volume with finer mesh
g_i.BoreholeVolume_1_Volume_1_Volume_3_Volume_4_1.CoarsenessFactor=0.1
g_i.BoreholeVolume_1_Volume_1_Volume_3_Volume_5_1.CoarsenessFactor=0.1
g_i.BoreholeVolume_1_Volume_1_Volume_2_Volume_3_Volume_4_1.CoarsenessFactor=0.1
g_i.BoreholeVolume_1_Volume_1_Volume_2_Volume_3_Volume_5_1.CoarsenessFactor=0.1
g_i.BoreholeVolume_1_Volume_1_Volume_3_1.CoarsenessFactor=0.1
g_i.BoreholeVolume_1_Volume_1_Volume_2_Volume_3_1.CoarsenessFactor=0.1
g_i.BoreholeVolume_1_Volume_1_Volume_2_Volume_3_2.CoarsenessFactor=0.1

g_i.mesh() # Generating mesh

# Selecting nodes and stress points in the output server
g_i.selectmeshpoints() #Opening the output

g_o.addcurvepoint("Node", (0,0,((slice_top+slice_bot)/2)))

g_o.update()

#############################################################################
######################### StageConstruction #################################

g_i.gotostages()

##### Initial phase, do not need to enter the phase

# Assigning material
g_i.set(g_i.Soil_1_Soil_2_Soil_5_1.Material,(g_i.InitialPhase),clay)
g_i.set(g_i.Soil_1_Soil_2_Soil_6_1.Material,(g_i.InitialPhase),clay)
g_i.set(g_i.Soil_1_Soil_2_Soil_4_Soil_5_1.Material,(g_i.InitialPhase),clay)
g_i.set(g_i.Soil_1_Soil_2_Soil_4_Soil_6_1.Material,(g_i.InitialPhase),clay)
g_i.set(g_i.Soil_1_Soil_2_Soil_4_1.Material,(g_i.InitialPhase),clay)
g_i.set(g_i.Soil_1_Soil_2_1.Material,(g_i.InitialPhase),clay)
g_i.set(g_i.Soil_1_Soil_2_Soil_3_Soil_4_Soil_6_1.Material,
        (g_i.InitialPhase),clay)
g_i.set(g_i.Soil_1_Soil_2_Soil_3_Soil_4_Soil_5_1.Material,
        (g_i.InitialPhase),clay)
g_i.set(g_i.Soil_1_Soil_2_Soil_3_Soil_4_1.Material,(g_i.InitialPhase),clay)
g_i.set(g_i.Soil_1_Soil_2_Soil_3_Soil_4_2.Material,(g_i.InitialPhase),clay)


####### Phase 1: Installation of pile + interface

g_i.phase(g_i.InitialPhase) #Add Initial phase
g_i.setcurrentphase(g_i.Phase_1) #Make Phase 1 current

g_i.Phase_1.Identification = "Installation" # IDENTIFICATION

# Pile material assigned to soil volume
g_i.set(g_i.Soil_1_Soil_2_Soil_3_Soil_4_Soil_6_1.Material,(g_i.Phase_1),pile)
g_i.set(g_i.Soil_1_Soil_2_Soil_3_Soil_4_Soil_5_1.Material,(g_i.Phase_1),pile)
g_i.set(g_i.Soil_1_Soil_2_Soil_3_Soil_4_1.Material,(g_i.Phase_1),pile)
g_i.set(g_i.Soil_1_Soil_2_Soil_3_Soil_4_2.Material,(g_i.Phase_1),pile)

g_i.Surface_2.activate(g_i.Phase_1)
g_i.NegativeInterface_1.activate(g_i.Phase_1) #Activating interface

######## Vertical loading
# Applying vertical loads equal to [0, 0.2, 0.4, 0.6, 0.8]*Vertical capacity

nr=2 # start of phases
lastnr=1

# Creating a loop for applying the vertical load, creating the slice
# and loading the slice laterally by assigning a prescribed displacement (ux)

for x in verticalload:
    # VERTICAL LOADING
    g_i.phase(g_i.Phases[lastnr])
    g_i.setcurrentphase(g_i.Phases[nr])
    g_i.Phases[nr].Identification = "Vertical_load_test"
    g_i.SurfaceLoads[0].activate(g_i.Phases[nr])
    g_i.set(g_i.SurfaceLoad_1_1.sigz,g_i.Phases[nr],x)
```

```
    # CREATING THE SLICE
    g_i.phase(g_i.Phases[nr])
    g_i.setcurrentphase(g_i.Phases[nr+1])
    g_i.Phases[nr+1].Identification = "creating_slice"
    g_i.Phases[nr+1].Deform.ResetDisplacementsToZero=True
    g_i.Phases[nr+1].Solver=1
    g_i.Phases[nr+1].Deform.UseDefaultIterationParams=False
    g_i.Phases[nr+1].Deform.UseGradualError=True

    # The new boundary conditions for the slice
    g_i.SurfaceDisplacement_1.activate(g_i.Phases[nr+1])
    g_i.SurfaceDisplacement_2.activate(g_i.Phases[nr+1])

    # Deactivating soil and pile above and below slice
    g_i.BoreholeVolume_1_Volume_1_Volume_4_1.deactivate(g_i.Phases[nr+1])
    g_i.BoreholeVolume_1_Volume_1_Volume_5_1.deactivate(g_i.Phases[nr+1])
    g_i.BoreholeVolume_1_Volume_1_Volume_3_Volume_4_1.deactivate(
            g_i.Phases[nr+1])
    g_i.BoreholeVolume_1_Volume_1_Volume_3_Volume_5_1.deactivate(
            g_i.Phases[nr+1])
    g_i.BoreholeVolume_1_Volume_1_Volume_2_Volume_3_Volume_4_1.deactivate(
            g_i.Phases[nr+1])
    g_i.BoreholeVolume_1_Volume_1_Volume_2_Volume_3_Volume_5_1.deactivate(
            g_i.Phases[nr+1])
    g_i.SurfaceLoads[0].deactivate(g_i.Phases[nr+1])
    g_i.NegativeInterface_1_1.deactivate(g_i.Phases[nr+1])
    g_i.NegativeInterface_1_4.deactivate(g_i.Phases[nr+1])

    # LATERAL LOADING (PRESCRIBED DISPLACEMENT u_x)
    s=nr+1 # nr last phase, "start from"
    vec=[x*step for x in range(-s+1,numb+1)] # List with displacements
    list1=list(range(s,s+numb)) # List starting from last phase, here phase 1
    for b in list1:
        g_i.phase(g_i.Phases[int(b)])
        g_i.setcurrentphase(g_i.Phases[int(b+1)])
        g_i.Phases[int(b+1)].Identification = "Load"

        # Activating the prescribed lateral displacement
        g_i.SurfaceDisplacement_3.activate(g_i.Phases[int(b+1)])
        g_i.set(g_i.SurfaceDisplacement_3_1.Displacement_x,
                (g_i.Phases[int(b+1)]),"Prescribed")
        g_i.set(g_i.SurfaceDisplacement_3_1.ux,(g_i.Phases[int(b+1)]),vec[b])

        # Changing the numerical control parameters
        g_i.Phases[int(b+1)].MaxStepsStored=100
        g_i.Phases[int(b+1)].Deform.UseDefaultIterationParams=False
        g_i.Phases[int(b+1)].Deform.MaxLoadFractionPerStep=0.005
        g_i.Phases[int(b+1)].Deform.MaxUnloadingSteps=50
        g_i.Phases[int(b+1)].Deform.DesiredMinIterations=10
        g_i.Phases[int(b+1)].Deform.DesiredMaxIterations=10
        g_i.Phases[int(b+1)].Deform.UseGradualError=True
        g_i.Phases[int(b+1)].Solver=1


    if lastnr==1:
        lastnr=2
    else:
        lastnr=nr

    nr=nr+2+numb


################################# CALCULATE ###################################
g_i.calculate()
############################ Saving the project ###############################
g_i.save(save_path)
```

D.3 Script for modelling Slice model 2

```
################################################################################
######################### SLICE MODEL 2 ########################################

########## LIBRARIES AND CONNECTION TO PLAXIS APPLICATION ####################
import os
import imp

plaxis_path=r'C:\Program Files\Plaxis\PLAXIS 3D'
plaxis_python_path=r'python\Lib\site-packages'
port_num = 10000
port_num_output = 10001
pw = 'yourpassword'  #change for your password

plx_modules = ['plxscripting','encryption']

for plx_module in plx_modules:
    print('importing module %s'%plx_module)
    found_module = imp.find_module(plx_module,
                                   [os.path.join(plaxis_path,
                                                 plaxis_python_path)])
    plxscripting = imp.load_module(plx_module,*found_module)

from plxscripting.easy import *

s_i, g_i = new_server('localhost', port_num, password=pw)
s_o, g_o=new_server('localhost', port_num_output, password=pw)

################################################################################
################ Based on a vertical capacity analysis ########################

vc_60_ld3=1359 # [kPa]

#For vertial loading of the pile
vc=-vc_60_ld3 # vertical capacity
su=60
verticalload=[0, 0.2*vc, 0.4*vc, 0.6*vc, 0.8*vc]
step=0.6 # Load step/displacement
numb=1 # Number of displacement steps

# Path and name for saving the project
save_path=r'C:\karianne\Slice_model_2'

################################################################################
############################## INPUT ###########################################

# Creating a new project
s_i.new()

# Set model and elements properties
g_i.setproperties("ModelType", "Full", "ElementType", "10-Noded")

LDratio=3
pile_length = 15
diameter=pile_length/LDratio
radius=diameter/2

# Model boundaries
xmin = -10*diameter
ymin = 0
zmin= -pile_length-(5*diameter)
xmax = 10*diameter
ymax = 10*diameter
zmax = 0
g_i.SoilContour.initializerectangular(xmin, ymin, xmax, ymax)

# The chosen depth of the slice
slice_top=-9
slice_bot=-10

################################################################################
############### Soil model and properties ######################################

# Clay
clay = g_i.soilmat() # Create a soil material set
clay.setproperties("MaterialName", "clay",
                   "Colour", 15262369,
                   "SoilModel", 3,
                   "DrainageType", "Undrained (B)",

                   "gammaUnsat", 20,
                   "gammaSat", 20,

                   "E50ref", 20000,
                   "cref", su,

                   "K0Determination","Manual",
                   "K0Primary",1,
```

```
                    "K0Secondary",1,
                    "powerm",1)


# Soil-structure interface
inter = g_i.soilmat()
inter.setproperties("MaterialName", "inter",
                    "Colour", 964844,
                    "SoilModel", 3,
                    "DrainageType", "Undrained (B)",

                    "gammaUnsat", 20,
                    "gammaSat", 20,

                    "E50ref", 20000,
                    "cref", su,

                    "K0Determination","Manual",
                    "K0Primary",1,
                    "K0Secondary",1,
                    "powerm",1)

# Interface for the slice
inter2 = g_i.soilmat()
inter2.setproperties("MaterialName", "inter_2",
                    "Colour", 964844,
                    "SoilModel", 1,
                    "DrainageType", "Undrained (A)",

                    "gammaUnsat", 20,
                    "gammaSat", 20,

                    "Eref", 300,
                    "Gref", 150,
                    "cref", su,

                    "K0Determination","Manual",
                    "K0Primary",1,
                    "K0Secondary",1,
                    "InterfaceStrength", "Manual",
                    "Rinter", 0)

# Pile
pile = g_i.soilmat()
pile.setproperties("MaterialName", "pile",
                    "Colour",10283244,
                    "SoilModel", 1,
                    "DrainageType", 4,
                    "Gref", 76923076.9230769,
                    "cref", 0,
                    "gammaUnsat", 20,
                    "Eref", 200000000,
                    "nu", 0.3,
                    "K0Determination","Manual",
                    "K0Primary",1,
                    "K0Secondary",1)
###############################################################################
############################## Borehole ########################################

borehole = g_i.borehole(0, 0) # x,y-coordinate of the borehole
borehole.setproperties("Head", 0) # z-coordinate of the water head
g_i.soillayer(-zmin) # Define a layer with z-coordinate of the lower boundary

###############################################################################
############################## Structures ######################################

g_i.gotostructures()

#Create soil polygon for the clay
soil=g_i.surface((xmin,ymin,zmax),(ymax,ymin,zmax),
                 (xmax,ymax,zmax),(xmin,ymax,zmax))
g_i.extrude(soil,(0,0,zmin))
g_i.delete(soil)
g_i.Volume_1.Soil.Material=clay

# Create polycurve for the pile
p=g_i.polycurve(0, 0, 0, radius, 0, 0, 0, radius, 0)
p.Offset1=radius
p.Offset2=0
p.add()
p.Segments[-1].SegmentType = "Arc"
p.Segments[-1].ArcProperties.RelativeStartAngle1=90
p.Segments[-1].ArcProperties.Radius=radius
p.Segments[-1].ArcProperties.CentralAngle=180
s=p.close() # Close to create volume

# Create lines along polycurve
```

```
lin=g_i.extrude(p,(0,0,-pile_length))

# Create solid surface
sur=g_i.surface(p)

# Creating surface load for verical loading
g_i.surfload(sur)
g_i.SurfaceLoad_1.setproperties("sigx",0,"sigy",0,"sigz",0)

# Create volume for pile
g_i.extrude(sur,(0,0,-pile_length))
g_i.Volume_2.Soil.Material=pile

# Create intephase along lines
g_i.delete(s) #delete line along BC (closed curve), to avoide interface
g_i.delete(lin) #delete surface created for volume
f=g_i.extrude(p,(0,0,-pile_length))

g_i.neginterface(f) #NegativeInterface_1, Default - from Adjacent soil
g_i.NegativeInterface_1.MaterialMode = "custom"
g_i.NegativeInterface_1.Material=inter # Assigning material

################## Creating volume for mesh

# Create polycurve
v8=g_i.polycurve(0, 0, 0, 3*radius, 0, 0, 0, 3*radius, 0)
v8.Offset1=3*radius
v8.Offset2=0
v8.add()
v8.Segments[-1].SegmentType = "Arc"
v8.Segments[-1].ArcProperties.RelativeStartAngle1=90
v8.Segments[-1].ArcProperties.Radius=3*radius
v8.Segments[-1].ArcProperties.CentralAngle=180
v9=v8.close() # Close to create volume

# Create solid surface
v10=g_i.surface(v8)

# Create volume
g_i.extrude(v10,(0,0,-pile_length-(2*radius)))

g_i.delete(v10)
g_i.delete(v8)

################### CREATE A SOIL SLICE, with interfaces
soil1=g_i.surface((xmin,ymin,slice_top),(xmax,ymin,slice_top),
                  (xmax,ymax,slice_top),(xmin,ymax,slice_top))

g_i.posinterface(soil1)

g_i.PositiveInterface_1.MaterialMode = "custom"
g_i.PositiveInterface_1.Material=inter

soil2=g_i.surface((xmin,ymin,slice_bot),(xmax,ymin,slice_bot),
                  (xmax,ymax,slice_bot),(xmin,ymax,slice_bot))

g_i.neginterface(soil2)

g_i.NegativeInterface_2.MaterialMode = "custom"
g_i.NegativeInterface_2.Material=inter

################## CREATE SURFACE FOR LOAD, CENTER OF SLICE

# Create polycurve
v5=g_i.polycurve((xmax+xmin)/2, ymin, (slice_top+slice_bot)/2,
                 radius, ymin, (slice_top+slice_bot)/2,
                 (xmax+xmin)/2, radius, (slice_top+slice_bot)/2)
v5.Offset1=radius
v5.Offset2=0
v5.OrientationAxis1X=1
v5.OrientationAxis1Y=0
v5.OrientationAxis1Z=0
v5.OrientationAxis2X=0
v5.OrientationAxis2Y=1
v5.OrientationAxis2Z=0
v5.add()
v5.Segments[-1].SegmentType = "Arc"
v5.Segments[-1].ArcProperties.RelativeStartAngle1=90
v5.Segments[-1].ArcProperties.Radius=radius
v5.Segments[-1].ArcProperties.CentralAngle=180
v6=v5.close() # Close to create volume

# Create solid surface
v7=g_i.surface(v5)

############################ Boundary conditions for slice model
```

```
# top
g_i.surfdispl((xmin,ymin,slice_top),(xmax,ymin,slice_top),
              (xmax,ymax,slice_top),(xmin,ymax,slice_top))
g_i.SurfaceDisplacement_1.setproperties("Displacement_x","Free",
                                        "Displacement_y","Free",
                                        "Displacement_z","Fixed")
# bottom
g_i.surfdispl((xmin,ymin,slice_bot),(xmax,ymin,slice_bot),
              (xmax,ymax,slice_bot),(xmin,ymax,slice_bot))
g_i.SurfaceDisplacement_2.setproperties("Displacement_x","Free",
                                        "Displacement_y","Free",
                                        "Displacement_z","Fixed")

# Surface displacement for lateral load
g_i.surfdispl(v7)
g_i.SurfaceDisplacement_3.setproperties("Displacement_x","Free",
                                        "Displacement_y","Free",
                                        "Displacement_z","Free")


################################################################################
###################### GroundWaterFlow ########################################

#Set as default if not changed

################################################################################
########################### Mesh###############################################

g_i.gotomesh()

# Soil volume outside
g_i.BoreholeVolume_1_Volume_1_1.CoarsenessFactor=1
g_i.BoreholeVolume_1_Volume_1_2.CoarsenessFactor=1
g_i.BoreholeVolume_1_Volume_1_3.CoarsenessFactor=1
#Pile and soil volume with finer mesh
g_i.BoreholeVolume_1_Volume_1_Volume_2_Volume_3_1.CoarsenessFactor=0.1
g_i.BoreholeVolume_1_Volume_1_Volume_2_Volume_3_2.CoarsenessFactor=0.1
g_i.BoreholeVolume_1_Volume_1_Volume_2_Volume_3_3.CoarsenessFactor=0.1
g_i.BoreholeVolume_1_Volume_1_Volume_2_Volume_3_4.CoarsenessFactor=0.1
g_i.BoreholeVolume_1_Volume_1_Volume_3_1.CoarsenessFactor=0.1
g_i.BoreholeVolume_1_Volume_1_Volume_3_2.CoarsenessFactor=0.1
g_i.BoreholeVolume_1_Volume_1_Volume_3_3.CoarsenessFactor=0.1


g_i.mesh() # Generating mesh

# Selecting nodes and stress points in the output server
g_i.selectmeshpoints() #Opening the output


g_o.addcurvepoint("Node", (0,0,((slice_top+slice_bot)/2))) # Nodes[0]

g_o.addcurvepoint("Node", (3,0,((slice_top+slice_bot)/2)))
g_o.addcurvepoint("Stresspoint",(3,0,((slice_top+slice_bot)/2)))

g_o.addcurvepoint("Node", (5,0,((slice_top+slice_bot)/2)))
g_o.addcurvepoint("Stresspoint",(5,0,((slice_top+slice_bot)/2)))

g_o.addcurvepoint("Node", (7.5,0,((slice_top+slice_bot)/2)))
g_o.addcurvepoint("Stresspoint",(7.5,0,((slice_top+slice_bot)/2)))

g_o.addcurvepoint("Node", (12.5,0,((slice_top+slice_bot)/2)))
g_o.addcurvepoint("Stresspoint",(12.5,0,((slice_top+slice_bot)/2)))

g_o.addcurvepoint("Node", (17.5,0,((slice_top+slice_bot)/2)))
g_o.addcurvepoint("Stresspoint",(17.5,0,((slice_top+slice_bot)/2)))

g_o.addcurvepoint("Node", (22.5,0,((slice_top+slice_bot)/2)))
g_o.addcurvepoint("Stresspoint",(22.5,0,((slice_top+slice_bot)/2)))


g_o.update()

################################################################################
######################### StageConstruction ####################################

g_i.gotostages()

##### Initial phase, do not need to enter the phase

# Assigning material
g_i.set(g_i.Soil_1_Soil_2_1.Material,(g_i.InitialPhase),clay)
g_i.set(g_i.Soil_1_Soil_2_2.Material,(g_i.InitialPhase),clay)
g_i.set(g_i.Soil_1_Soil_2_3.Material,(g_i.InitialPhase),clay)
g_i.set(g_i.Soil_1_Soil_2_Soil_3_Soil_4_1.Material,(g_i.InitialPhase),clay)
g_i.set(g_i.Soil_1_Soil_2_Soil_3_Soil_4_2.Material,(g_i.InitialPhase),clay)
g_i.set(g_i.Soil_1_Soil_2_Soil_3_Soil_4_3.Material,(g_i.InitialPhase),clay)
```

```
g_i.set(g_i.Soil_1_Soil_2_Soil_3_Soil_4_4.Material,(g_i.InitialPhase),clay)
g_i.set(g_i.Soil_1_Soil_2_Soil_4_1.Material,(g_i.InitialPhase),clay)
g_i.set(g_i.Soil_1_Soil_2_Soil_4_2.Material,(g_i.InitialPhase),clay)
g_i.set(g_i.Soil_1_Soil_2_Soil_4_3.Material,(g_i.InitialPhase),clay)



####### Phase 1: Installation of pile + interface
g_i.phase(g_i.InitialPhase) #Add Initial phase
g_i.setcurrentphase(g_i.Phase_1) #Make Phase 1 current

g_i.Phase_1.Identification = "Installation" # IDENTIFICATION

# Pile material assigned to soil volume
g_i.set(g_i.Soil_1_Soil_2_Soil_3_Soil_4_1.Material,(g_i.Phase_1),pile)
g_i.set(g_i.Soil_1_Soil_2_Soil_3_Soil_4_2.Material,(g_i.Phase_1),pile)
g_i.set(g_i.Soil_1_Soil_2_Soil_3_Soil_4_3.Material,(g_i.Phase_1),pile)
g_i.set(g_i.Soil_1_Soil_2_Soil_3_Soil_4_4.Material,(g_i.Phase_1),pile)

g_i.Surface_2.activate(g_i.Phase_1)
g_i.NegativeInterface_1.activate(g_i.Phase_1) #Activating interface

######## Vertical loading
# Applying vertical loads equal to [0, 0.2, 0.4, 0.6, 0.8]*Vertical capacity

nr=2 # start of phases
lastnr=1

# Creating a loop for applying the vertical load, creating the slice
# and loading the slice laterally by assigning a prescribed displacement (ux)

for x in verticalload:
    #VERTICAL LOADING
    g_i.phase(g_i.Phases[lastnr])
    g_i.setcurrentphase(g_i.Phases[nr])
    g_i.Phases[nr].Identification = "Vertical_load_test"
    g_i.SurfaceLoads[0].activate(g_i.Phases[nr])
    g_i.set(g_i.SurfaceLoad_1_1.sigz,g_i.Phases[nr],x)

    g_i.NegativeInterface_2.activate(g_i.Phases[nr])
    g_i.PositiveInterface_1.activate(g_i.Phases[nr])

    # CREATING THE SLICE
    g_i.phase(g_i.Phases[nr])
    g_i.setcurrentphase(g_i.Phases[nr+1])
    g_i.Phases[nr+1].Identification = "reset_displacements"
    g_i.Phases[nr+1].Deform.ResetDisplacementsToZero=True
    g_i.Phases[nr+1].Solver=1
    g_i.Phases[nr+1].Deform.UseDefaultIterationParams=False
    g_i.Phases[nr+1].Deform.UseGradualError=True

    # The new boundary conditions for the slice
    g_i.SurfaceDisplacement_1.activate(g_i.Phases[nr+1])
    g_i.SurfaceDisplacement_2.activate(g_i.Phases[nr+1])

    # The interfaces used for creating the slice
    g_i.set(g_i.NegativeInterface_2_1.Material,(g_i.Phases[nr+1]),inter2)
    g_i.set(g_i.NegativeInterface_2_2.Material,(g_i.Phases[nr+1]),inter2)
    g_i.set(g_i.NegativeInterface_2_3.Material,(g_i.Phases[nr+1]),inter2)
    g_i.set(g_i.PositiveInterface_1_1.Material,(g_i.Phases[nr+1]),inter2)
    g_i.set(g_i.PositiveInterface_1_2.Material,(g_i.Phases[nr+1]),inter2)
    g_i.set(g_i.PositiveInterface_1_3.Material,(g_i.Phases[nr+1]),inter2)


    # LATERAL LOADING (PRESCRIBED DISPLACEMENT u_x)
    s=nr+1 # nr last phase, "start from"
    vec=[x*step for x in range(-s+1,numb+1)] # List with displacements
    list1=list(range(s,s+numb)) # List starting from last phase, here phase 1
    for b in list1:
        g_i.phase(g_i.Phases[int(b)])
        g_i.setcurrentphase(g_i.Phases[int(b+1)])
        g_i.Phases[int(b+1)].Identification = "Load"

        # Activating the prescribed lateral displacement
        g_i.SurfaceDisplacement_3.activate(g_i.Phases[int(b+1)])
        g_i.set(g_i.SurfaceDisplacement_3_1.Displacement_x,
                (g_i.Phases[int(b+1)]),"Prescribed")
        g_i.set(g_i.SurfaceDisplacement_3_1.ux,(g_i.Phases[int(b+1)]),vec[b])

        # Changing the numerical control parameters
        g_i.Phases[int(b+1)].MaxStepsStored=100
        g_i.Phases[int(b+1)].Deform.UseDefaultIterationParams=False
        g_i.Phases[int(b+1)].Deform.MaxLoadFractionPerStep=0.005
        g_i.Phases[int(b+1)].Deform.MaxUnloadingSteps=50
        g_i.Phases[int(b+1)].Deform.DesiredMinIterations=10
        g_i.Phases[int(b+1)].Deform.DesiredMaxIterations=10
        g_i.Phases[int(b+1)].Deform.UseGradualError=True
```

```
        g_i.Phases[int(b+1)].Solver=1


    if lastnr==1:
        lastnr=2
    else:
        lastnr=nr

    nr=nr+2+numb


################################# CALCULATE ###################################
g_i.calculate()
########################### Saving the project ################################
g_i.save(save_path)
```

D.4 Script for modelling only a slice

```
################################################################################
######################### SLICE MODEL 1 ########################################

########## LIBRARIES AND CONNECTION TO PLAXIS APPLICATION ######################
import os
import imp

plaxis_path=r'C:\Program Files\Plaxis\PLAXIS 3D'
plaxis_python_path=r'python\Lib\site-packages'
port_num = 10000
port_num_output = 10001
pw = 'yourpassword'   #change for your password

plx_modules = ['plxscripting','encryption']

for plx_module in plx_modules:
    print('importing module %s'%plx_module)
    found_module = imp.find_module(plx_module,
                                   [os.path.join(plaxis_path,
                                                 plaxis_python_path)])
    plxscripting = imp.load_module(plx_module,*found_module)

from plxscripting.easy import *

s_i, g_i = new_server('localhost', port_num, password=pw)
s_o, g_o=new_server('localhost', port_num_output, password=pw)

################################################################################
################## Based on a vertical capacity analysis #######################

vc_60_ld3=1359 # [kPa]

#For vertial loading of the pile
vc=-vc_60_ld3 # vertical capacity
su=60

verticalload=[0]
dis=0.6 # Prescribed displacement


# Path and name for saving the project
save_path=r'C:\karianne\Slice'

################################################################################
############################## INPUT ###########################################

# Creating a new project
s_i.new()

# Set model and elements properties
g_i.setproperties("ModelType", "Full", "ElementType", "10-Noded")

# Pile geometry
ldratio=3
pile=15 # Length of the pile
diameter=pile/ldratio
radius=diameter/2

# Length of the pile in the model, 1m thickness of the slice
pile_length = 1

# Model boundaries
xmin = -10*diameter
ymin = 0
zmin= -pile_length # 1m thickness of the slice
xmax = 10*diameter
ymax = 10*diameter
zmax = 0
g_i.SoilContour.initializerectangular(xmin, ymin, xmax, ymax)

slice_top=0
slice_bot=-1

################################################################################
############### Soil model and properties ######################################

# Clay
clay = g_i.soilmat() # Create a soil material set
clay.setproperties("MaterialName", "clay",
                   "Colour", 15262369,
                   "SoilModel", 3,
                   "DrainageType", "Undrained (B)",

                   "gammaUnsat", 20,
                   "gammaSat", 20,

                   "E50ref", 20000,
```

```
                    "cref", su,

                    "K0Determination","Manual",
                    "K0Primary",1,
                    "K0Secondary",1,
                    "powerm",1)

# Soil-structure interface
inter = g_i.soilmat()
inter.setproperties("MaterialName", "inter",
                    "Colour", 964844,
                    "SoilModel", 3,
                    "DrainageType", "Undrained (B)",

                    "gammaUnsat", 20,
                    "gammaSat", 20,

                    "E50ref", 20000,
                    "cref", su,

                    "K0Determination","Manual",
                    "K0Primary",1,
                    "K0Secondary",1,
                    "powerm",1)

# Pile
pile = g_i.soilmat()
pile.setproperties("MaterialName", "pile",
                    "Colour",10283244,
                    "SoilModel", 1,
                    "DrainageType", 4,
                    "Gref", 76923076.9230769,
                    "cref", 0,
                    "gammaUnsat", 20,
                    "Eref", 200000000,
                    "nu", 0.3,
                    "K0Determination","Manual",
                    "K0Primary",1,
                    "K0Secondary",1)

################################################################################
############################## Borehole ########################################

borehole = g_i.borehole(0, 0) # x,y-coordinate of the borehole
borehole.setproperties("Head", 0) # z-coordinate of the water head
g_i.soillayer(-zmin) # Define a layer with z-coordinate of the lower boundary

################################################################################
############################## Structures ######################################

g_i.gotostructures()

#Create soil polygon for the clay
soil=g_i.surface((xmin,ymin,zmax),(ymax,ymin,zmax),
                 (xmax,ymax,zmax),(xmin,ymax,zmax))
g_i.extrude(soil,(0,0,zmin))
g_i.delete(soil)
g_i.Volume_1.Soil.Material=clay

# Create polycurve for pile
p=g_i.polycurve(0, 0, 0, radius, 0, 0, 0, radius, 0)
p.Offset1=radius
p.Offset2=0
p.add()
p.Segments[-1].SegmentType = "Arc"
p.Segments[-1].ArcProperties.RelativeStartAngle1=90
p.Segments[-1].ArcProperties.Radius=radius
p.Segments[-1].ArcProperties.CentralAngle=180
s=p.close() # Close to create volume

# Create lines along polycurve
lin=g_i.extrude(p,(0,0,-pile_length))

# Create solid surface
sur=g_i.surface(p)

# Creating surface load for verical loading
g_i.surfload(sur)
g_i.SurfaceLoad_1.setproperties("sigx",0,"sigy",0,"sigz",0)

# Create volume for pile
g_i.extrude(sur,(0,0,-pile_length))
g_i.Volume_2.Soil.Material=pile

# Create intephase along lines
g_i.delete(s) #delete line along BC (closed curve), to avoide interface
g_i.delete(lin) #delete surface created for volume
```

```
f=g_i.extrude(p,(0,0,-pile_length))

g_i.neginterface(f) #NegativeInterface_1, Default - from Adjacent soil
g_i.NegativeInterface_1.MaterialMode = "custom"
g_i.NegativeInterface_1.Material=inter # Assigning material

################## Creating volume for mesh

# Create polycurve
v8=g_i.polycurve(0, 0, 0, 3*radius, 0, 0, 0, 3*radius, 0)
v8.Offset1=3*radius
v8.Offset2=0
v8.add()
v8.Segments[-1].SegmentType = "Arc"
v8.Segments[-1].ArcProperties.RelativeStartAngle1=90
v8.Segments[-1].ArcProperties.Radius=3*radius
v8.Segments[-1].ArcProperties.CentralAngle=180
v9=v8.close() # Close to create volume

# Create solid surface
v10=g_i.surface(v8)

# Create volume
g_i.extrude(v10,(0,0,-pile_length))

g_i.delete(v10)
g_i.delete(v8)

################# CREATE SURFACE FOR LOAD, CENTER OF SLICE

# Create polycurve
v5=g_i.polycurve((xmax+xmin)/2, ymin, (slice_top+slice_bot)/2,
                 radius, ymin, (slice_top+slice_bot)/2,
                 (xmax+xmin)/2, radius, (slice_top+slice_bot)/2)
v5.Offset1=radius
v5.Offset2=0
v5.OrientationAxis1X=1
v5.OrientationAxis1Y=0
v5.OrientationAxis1Z=0
v5.OrientationAxis2X=0
v5.OrientationAxis2Y=1
v5.OrientationAxis2Z=0
v5.add()
v5.Segments[-1].SegmentType = "Arc"
v5.Segments[-1].ArcProperties.RelativeStartAngle1=90
v5.Segments[-1].ArcProperties.Radius=radius
v5.Segments[-1].ArcProperties.CentralAngle=180
v6=v5.close() # Close to create volume

# Create solid surface
v7=g_i.surface(v5)

################# Boundary conditions for slice model

# top
g_i.surfdispl((xmin,ymin,slice_top),(xmax,ymin,slice_top),
              (xmax,ymax,slice_top),(xmin,ymax,slice_top))
g_i.SurfaceDisplacement_1.setproperties("Displacement_x","Free",
                                        "Displacement_y","Free",
                                        "Displacement_z","Fixed")
# bottom
g_i.surfdispl((xmin,ymin,slice_bot),(xmax,ymin,slice_bot),
              (xmax,ymax,slice_bot),(xmin,ymax,slice_bot))
g_i.SurfaceDisplacement_2.setproperties("Displacement_x","Free",
                                        "Displacement_y","Free",
                                        "Displacement_z","Fixed")

#Surface displacement for lateral load
g_i.surfdispl(v7)
g_i.SurfaceDisplacement_3.setproperties("Displacement_x","Free",
                                        "Displacement_y","Free",
                                        "Displacement_z","Free")


###############################################################################
###################### GroundWaterFlow ########################################

#Set as default if not changed

###############################################################################
############################ Mesh##############################################

g_i.gotomesh()

# Soil volume outside
g_i.BoreholeVolume_1_Volume_1_1.CoarsenessFactor=1
```

```
#Pile and soil volume with finer mesh
g_i.BoreholeVolume_1_Volume_1_Volume_2_Volume_3_1.CoarsenessFactor=0.1
g_i.BoreholeVolume_1_Volume_1_Volume_2_Volume_3_2.CoarsenessFactor=0.1
g_i.BoreholeVolume_1_Volume_1_Volume_3_1.CoarsenessFactor=0.1

g_i.mesh() # Generating mesh

# Selecting nodes and stress points in the output server
g_i.selectmeshpoints()

g_o.addcurvepoint("Node", (0,0,((slice_top+slice_bot)/2)))

g_o.update()

##############################################################################
######################### StageConstruction ##################################

g_i.gotostages()

##### Initial phase, do not need to enter the phase

# Assigning material
g_i.set(g_i.Soil_1_Soil_2_1.Material,(g_i.InitialPhase),clay)
g_i.set(g_i.Soil_1_Soil_2_Soil_3_Soil_4_1.Material,(g_i.InitialPhase),clay)
g_i.set(g_i.Soil_1_Soil_2_Soil_3_Soil_4_2.Material,(g_i.InitialPhase),clay)
g_i.set(g_i.Soil_1_Soil_2_Soil_4_1.Material,(g_i.InitialPhase),clay)

g_i.set(g_i.Deformations.BoundaryZMin,g_i.InitialPhase,"Free")
g_i.set(g_i.Deformations.BoundaryZMax,g_i.InitialPhase,"Free")

####### Phase 1: Installation of pile + interface

g_i.phase(g_i.InitialPhase) #Add Initial phase
g_i.setcurrentphase(g_i.Phase_1) #Make Phase 1 current

g_i.Phase_1.Identification = "Installation" # IDENTIFICATION

#Pile material assigned to soil
g_i.set(g_i.Soil_1_Soil_2_Soil_3_Soil_4_1.Material,(g_i.Phase_1),pile)
g_i.set(g_i.Soil_1_Soil_2_Soil_3_Soil_4_2.Material,(g_i.Phase_1),pile)

g_i.Surface_2.activate(g_i.Phase_1)
g_i.NegativeInterface_1.activate(g_i.Phase_1) #Activating interface

g_i.set(g_i.Deformations.BoundaryZMin,g_i.Phase_1,"Vertically fixed")
g_i.set(g_i.Deformations.BoundaryZMax,g_i.Phase_1,"Vertically fixed")

######## Reset displacements

g_i.phase(g_i.Phase_1)
g_i.setcurrentphase(g_i.Phase_2)
g_i.Phase_2.Identification = "Reset_displacements"
g_i.Phase_2.Deform.ResetDisplacementsToZero=True

# The boundary conditions for the slice
g_i.SurfaceDisplacement_1.activate(g_i.Phase_2)
g_i.SurfaceDisplacement_2.activate(g_i.Phase_2)

# Changing the numerical control parameters
g_i.Phase_2.Solver=1
g_i.Phase_2.Deform.UseDefaultIterationParams=False
g_i.Phase_2.Deform.UseGradualError=True

######## Lateral loading
g_i.phase(g_i.Phase_2)
g_i.setcurrentphase(g_i.Phase_3)
g_i.Phase_3.Identification = "Load"

g_i.SurfaceDisplacement_3.activate(g_i.Phase_3)
g_i.set(g_i.SurfaceDisplacement_3_1.Displacement_x,(g_i.Phase_3),"Prescribed")
g_i.set(g_i.SurfaceDisplacement_3_1.ux,(g_i.Phase_3),dis)

# Changing the numerical control parameters
g_i.Phase_3.MaxStepsStored=100
g_i.Phase_3.Deform.UseDefaultIterationParams=False
g_i.Phase_3.Deform.MaxLoadFractionPerStep=0.005
g_i.Phase_3.Deform.MaxUnloadingSteps=50
g_i.Phase_3.Deform.DesiredMinIterations=10
g_i.Phase_3.Deform.DesiredMaxIterations=10
g_i.Phase_3.Deform.UseGradualError=True
g_i.Phase_3.Solver=1

################################# CALCULATE ##################################
g_i.calculate()
########################### Saving the project ###############################
g_i.save(save_path)
```

D.5 Script for extracting results

```
##########################################################################
######## Function for extracting force Fx and displacement ux #############

# The fuction creates a file with name selected by the user (filename)
# where the data is storred, the data is extracted from a calaculation
# phase (phaseorder)


def gettable_fx_vs_ux(filename=None, phaseorder=None):
    # Creating empty lists for data
    stepids = []
    uxAs = []
    force = []
    phasenames = []

    # Look into all phases, all steps:
    r=phaseorder.Steps.value
    for step in r:
        phasenames.append(phaseorder.Name.value)
        stepids.append(int(step.Name.value.replace("Step_","")))
        uxAs.append(g_o.getcurveresults(g_o.Nodes[0],step,
                                        g_o.ResultTypes.Soil.Ux))
        forcevalue = "-"
        if hasattr(step, 'Reached'):
            if hasattr(step.Reached, 'ForceX'):
                forcevalue = step.Reached.ForceX.value
        force.append(forcevalue)

    # Storing the data in file
    if filename:
        with open(filename, "w") as file:
            file.writelines(["{}\t{}\t{}\t{}\n".format(ph, nr, f, uxA)
                             for ph, nr,f, uxA, in zip(phasenames,stepids,
                                                       force,uxAs)])

    # Creating a file with data: [phaseorder stepid Fx ux]



##########################################################################
##########################################################################
#################### Example of use ######################################


# The location of the project of interest "filename"
open_path=r'C:\Dokumenter\Master\filename'

# Calculation phase of interest
ph00=g_o.Phase_4

# Open the project "filename"
s_i.open(open_path)
g_i.view(g_i.Phase_1)
s_o.open(open_path) # Open Plaxis output



# Calling on the fuction gettable_fx_vs_ux to extract force - displacement

gettable_fx_vs_ux(filename= r'C:\Dokumenter\Master\file_phase4_fx_ux.txt',
                  phaseorder = ph00)


# The data from phase 4 in the project "filename" is storred in file:
# "file_phase4_fx_ux.txt"
```

```
################################################################################
######## Function for extracting Mstage and displacement uz ###############

# The fuction creates a file with name selected by the user (filename)
# where the data is storred, the data is extracted from a calaculation
# phase (phaseorder)


def gettable_mstage_vs_uz(filename=None, phaseorder=None):
    # Creating empty lists for data
    stepids = []
    uzAs = []
    mstage = []
    phasenames = []

    # look into all phases, all steps:
    r=phaseorder.Steps.value
    for step in r:
        phasenames.append(phaseorder.Name.value)
        stepids.append(int(step.Name.value.replace("Step_","")))
        uzAs.append(g_o.getcurveresults(g_o.Nodes[0],step,
                                        g_o.ResultTypes.Soil.Uz))
         # make sure step info on time is available, then add it:
        mstagevalue = "-"
        if hasattr(step, 'Reached'):
            if hasattr(step.Reached, 'SumMstage'):
                mstagevalue = step.Reached.SumMstage.value
        mstage.append(mstagevalue)

    # Storing the data in file
    if filename:
        with open(filename, "w") as file:
            file.writelines(["{}\t{}\t{}\t{}\n".format(ph, nr, m, uzA)
                             for ph, nr, m, uzA, in zip(phasenames, stepids,
                                                        mstage,uzAs)])

    # Creating a file with data: [phaseorder stepid Mstage uz]



################################################################################
################################################################################
#################### Example of use ############################################


# The location of the project of interest "filename"
open_path=r'C:\Dokumenter\Master\filename'

# Calculation phase of interest
ph00=g_o.Phase_2

# Open the project "filename"
s_i.open(open_path)
g_i.view(g_i.Phase_1)
s_o.open(open_path) # Open Plaxis output



# Calling on the fuction gettable_mstage_vs_uz to extract mstage - displacement

gettable_mstage_vs_uz(filename= r'C:\Dokumenter\Master\file_phase2_mstage_uz',
                      phaseorder = ph00)


# The data from phase 4 in the project "filename" is storred in file:
# "file_phase4_mstage_uz.txt"
```